T-4560

DEVELOPMENT OF A BLOW-DOWN COMBUSTION BOMB FOR IN-CYLINDER CHEMICAL KINETIC STUDIES

by

Richard K. Mackay

T-4560

A thesis submitted to the Faculty and Board of Trustees of the Colorado School of Mines in partial fulfillment of the requirements for the degree of Master of Science (Applied Mechanics).

Golden, Colorado

Date March 14, 1994

Signed: _____
Richard K. Mackay

Approved: _____
Dr. Mark A. Linne
Thesis Advisor

Golden, Colorado

Date March 14, 1994

_____
Dr. Joan P. Gosink
Professor and Head,
Division of Engineering

ABSTRACT

With increasing pressure being placed on Internal Combustion (IC) engine manufacturers to increase specific output, improve efficiency and simultaneously reduce emissions, a greater emphasis is being directed toward understanding completely the process of combustion. In order for this to occur, a controlled experiment must be utilized. The design of the apparatus introduced here emulates the pressure-time histories found in IC engines without the use of piston motion. In this manner, variations brought about by turbulent flow fields are reduced. This makes it possible to observe chemical kinetics in a reproducible pressure-time curve while minimizing fluid mechanical influences.

The Blow-Down Combustion Bomb (BDCB) is divided into two chambers separated by an orifice plate. The test section incorporates windows in order that flame propagation rates and species concentrations can be determined using laser diagnostic techniques. Also included in this region is a spark plug to initiate combustion, a port to allow the introduction of fuel and air into the BDCB, and a piezoelectric transducer to measure the cylinder pressure. Because of this configuration, the pressure in the BDCB

rises rapidly upon ignition, behaving much like a Constant Volume Combustion Bomb. On the other side of the orifice plate is a back-pressure section, which is responsible for containing the gases within the BDCB until a fast-acting dump valve is actuated. With the valve opened, gases in the test section are expelled at a rate controlled by the orifice plate, producing the desired pressure decay. The combination of these two processes gives a realistic pressure pulse.

In order for the experimental viability of the BDCB to be affirmed, a two-zone thermodynamic model was employed using experimental pressure-time data. The two zones referred to here are the independent regions of burned and unburned gases. As the experiment progresses, the burned volume will expand at the expense of the unburned volume. With this model, information is gained concerning the temperature, volume and mass of the reactants and products at each instant in time.

TABLE OF CONTENTS

LIST OF FIGURES

LIST OF VARIABLES

a - inner radius
b - outer radius or frictional loss term
d - quenching distance
e - ratio of width to length
h - thickness or enthalpy
k - ratio of specific heats
k_e - effective thermal conductivity
k′ - spring constant
m - mass
q - heat transfer per unit area
t - time
u - internal energy
w - width
x - displacement
A - area
C_p - constant pressure specific heat
C_v - constant volume specific heat
P - pressure
Q - heat transfer
R - specific gas constant
S_L - laminar flame speed
T - temperature
V - volume
δ - thermal boundary layer thickness
M - bending moment per unit width
μ - viscosity
σ - stress
ϕ - fuel-air equivalence ratio

SUBSCRIPTS

b - burned gas constituents
f - final state
o - initial or standard state or choked flow variable
p - piston variables
u - unburned gas constituents
v - valve variables
w - wall or wetted surface
ac - adiabatic core
rr - radial direction
zz - axial direction
$\theta\theta$ - circumferential direction

ACKNOWLEDGMENTS

The author wishes to thank Dr. Mark A. Linne for his valued support. In addition to providing creative solutions to otherwise insurmountable obstacles, he was instrumental in pointing out those areas which would have otherwise been overlooked. Special acknowledgment goes to William Bahn for his outstanding work in developing the digital control system used in the experiment. Thanks also to Jim Lally of PCB Piezotronics for providing insightful information and donation of a model 308M117 accelerometer along with a model 480B battery power supply. The Colorado Institute for Fuels and High Altitude Engine Research made available the funds necessary for the purchase of the pressure transducer. The digital equipment used in the experiment was provided thanks to funds derived from the Parsons Foundation. This included several Phillips digital storage oscilloscopes, a Phillips function generator and plotter, a Fluke Helios I analog to digital converter, and a Fluke digital multimeter. Through the efforts of Mary M. Nijhout from Sigma Xi, $382.00 was made available to cover research expenditures. This endowment is the result of income derived from the Gordon B. and Bet L. Carson Fund. Lastly, thanks to Jack Kitner for his valued advice on manufacturing techniques.

INTRODUCTION

While Internal Combustion (IC) engines have been employed in every walk of life over the last 100 years, complete understanding of the combustion process has, to this day, evaded their designers. It is this process which dictates the overall performance of a particular engine, as combustion is the conversion of chemical energy into usable heat energy. Physical considerations, such as valve positioning and number, piston shape, cylinder head geometry, and intake manifold design, all affect the amount of turbulence introduced. This in turn affects engine performance by enhancing or impeding the combustion process. It is therefore difficult to formulate conclusions as to individual contributing factors which affect combustion directly.

With increasing demands from government to improve efficiency and reduce emissions, the task of engine manufacturers is a difficult one as these are mutually exclusive requests. Standards for 1995 would have Spark Ignition (SI) engine designers reduce emissions to 3.4 gm/mi for hydrocarbons, 0.25 gm/mi for carbon monoxide, and 0.4 gm/mi for nitric oxides. Corporate Average Fuel Economy

standards for 1995 and 2000 have been increased to 33 and 40 miles per gallon (mpg) respectively, up from the 27.5 mpg standard that has existed since 1985. In addition, pressure from the consumers of these products dictates that specific output not be compromised. It is clear that a greater understanding of the combustion process itself will have to be attained in order that the demands be met in the years to come.

One might conclude that research should be directed toward developing an engine design which optimizes the physical parameters previously mentioned to meet the goals of society, ignoring the need for a more fundamental understanding of the combustion process. This would not be prudent however, as each engine design is specific to its application. While one engine may be capable of producing high specific output for short periods of time, the design would limit its usefulness for applications requiring reasonable fuel consumption and dependability. As such, even with the many diagnostic tools available to the designer, little is gained in the pursuit of generalized conclusions by this approach.

The key problem in using engines as a diagnostic technique for fundamental research is the introduction of turbulent flow fields. This turbulence greatly affects flame

propagation, making it difficult to determine the factors controlling chemistry. Over the years, devices have been developed which were designed to direct research toward a more fundamental approach. These devices basically fall into one of two categories, Rapid-Compression Machines (RCM) and Constant-Volume Combustion Bombs (CVCB).

With RCM, a quiescent mixture of fuel and air is rapidly compressed, ignited and expanded and duplicates those same processes found in IC engines. The ignition can be either SI or Compression Ignition (CI) depending on the fuel and the compression ratio (2,3). The advantage of such a device is the elimination of the intake and exhaust processes from the cycle, which in turn greatly reduces turbulence in the cylindrical combustion chamber. The gases within the combustion chamber, both reactants and products, experience similar temperatures and pressures to those found in IC engine, adding to their usefulness as experimental devices.

The manner in which they operate is usually by means of a high-speed hydraulic ram. This ram is connected to a piston which moves back and forth in the experimental cylinder. Motion of the ram is controlled by a two-way actuator valve, one circuit being used for compression and the other, for expansion. While RCM serve a key role in

fundamental engine research, the motion of the piston dictates that a reasonably high degree of turbulence will always be present, making studies of chemical kinetics difficult.

In order for flow turbulence to be eliminated, a second diagnostic technique using CVCB has, for many years, been employed. In doing so, the resulting studies are concentrated on chemistry and not on the effects of turbulent mixing in the combustion process. Chemistry and turbulence are therefore distinctly separated. These devices are particularly useful in determining such things as laminar flame speed (5), and represent the most fundamental of approaches when considering constrained combustion. Like RCM, they can be used for studies involving both SI and CI (6). Research involving the CVCB has a more limited scope than that of the RCM in that no effort is made to imitate the pressure history of IC engines (see Fig. 1). In these cases, the pressure decay is elevated when compared to IC engine pressure traces and falls only as a result of heat transfer from the vessel (see Fig. 2). This elevated pressure also implies higher temperatures for the combustion products in relation to those found in real engines. This being the case, information is gained concerning the compression and ignition phase of IC engine operation, but

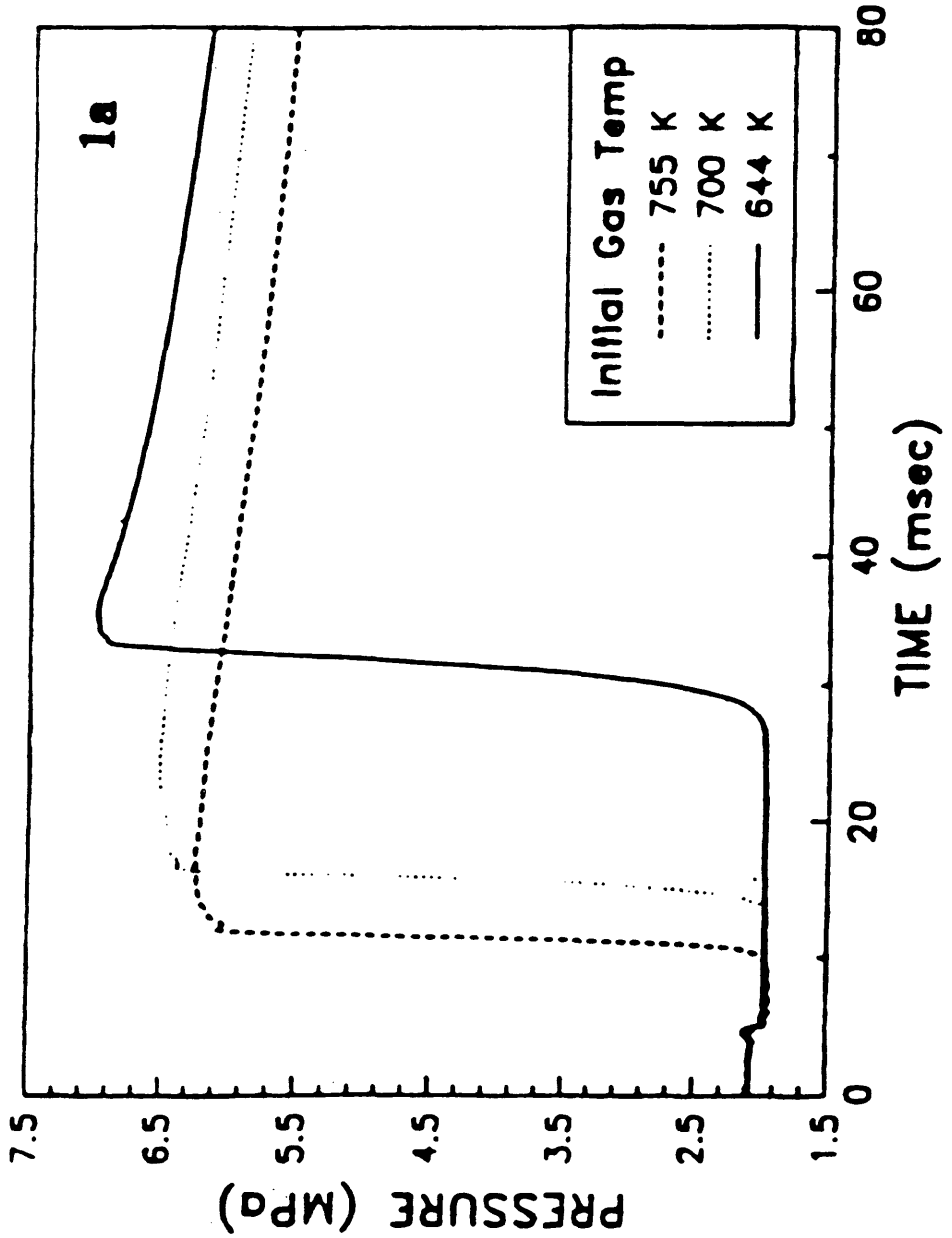

Figure 1 - Pressure-time curve for a Constant-Volume Combustion Bomb using three different initial gas temperatures (Ref. 6).

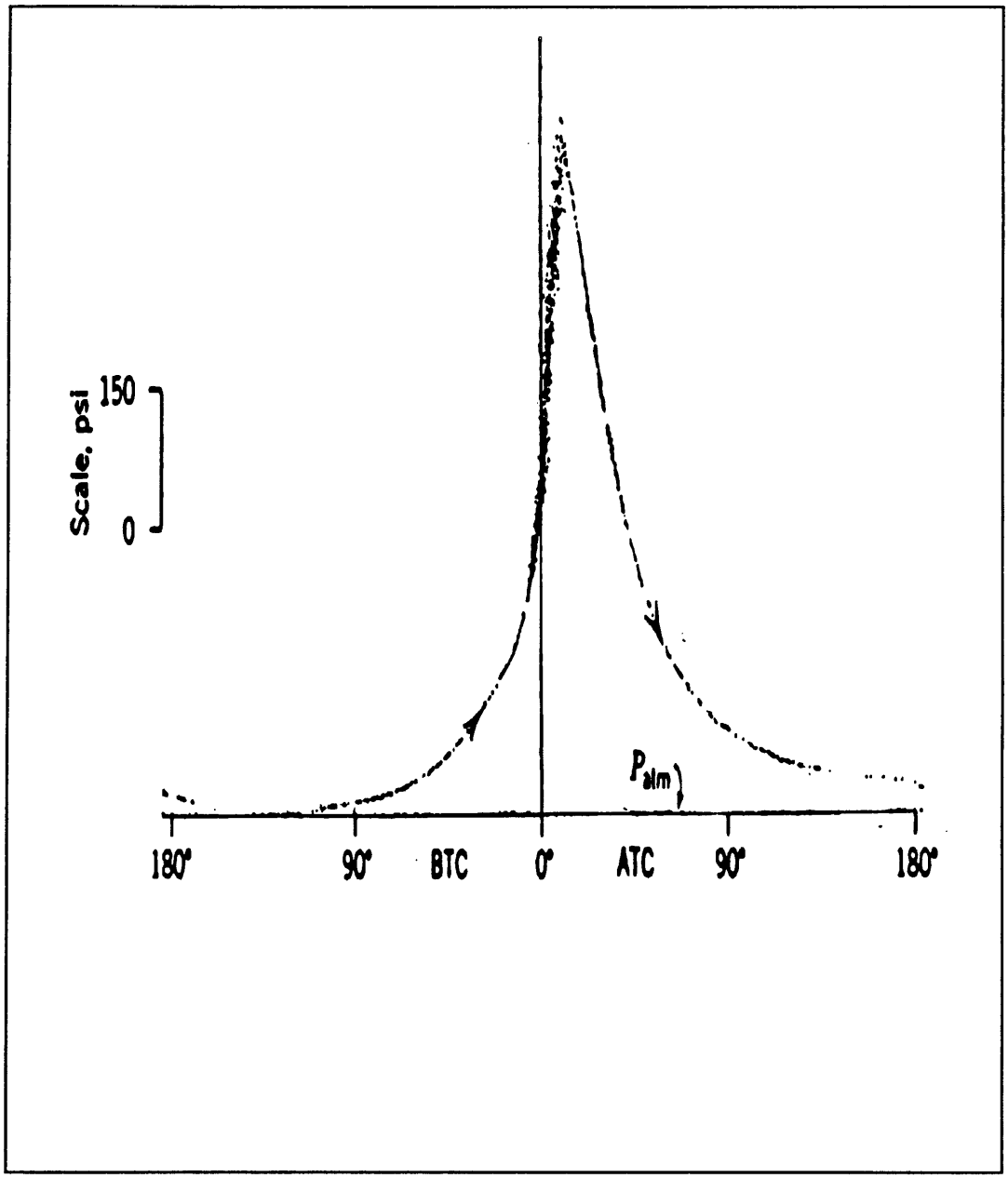

Figure 2 - Cylinder pressure versus crank angle degrees using an indicator card for a CFR Spark Ignition engine operating at 1200 rpm (Ref. 11).

not the expansion phase. It is during expansion, when three body recombination reactions which take combustion to completion are slowed, that many of the species associated with pollution are formed. These species show a high degree of dependency on pressure, temperature and time (7,8).

The development of the BDCB is basically the amalgamation of the two previously cited devices into one which serves a broader goal. Once ignited, reactants are converted into products, causing a pressure rise which is essentially the same as that of a CVCB. An orifice plate with several evenly distributed holes is used to separate the test section from the back-pressure zone. By rapidly evacuating the back-pressure zone, flow across the orifice plate becomes choked and a pressure decay similar to that found in IC engines is produced in the test section. In this manner, the pressure history found in IC engines is emulated, but with turbulence levels greatly diminished from RCM. Additionally, the cyclic variation that IC engines exhibit is significantly reduced (see Fig. 3).

While pressure histories are certainly a large part of verifying a design as an alternative to IC engine studies, the information gained is limited if the temperature regime varies greatly from its engine counterpart. When one considers the duration of one cycle of an engine at typical

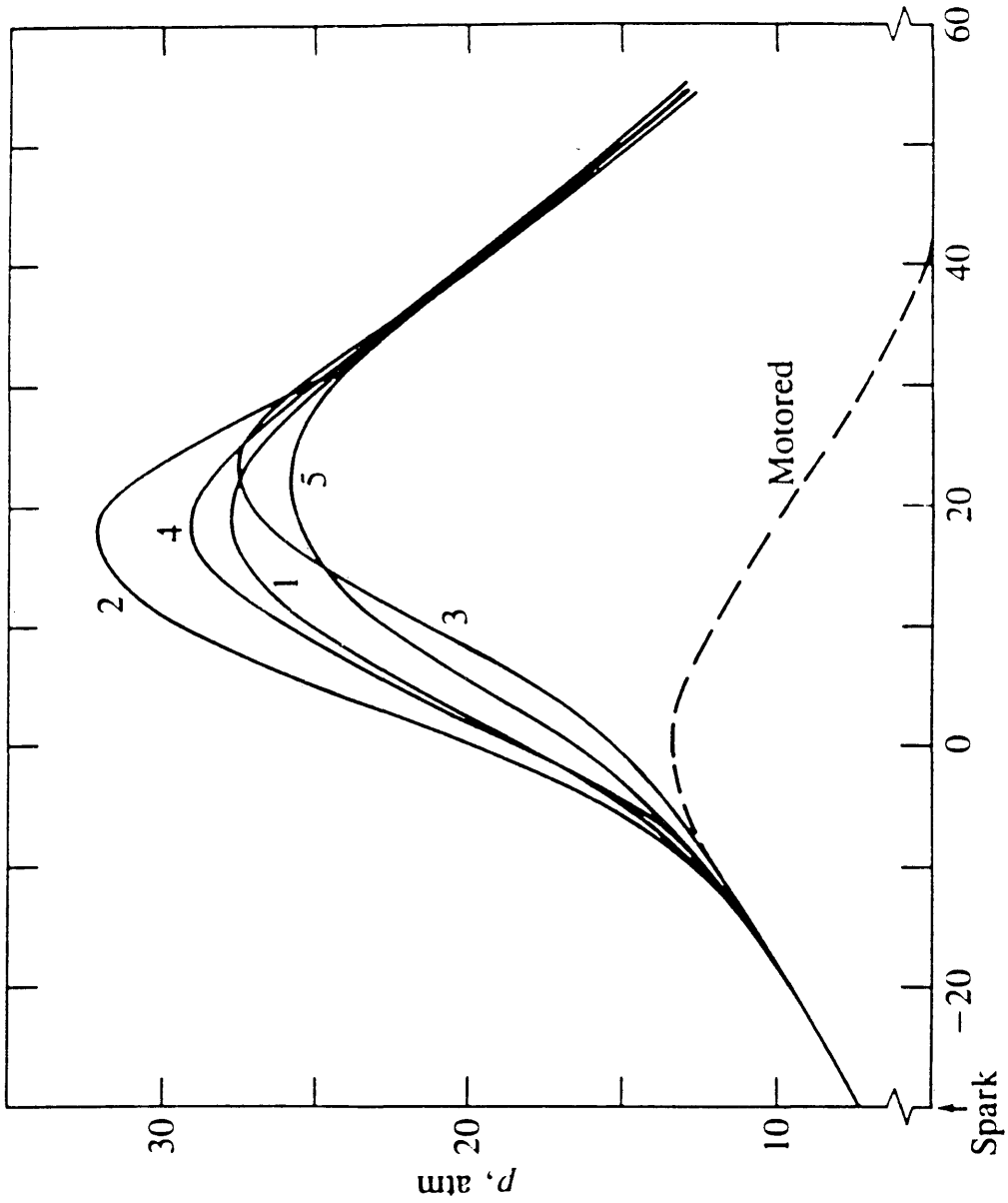

Figure 3 - Cylinder pressure versus crank angle degrees for five consecutive cycles of a Spark Ignition engine (Ref. 4).

operating speeds, determining the temperatures at various locations within the cylinder by direct measurement would be most difficult. Instead, it is standard practice to employ thermodynamic models which are driven by the experimental pressure traces.

Some of the earliest models developed using pressure data were by Rassweiler and Withrow (9). In their evaluation, the burned mass was taken to be proportional to the deviation between the experimental pressure and the pressure that would result from polytropic compression or expansion. While this technique is easy to employ for IC engines, the lack of volume change in the BDCB renders it ineffectual in this application. In addition, no information is given as to the energy change represented by the pressure-time curve.

With the introduction of digital computers and their ability to perform large computational tasks, a thermodynamic first law evaluation could be undertaken. Some of the first work done in this area was by Olikara and Borman (10). Previously, no such analysis could be performed owing to the difficulty in determining the equilibrium concentrations of the major product species at every instant in the experiment. It is these species that control thermochemistry, which is the driving force behind pressure

and temperature profiles. Equilibrium will not, however, provide information concerning the trace species. With the ability to determine the thermochemical properties in hand, one- and two-zone, zero-dimensional thermodynamic models were developed. One-zone models are used in studies of CI while two-zone models are used for SI experiments. The term "zero-dimensional" describes those models which are void of any spatial relations. Figure 4 is included to illustrate the temperature regimes which result from the application of a two-zone model. The temperature of the burned gases are much higher than that of the unburned gases as chemical energy is converted to sensible energy, thereby giving rise to the two-zones, each unique from the other.

The diagram (Fig. 4) that has been included shows that period of the experiment between ignition and exhaust. When using a first law analysis to evaluate pressure data for IC engines, a different equation must be developed for each of the four processes, intake, compression, combustion and expansion, and exhaust. Of these, only combustion and expansion are of interest in heat release analysis. These are the only processes addressed by studies involving the BDCB.

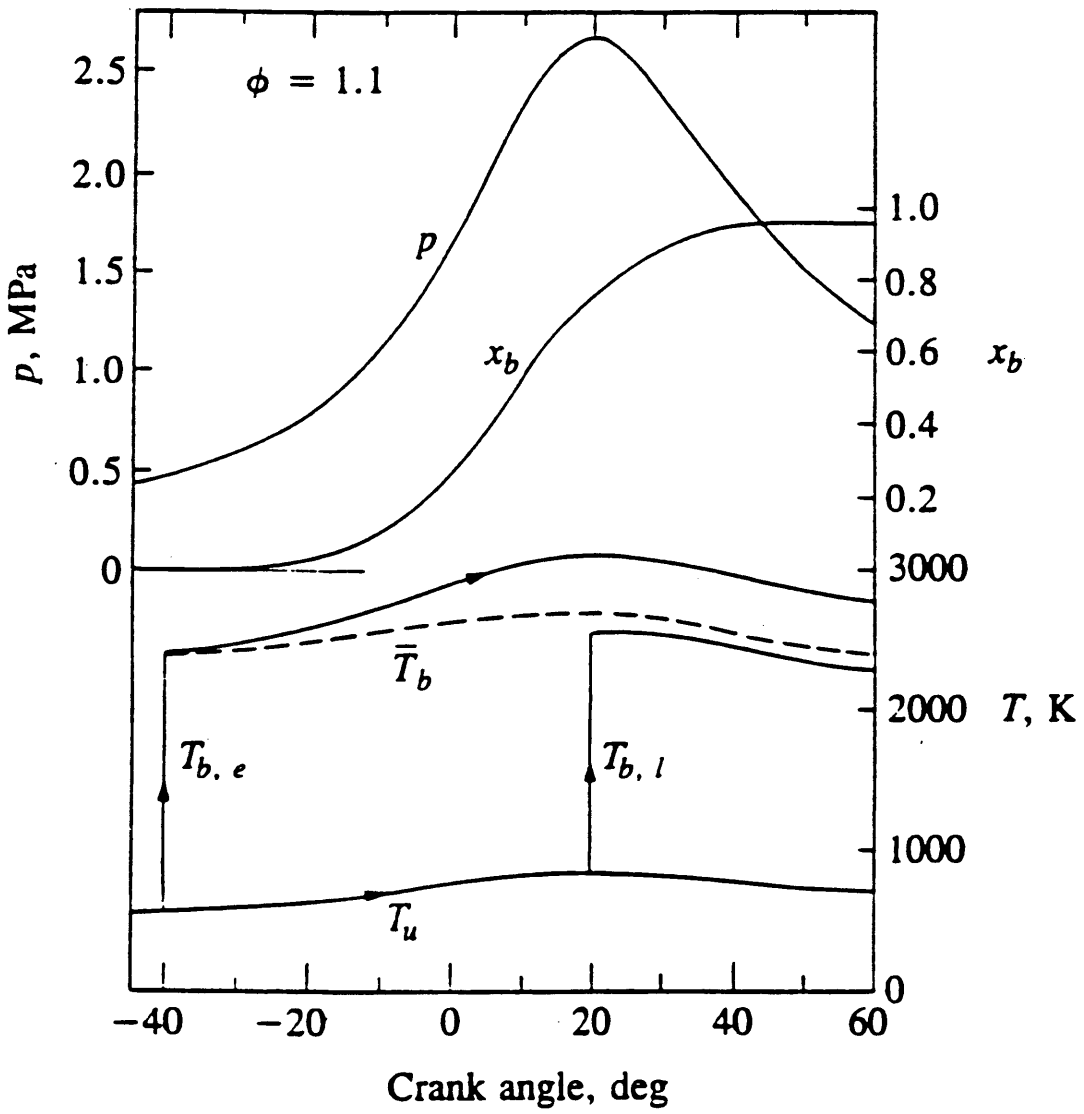

Figure 4 - Burned and unburned gas temperatures resulting from a two-zone thermodynamic model (Ref. 20).

BLOW-DOWN COMBUSTION BOMB DESIGN

Design Criterion

Before proceeding with the details of the design, the criteria used in the solution approach must be addressed. The most critical of these considerations is the pressure history which the BDCB will produce. In order for a meaningful correlation to exist between this device and a real engine, the pressure-time relationships must be coincidental. Design modeling for the BDCB was therefore done using the engine pressure trace illustrated previously (see Fig. 3), obtained from Taylor (11). The CFR Spark Ignition engine used in that work has a bore of 82.55 mm and a stroke of 114.3 mm, as specified in the ASTM book of standards (volume 05.04 page 338). At the time Figure 2 was obtained, the engine was operating at 1200 rpm and had a compression ratio of 8.35. The mass ratio of iso-octane (iso-C_8H_{18}) to air was stated to be 0.0782.

Another consideration addressed the need to limit the contributions of fluid mechanics. By restricting these effects, a study of chemical kinetics can be conducted without the interference of turbulent mixing. It was also

desired that the BDCB produce results which were highly reproducible.

An additional criterion important to the design was that the test section be of sufficient size to accommodate laser diagnostics. Because the final outcome of this design is to investigate flame propagation and emission formation kinetics, adequate optical access is essential.

Lastly, this device is, as the name implies, a bomb. It is to be used in the study of rapid combustion. As such, considerations must be taken to ensure sufficient safety by utilizing a large margin of error. This factor of safety is to be applied to all materials whose fragmentation could potentially put the laboratory occupants at risk.

Design Overview

Due to the speed at which real IC engines operate, portions of the pressure-time characteristics are very difficult to duplicate. The exponential pressure rise is caused by the conversion of chemical energy of the reactant into sensible energy of the products. This process is due to combustion and is independent of the BDCB design. The BDCB exponential pressure decay is duplicated by choking the flow

of gases across an orifice plate, thereby expelling mass and reducing pressure at the desired rate. If this method of exhausting mass were not used, a means of setting the flow of gases would have to be provided by some type of control system. As has just been mentioned, the short duration of the experiment involved here would make this almost impossible. By setting the desired moment at which the exponential decay is introduced, a pressure history is obtained which greatly resembles that of an IC engine.

The design which resulted from this consideration is illustrated on the following page (see Fig. 5). This apparatus is composed of several components which will be briefly discussed here. The test section is designed to provide the facility through which combustion diagnostics can be performed. It is in this section that the pressure emulates that of a real engine. The fuel and air mixtures to be studied are introduced into the test section through the cylinder head. This component also houses a piezoelectric pressure transducer and a spark plug, used to initiate the combustion process. The test section is separated from the exhaust port by the orifice plate. Finally, the blow-down gases are expelled from the bomb through the exhaust valve. This valve is opened by applying a pressure to the actuating piston, located in the valve body.

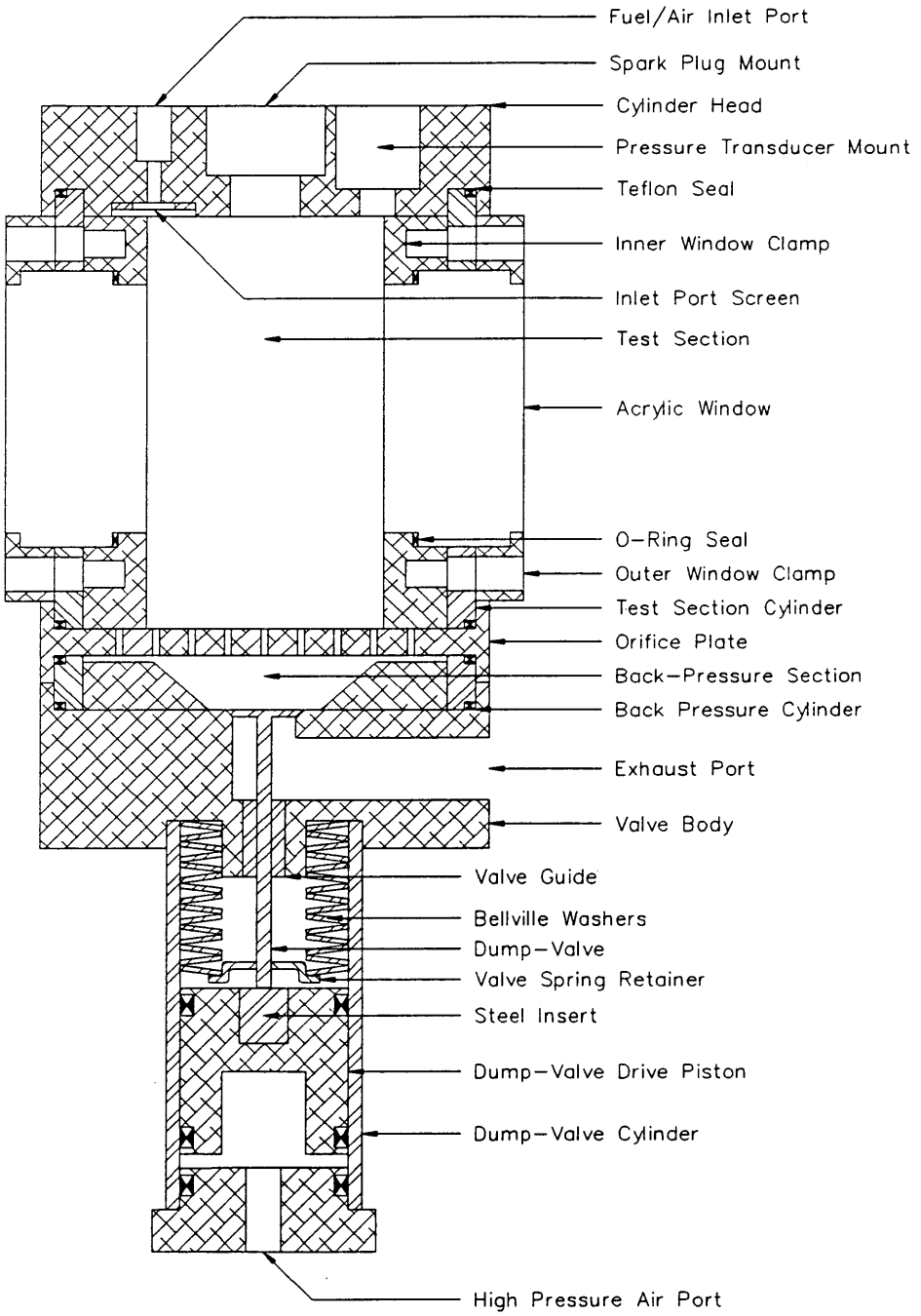

Figure 5 - Cross-sectional view of the BDCB.

Pressure Decay Design Model

The first step taken in establishing a model for the pressure fall was to determine the mathematical relationship between the cylinder pressure and the corresponding time. From Figure 2, it was apparent that this relationship , like the pressure rise, is exponential in nature. A linear regression was performed and a "best fit" curve was established. The results of this approximation and the subsequent error, are presented in Table I of Appendix A. The exponential equation for the pressure fall is of the following form:

$$P = P_o \exp^{-Ct} \tag{1}$$

The initial condition represented here is the peak pressure, as this is the starting point of the decay.

By considering the theory of isentropic flow of an ideal gas through a nozzle, as presented by Shapiro (12), a method of experimentally matching the above constant (C) was obtained. With this theory, the flow in the nozzle is said to be choked if the downstream pressure (P^*) is kept below the following limit.

$$P^* \leq P_o \left(\frac{2}{k+1}\right)^{k/(k+1)} \tag{2}$$

Because the flow is choked, the Mach number in the nozzle will be equal to unity, indicating that the velocity of the gas is sonic. In addition, once the downstream pressure has dropped below the critical value (P^*), the mass flow is solely a function of the upstream stagnation pressure as long as the differential is maintained.

With the nozzle choked, the equation governing the mass flow rate of the gases in the test section becomes;

$$\dot{m} = P\,A^* \sqrt{\frac{k}{RT_o}} \left(\frac{k+1}{2}\right)^{-(k+1)/2(k-1)} \qquad (3)$$

$$where\ \dot{m} = \frac{dm}{dt}$$

In this equation (Eqn. 3), all of the terms on the right-hand side are constant, except the pressure. This pressure is related to the mass using the ideal gas equation PV = mRT such that a differential equation is obtained.

$$\frac{dP}{P} = \frac{A^*}{V} \sqrt{kRT_o} \left(\frac{k+1}{2}\right)^{-(k+1)/2(k-1)} dt \qquad (4)$$

Once integrated, this equation yields the desired constant (C), which is equal to the terms on the right-hand side of equation (4). All of these terms are invariant and previously defined, except for the total throat area (A^*), which is now determined.

Fast-Acting Valve Design

In order for the transition between the pressure rise and decay in Figure 2 to be as small as possible, a fast-acting dump valve must be employed. This valve is responsible for expelling the gases downstream of the orifice plate, thereby bringing the back-pressure section to atmospheric pressure as rapidly as possible. It is in this manner that the critical pressure differential is obtained. From the development work done by Renault, termed "Distribution Pneumatique," it was noted that a pneumatic valve can be made to respond much more quickly than a mechanical one. This was also the direction taken by Lo Russo et al. (13) in their formulation of a gas sampling valve used in hydrocarbon emission studies. Currently, there are commercially available units that have the desired 1.5 ms response time, but at very small flow rates. They are also extremely expensive, thus prohibiting their use.

The design that the following discussion encompasses is for a valve that will open into the combustion chamber upon activation (see Fig. 5). In this manner, the cylinder pressure, acting on the valve face, will serve to enhance the seal between the valve and the seat prior to opening. The disadvantage of this type of design is that a very large

force must be applied behind the valve to overcome the sealing force. While achieving the opening force itself is not difficult, providing a restoring force is.

In this design, a spring is used to limit the travel of the valve, as its restoring force increases with deflection. If the valve were allowed to move unrestrained, the force acting on the end of the valve would cause it to move until some obstruction was encountered. This would be a very destructive means of controlling the valve motion. Additionally, this spring supplies a force that serves to enhance sealing at lower cylinder pressures.

As mentioned previously, the entire duration of the experiment is in the order of milliseconds. Because of this, any attempt to externally control the valve and its motion would be difficult, making the above configuration a realistic approach.

The valve is activated by applying air pressure to a piston that rests on the end of the valve stem. As the combustion pressure acting on the valve face serves to keep it closed, motion of the piston, which is coupled to the valve, will not be initiated until the pressure behind the piston reaches a critical value. This has the advantage of improving the response time of the valve, as any delay associated with pressure build up is eliminated.

It was decided early in the development of this design that the valve itself should be one which is used in some IC engine application. In this manner, a valve and retainer would not have to be fabricated as this is a difficult process. In addition, the economy of scale dictates that this would be a prudent choice in terms of incurred expenditures. One of the restrictions used in the selection of this valve is that it be large enough to facilitate an adequate mass flow rate. A limitation to this existed because the valve face area is directly proportional to the force acting to keep it closed. After considering many alternatives, a valve was selected which had a valve face diameter of 17.8 mm (Honda PN - 14721 ZE6 001). This results in a valve face area (A_v) of 248 mm^2 and a flow area of 228 mm^2.

The driving pressure needed to overcome the force acting on the valve face is given by the following relation.

$$P_p = P_f \frac{A_v}{A_p} \tag{5}$$

As was stated previously, P_f is the maximum pressure reached in the cylinder, which in the case of the CFR SI engine is 5090 kPa. Using a 38.1 mm diameter piston, the driving pressure must be greater than or equal to 1379 kPa.

The differential equation governing the motion of the valve then becomes:

$$m\frac{d^2x}{dt^2} + b\frac{dx}{dt} + k'x = P_pA_p \tag{6}$$

where the force on the right-hand side is the Heaviside function. The solution to this equation, as outlined by Guterman and Nitecki (14), is the following.

$$x = \frac{P_pA_p}{k'} + \exp^{-\lambda t}\,(C_1 \cos\omega t + C_2 \sin\omega t)$$

$$\text{where } \lambda = \frac{b}{2m}$$

$$\omega = \frac{\sqrt{4mk' - b^2}}{2m} \tag{7}$$

$$C_1 = \frac{-P_pA_p}{k'}$$

$$C_2 = C_1\frac{\lambda}{\omega}$$

The mass (m) was readily determined using the densities of the materials and found to be 0.10 kg. Several attempts were made to employ a conventional coil spring using the theory put forth by Deutschman et al (15). It was determined however that the stress and size requirements could not be met simultaneously. A set of 14 Bellville washers (Associated Spring PN - B1500-045) in series were used instead, giving a spring constant (k') of 124 kN/m. A value

for the friction term (b) was obtained from data presented by Taylor (11). Here, the frictional horsepower loss was plotted versus engine speed. At higher velocities, the relationship between these two terms could be approximated by a linear equation. After converting to the desired units, the friction term was estimated to be 21.2 Ns/m. With this arrangement, the valve will be completely open in 1.35 ms. To eliminate any detrimental effects of the piston compressing the air in the region of the valve springs, an exhaust hole was drilled at the base of the piston cylinder.

The maximum deflection of the dump valve is limited to 15 mm, as otherwise interference with the orifice plate would occur. As a consequence of the valve stem shape, any displacement above 5 mm will not serve to increase the mass flow rate. The valve is therefore considered to be open once this value is reached. The theoretical plot of the valve deflection due to a Heaviside function versus the time after activation is illustrated on the following page (see Fig. 6). In addition to the response resulting from the above design, other configurations are also illustrated. In this manner, the effect of varying the applied pressure, and the spring rate is shown. A wide range of response times are thereby achieved.

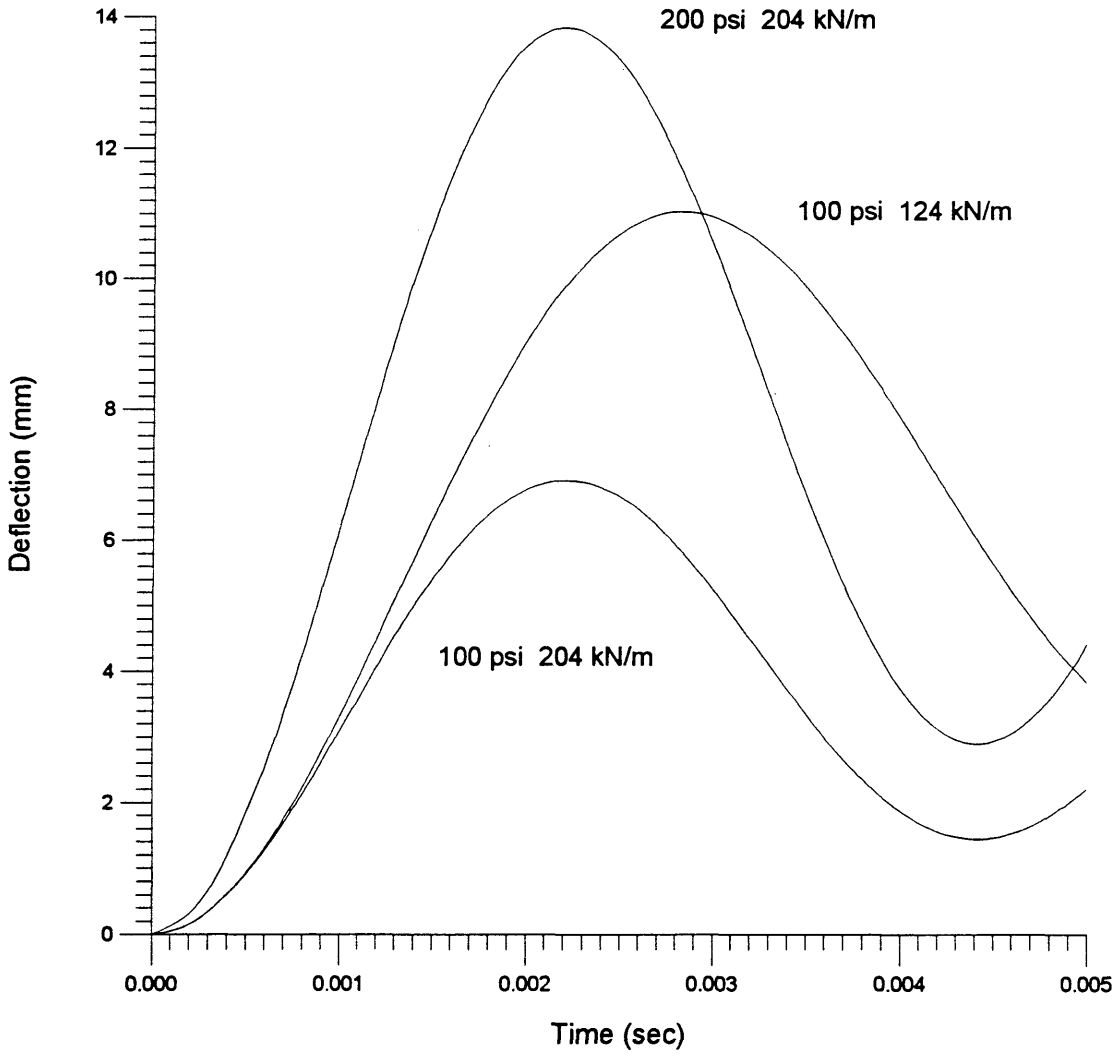

Figure 6 - Deflection of the Fast-Acting Dump Valve as a function of time for different spring rates and pressures.

BDCB Design Details

The design which resulted from the previous discussion is illustrated in Figure 5. The following paragraphs will be dedicated to some of the design details as well as material considerations.

For the pressure decay model to be valid, it was required that the total choked flow area be equal to 157 mm^2. By using several holes to make up this area, the fluid flow inside the test section will be more uniform. Additionally, these holes should be equidistant from one another such that limited flow migration occurs. The resulting orifice plate design utilizes 81 holes, 1.32 mm in diameter with one hole located at the center. The distance between the successive rings of holes is 8.9 mm with the first having 8, the second 16, the third 24 and the fourth 32. This configuration is illustrated in Drawing #2 of Appendix B. To reduce the volume in the back-pressure region down stream of the orifice plate, a disk was fabricated which is also presented in Appendix B. In limiting this volume, the time needed to blow down the back-pressure zone is greatly diminished. The only restriction placed on this design is that it not limit the exhausting of the blow-down zone. The 25.4 mm minor diameter provides a large enough

annulus that this was not a problem.

In the design of the valve actuating piston, aluminum was used so as to reduce the mass and thereby improve the response time. Initially, experiments were conducted using a 25.4 mm long piston in an attempt to keep the dynamic masses to a minimum. This proved to be an incorrect approach however as the piston was not of sufficient length to remain stable in the cylinder bore. To remedy this situation, a 38.1 mm piston was fabricated with a volume of 5.43 cm^3 removed from the actuator side of the piston (see Drawing #4 in Appendix B). Unfortunately, this void increased the valve delay from 3 ms to 17 ms as determined by experimental and computational results discussed later. Increasing the clearance volume increased the time for the drive air to be expanded and compressed. Because of this effect, hydraulic, rather than pneumatic, actuation should be employed in the future. This facility could be provided through the use of a Grainger model 7Z763 pump and 6Z628 regulator. The additional damping provided by hydraulic fluid would act only in the closing direction. This would serve to keep the valve open once actuated, eliminating the dampened oscillatory motion.

As a result of the piston being subjected to high loading exerted by the hardened steel valve, substantial

wear could occur. To alleviate this problem, a steel insert is used where the valve loading bears against the piston. This insert is installed into the aluminum using a standard interference fit.

In terms of possible structural failure, the test section is the area of greatest concern. A stress analysis was performed using a model for pressure vessels presented by Boresi and Sidebottom (16). In the case of the BDCB, the thickness to radius ratio is 0.154 which exceeds the 0.1 limit used for thin-wall analysis. As it is desired to use the BDCB for both CI and SI analyses, 8600 kPa was used for the internal pressure (P_1) in the following equations. Relative to this value, the atmospheric pressure (P_2) acting on the outside of the cylinder can be neglected. The results of this stress analysis are included following the equations.

$$\sigma_{pp} = \frac{P_1 a^2 - P_2 b^2}{b^2 - a^2} \tag{8}$$

$$\sigma_{qq} = \frac{a^2 b^2 \ (P_1 - P_2)}{r^2 \ (b^2 - a^2)} \tag{9}$$

$$\sigma_{rr} = \sigma_{pp} - \sigma_{qq} \tag{10}$$

$$\sigma_{\theta\theta} = \sigma_{pp} + \sigma_{qq} \tag{11}$$

$$\sigma_{zz} = \sigma_{pp} + \frac{P_{zz}}{\pi \ (b^2 - a^2)} \tag{12}$$

σ_{rr} = -8.6 MPa, $\sigma_{\theta\theta}$ = 51.3 MPa, σ_{zz} = 51.6 MPa

From equation (10), it should be noted that the maximum compressive stress in the radial direction (σ_{rr}) occurs at the inner fibers. The maximum circumferential stress ($\sigma_{\theta\theta}$), however, occurs where the radius (r) is the largest. The axial stress (σ_{zz}) is the result of the cylinder pressure acting on the end plates. In this analysis, the mode of failure is through yielding as the BDCB does not experience fatigue due to the small number of loadings. Using the more conservative maximum shear theory, a shear stress of 60.2 MPa is obtained. With the yield strength of structural steel being 250 MPa, this gives a safety factor of 4.15.

Additionally, one must consider the stresses sustained in the end plates and in the valve body. The cylinder pressure exerts a distributed load on the end plates, while the spring exerts a concentrated load on the valve body. Both of these conditions are addressed by Boresi and Sidebottom (16). For the end plates, the maximum principle stress is given by:

$$\sigma_{max} = \frac{3P_1a^2}{4A_{bore}h^2} \tag{13}$$

which gives rise to a maximum stress of 33.1 MPa. As the thickness (h) of the plate in this case is 6.35 mm, the

resulting safety factor is 8.3. For the valve body, the maximum stress occurs at the inside diameter of the Bellville washer, which is 19 mm. This gives an outer to inner diameter ratio of 44.5/19 = 2.33. The constant of proportionality that the authors present for this condition is 0.527. The maximum stress then becomes;

$$\sigma_{max} = 0.527 \frac{P_p A_p a^2}{h^2} \tag{14}$$

and results in a stress of 28.3 MPa with a safety factor of 10.1.

The design of the optical windows proved to be a more rigorous undertaking. As with preliminary tests of the BDCB itself, a means of containing gases at such high pressure evaded solution. To seal the cylinders that make up the BDCB, teflon hydraulic rings were used (PN 55000-60-152) with good results. A circular seal could not be used on the windows however as they are necessarily rectangular in shape. Instead, rubber O rings were employed and distorted into the desired shape. The windows were then placed between an inner and an outer clamp to maintain the sealing force necessary to prevent the expulsion of gases. These clamps, as well as the machining details for the windows, are illustrated in Appendix B. While this configuration does

reduce the volume in the test zone of the BDCB, it is manufactured so as to present a smooth, uninterrupted surface to the flame front.

Initially, Lex-gard (polycarbonate) was used for the windows because of its high yield strength. Unfortunately, it did not withstand the thermal gradient encountered inside the BDCB and its inner surface became crazed. Acrylic was then employed with a yield strength of 38 MPa. It is worth noting that, for the yield strengths of these materials, a solution would not converge with any degree of safety for cylindrically shaped windows. Using a uniformly loaded, flat-plate analysis with all edges fixed as presented by Westergaard (17), the maximum bending moment was found to occur at the outer edge of the window, in the middle of the long side. The bending moment per unit width is then given by

$$\mathbf{M} = \frac{P\, w^2}{12\ (1 + e^4)} \tag{15}$$

where e is the ratio of width (w) to length. The stress is then a function of window thickness which determines the desired dimension.

$$\sigma = \frac{6\ \mathbf{M}}{h^2} \tag{16}$$

Using the above stated yield strength and a window thickness of 31.75 mm, the maximum shear stress criterion for failure gives a safety factor of 3.45. Should sufficient funds become available in the future, Sapphire could be substituted in place of the acrylic windows. The advantage of such a substitution is a greater transparency to laser radiation as well as increased strength. With an ultimate strength of 338 MPa, Sapphire windows would need to be only 10.6 mm thick for the same factor of safety. Because Sapphire cannot be easily machined, the flat inner surface would have to be sacrificed in order to use this material.

One last remaining concern is the introduction of combustible gases into the BDCB. As has been previously stated indirectly, it is the purpose of this design to eliminate any spurious flame fronts which would adversely affect the experiment. The lines running from the gas cylinders to the BDCB therefore pose a problem both from the standpoint of forming a second flame front as well as introducing a serious safety risk. If the flame were allowed to travel up the fuel/air line, there is a chance that the resulting pressure rise could cause a rupture. One way to solve this problem is to use poppet valves in the cylinder head to introduce gases into the test section. Unfortunately, this in itself can be detrimental as there

will always be a small but measurable leakage associated with these valves. In addition, it would be exceedingly difficult to facilitate these devices in the cylinder head without altering its shape. Typically, cylinder heads of this design use a hemispherical combustion chamber to provide the space needed. Again, this results in a flame front which would differ significantly from that which is desired in this experiment.

The solution approach that was taken was to use a fundamental property of flame propagation, namely the quenching distance. This distance is defined to be the largest dimension that will just stop a flame from propagating. The problem in determining this distance is that it is dependent upon the air-fuel ratio, the length of the carbon chain in the fuel and the absolute pressure in the flame. Based on experimental data by Lewis and von Elbe (18), it has been shown that while heptane requires the smallest quenching distance for a given pressure, it varies only slightly from propane. Subsequent analysis is therefore directed toward propane due to the large amount of available data. This analysis is further simplified by considering only the oxygen-nitrogen ratio found in air, namely 21%. Because the BDCB is designed to operate to a maximum pressure of 5090 kPa, the minimum quenching distance was

found to be 0.185 mm as indicated in the following plot (see Fig. 7). This plot can also be used to determine the appropriate spacing for the spark plug gap. With a fill pressure of 862 kPa, propane would require a minimum spark plug gap size of 0.65 mm.

Initially, experiments were conducted using a single hole drilled with a #80 drill bit in order that the flame front be prevented from travelling up the line. This proved ineffective as a solution because a great deal of time was needed to fill the BDCB to the desired pressures. Even with a leak down of 0.2%, a large quantity of gases were expelled during this time. Additionally, this small hole would frequently become blocked by soot particles, making it necessary to disassemble the BDCB. This situation was corrected by using a stainless steel screen whose mesh was smaller than the quenching distance (0.04 mm). In this manner, several small openings allowed the gases to enter the BDCB and the fill time was significantly improved with no further blockage. A detrimental effect did result from this approach, however, caused by the heating of the stainless steel screen during combustion. Once the BDCB is exhausted down to the fill pressure, the methane-air mixture in the fill line is allowed to escape back into the test section unimpeded by the stainless steel screen. With the

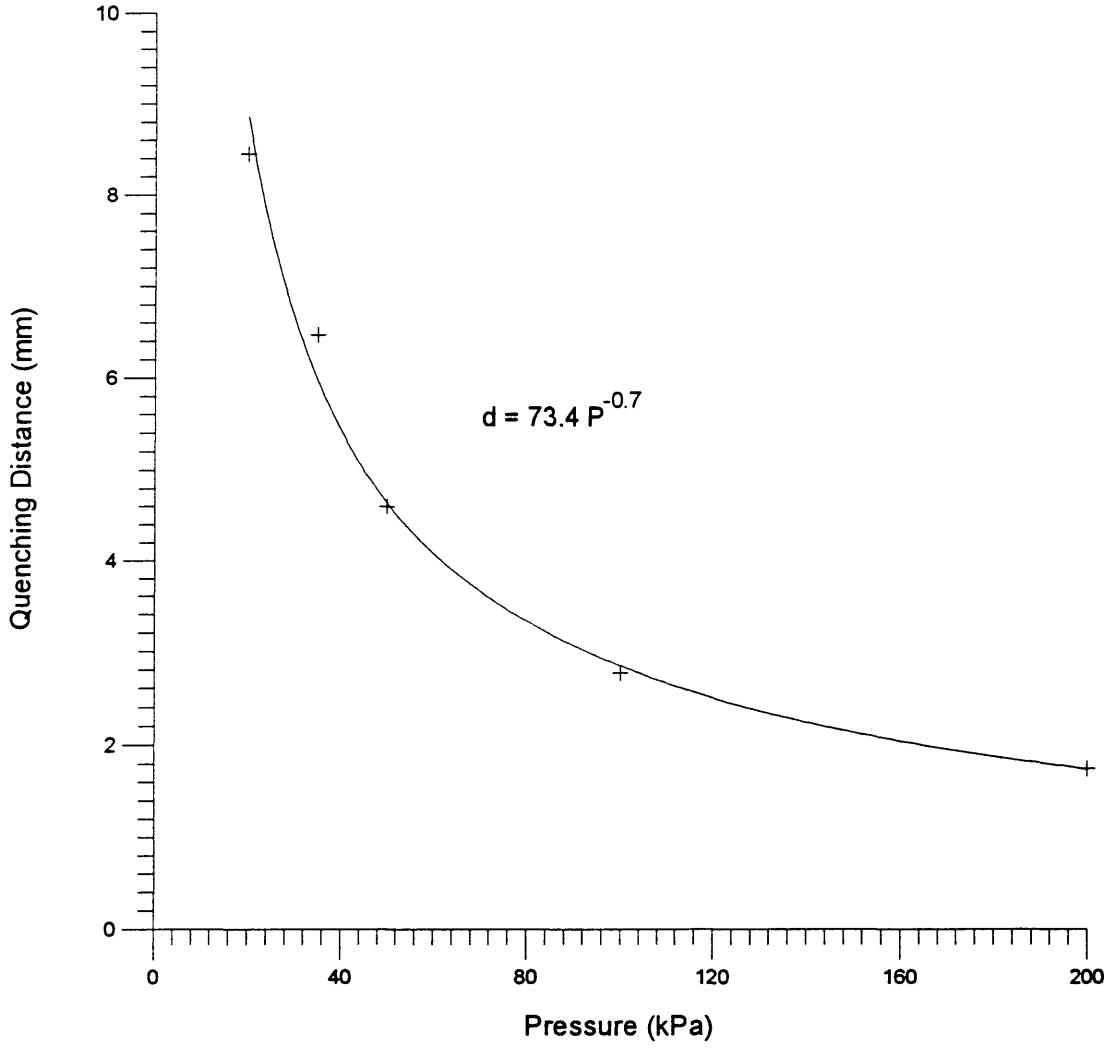

Figure 7 - Quenching distance as a function of pressure for propane.

screen sufficiently heated, these gases were then combusted causing a secondary pressure rise.

INSTRUMENTATION AND CONTROL

One of the desirable features of this apparatus is the simplicity through which it operates. As a result, flexibility and cost effectiveness were easily obtained. There are four instrumentation and control components used in performing an experiment: charging of the BDCB, combustion initiation, pressure data acquisition, and blow-down valve control.

It should be pointed out here that the opening of the fast-acting valve is triggered by a threshold pressure comparator, unless this system has failed to function correctly during the experiment. The reason that this is preferred to firing the valve at a fixed time delay after ignition has to do with the extremely large derivative values for pressure with respect to time. Experimentation has shown that variations in these values can be as much as 4.87 MPa/s. This condition is seen in real IC engine operation as well (see Fig. 3). If the control system were time dependent, large fluctuations in peak pressure would occur, as illustrated in Figure 8. These two pressure traces were obtained using the Helios digital-to-analog converter as a time-based control for the blow-down valve. The large

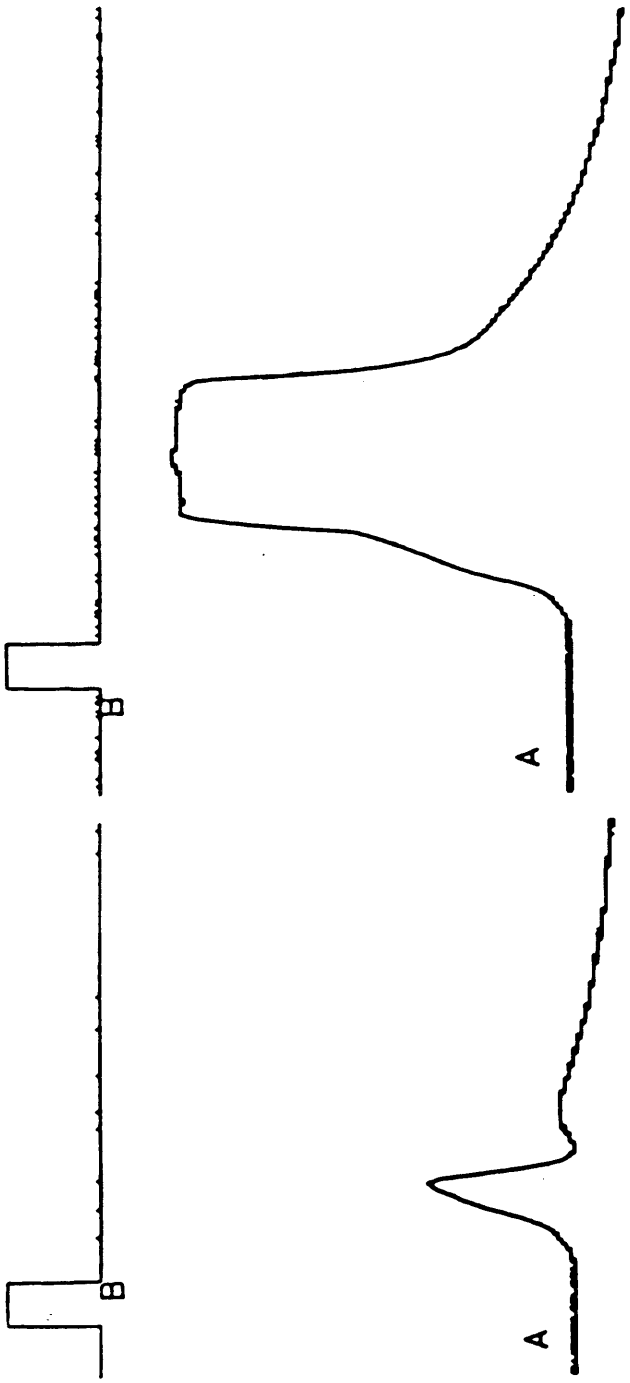

Figure 8 - Two pressure traces using the BDCB and Helios time-based control.

variation seen here is the result of a single time-step difference in the opening of the valve. As reproducibility was a key criterion in the BDCB design, this type of variation must be limited. Employing the pressure-based control system minimizes this behavior.

In contrast, the evacuation and filling processes prior to ignition required time-based control. These procedures require a great deal of time and the fill pressures are quite low, necessitating the use of a diaphragm type pressure transducer should pressure-based control be employed. Unfortunately, the experimental pressures are sufficient to cause the destruction of this type of device. Additionally, the fill rates are small enough that time-based control produces excellent results.

Pressure Data Acquisition

The first component of instrumentation to be discussed in detail is the acquisition of data relating the cylinder pressure to the representative time domain. This is achieved using a PCB model 111A22 piezoelectric pressure transducer along with the PCB model 482A single-channel/line power supply. The rise time of the transducer is 1 microsecond

which, for the purposes of the BDCB, yields a very favorable time resolution. One advantage in the above configuration is that a MOSFET IC amplifier is contained within the transducer, eliminating the need for a charge amplifier. Because of this, the expenditures incurred were about half that of a standard piezoelectric transducer. The output of the line power supply is equipped with a BNC coaxial connector to facilitate hook up with the Phillips PM3335/40 digital storage oscilloscope that is used to record the pressure trace. This voltage signal, which is proportional to pressure (1 psi = 1 mV), is also used to trigger the opening of the blow-down valve. Once the power supply is activated, the transducer must be allowed to stabilize for approximately one minute to ensure charging of the internal capacitor. With the transducer installed into the cylinder head, a vinyl coating is placed over its end to minimize spurious signals generated by thermal effects.

Automated Charging of Fuel and Air

The second component of control involves the automated introduction of gases into the BDCB. The purpose of this is to simplify the performance of the experiment and to reduce

the erroneous variation of experimental parameters. It also serves to significantly decrease the time required to complete experiments. To aid in interpreting the remaining discussions, Figure 9 has been included on the following page. Through the use of the program BDCB.BAS (see Appendix C), a personal computer is used to initiate +10 V, 20 mA output signals from a Helios digital-to-analog converter. For each channel activated, there is a corresponding solid-state relay (Potter and Brumfield PN SSRT-120D10) which in turn opens one of the Atkomatic stainless steel solenoids. Two high-pressure (1100 psi) and two low-pressure (250 psi) solenoid valves are used, each having a response time of 8 to 12 milliseconds.

Prior to charging the BDCB with a combustible mixture, it is evacuated using a mechanical vacuum pump. In this manner, the majority of the residual gases from a prior experiment are depleted. One of the high-pressure valves is used here, as the back side of the valve is directly exposed to the cylinder pressure. With the BDCB sufficiently evacuated, the vacuum valve is closed and the second high-pressure valve opened. This valve is in series with both the fuel and air valves as a second line of defense preventing a flame from propagating up the lines to the regulators. The valve controlling fuel flow is now opened and will remain so

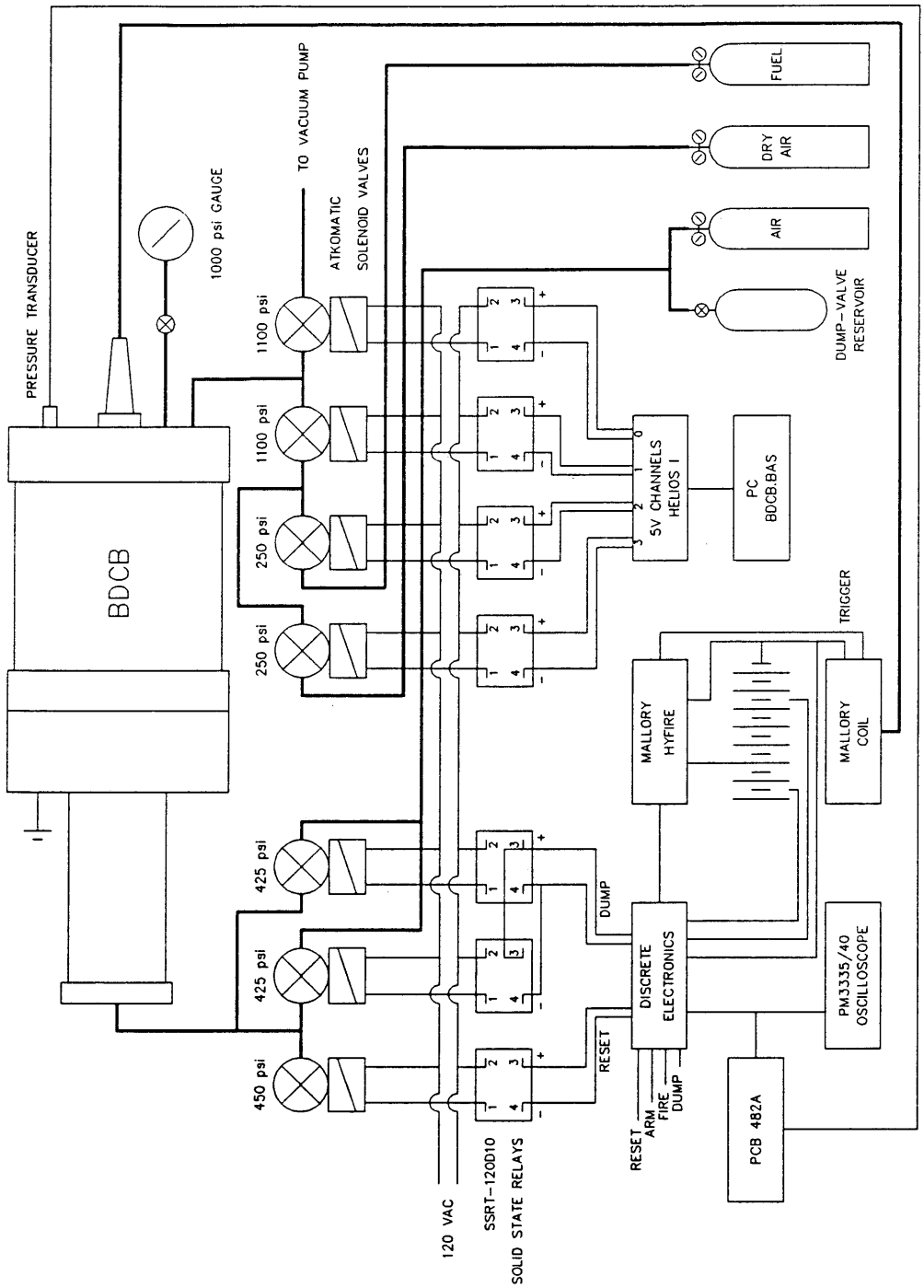

Figure 9 - Schematic of experimental layout for the BDCB.

until the desired fuel pressure is achieved. The fuel valve is then closed and the air valve opened. Again, this valve will remain open for a predetermined period of time necessary for the desired fill pressure to be achieved, as set by the regulators. Specification of these times is prompted in the driver program BDCB.BAS. In addition, the filling pressures were checked with a Wallace and Teirnan pressure gauge and found to be consistent. With the BDCB filled to the desired pressures of fuel and air, the air and high-pressure valves are now closed and the experiment is ready to commence. The operator is then prompted to "fire immediately," indicating ignition can now occur.

Ignition Initiation

The next aspect of instrumentation to be discussed is the initiation of the combustion process using a standard automotive spark plug. After several different combinations of spark plug and ignition systems were tried, the most successful seems to be the Bosch platinum spark plug used in conjunction with a Mallory Promaster Coil (PN 29440) and Mallory Hyfire (PN 29026). The purpose of the Hyfire is to further increase the output energy of the coil to an

advertized value of 150 mJ. Power for the coil and the Hyfire are provided from a 12 VDC battery. While such an intense spark is beneficial in initiating combustion, it produced unwanted RF emissions. Extensive shielding was necessary to prevent sporadic triggering of the blow-down valve. Opticouplers were employed to isolate the output signals from the output components.

As this ignition system was derived from automotive applications, its behavior deviated from that which is desired for digital control. Because an ignition spark occurs when the contacts to the primary coil are broken, the ignition control system must first be armed before a discharge can occur. In addition, no more than two seconds can pass before firing once the ignition system has been armed or a misfire will occur. This is due to the capacitive nature of the ignition system.

Blow-Down Valve Control

The fourth control system is used to trigger the opening of the blow-down valve and trigger the shutter release of an electronically controlled 35 mm camera. A block diagram is included with this discussion on the

following page to illustrate this system (see Fig. 10). If the exhaust valve were not to open, the cylinder pressure would be allowed to increase unchecked. To prevent this, several fail-safe mechanisms were employed.

Once the ignition system has been fired, the blow-down valve control system proceeds with two distinct paths. The first is a comparative analysis of the voltage input from the line power supply (cylinder pressure) whose output is given a gain of 10 by the comparator. Using an 8-pin dip switch and a toggle switch, the threshold and over-pressure generators can be set from 0 to 1990 psi in 10 psi increments. The toggle switch is used to add either 0 or 1000 psi to the dip-switch value. The 339 quad comparator will compare the output from the line power supply to that of the threshold and over-pressure generators. Once the BDCB pressure first exceeds the output from either of these circuits, the comparator will latch a flip-flop high and trigger the opening of the blow-down valve.

The desired triggering of the blow-down valve occurs in the threshold-pressure circuit. To increase the flexibility of this system, a threshold-pressure delay is also incorporated which will delay the opening of the valve from 0 to 90 ms in 10 ms increments, using two 4-pin dip switches. Should this pressure control circuit fail to open

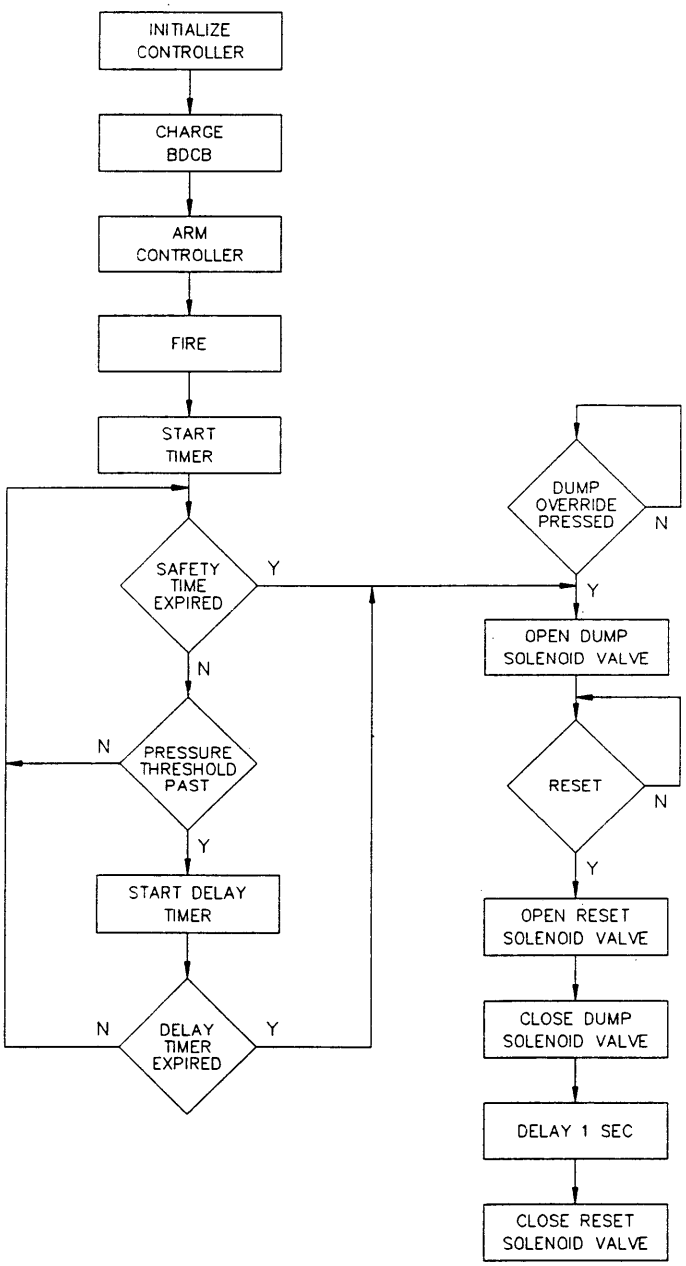

Figure 10 - Block diagram of Fast-Acting, Dump-Valve control system.

the valve, an excessive build up of pressure will result.

The second path taken by the control system involves the opening of the valve based on the time elapsed from the firing of the ignition. This duration limit can be set from 0 to 1990 ms in 10 ms increments in the same manner as the threshold- and over-pressure generators. This is then another fail safe which the system employs. The master time clock also drives the trigger system used to activate the camera shutter release using a TLC555 timer to deliver a 1 kHz square wave. The delay from the ignition time can be set from 0 to 1999 ms in 1 ms increments, again using three 4-pin dip switches and toggle switch. Once this time has elapsed, the I/O contacts of a MM54HC4066 quad analog switch will close and the cameras shutter will be activated.

To open the blow-down valve, the control system provides a 5 V, 20 mA output signal which trips a solid-state relay. This in turn activates two 425 psi Atkomatic solenoids which are connected to a compressed-air cylinder with the regulator set to the desired pressure to achieve a particular valve response. Two solenoids are used to increase the flow rate and to ensure that the valve opens should there be a solenoid failure. To reduce any variation in air pressure delivery due to the regulator, a 25 lbm propane cylinder is used as a pressure reservoir.

Once the dump valve has been opened by either the threshold pressure or the over pressure or the time delay, it must be closed so that another experiment can be performed. By depressing the reset on the control system, the two solenoids are closed and another 425 psi Atkomatic valve is opened to exhaust the air from the back side of the actuating valve. The circuits used here are illustrated in Appendix B.

ZERO-DIMENSIONAL, TWO-ZONE MODEL FOR THE BLOW-DOWN COMBUSTION BOMB

In order to analyze the pressure data obtained using the BDCB, a two-zone thermodynamic model was employed. It is therefore considered to be diagnostic, rather than predictive, in nature. This type of analysis has gained great favor in the combustion community and is used extensively for evaluating engine pressure traces. If the burning rate were to be irregular or if a discrepancy existed between the fuel chemical energy and the total energy released, a fault in the pressure data may be present. Thus a first law analysis provides a means of ascertaining the validity of a particular experiment as well as supplying the temperature-time curves necessary for kinetic studies.

With this type of model, spatial relations are ignored in favor of separate control volumes for burned and unburned constituents. As the BDCB was designed to reduce the effects of fluid mechanics, it seems reasonable to select a form of analysis which is limited in its use of spatial relations. The use of such a model yields a great deal of valuable information. In addition to giving information about

temperature, volume and mass of both burned and unburned components, concentrations of each of the major product species can be estimated.

Employing this type of analysis requires that certain assumptions be made. The reason for this is that the burned and unburned regions must be considered to be unique but homogeneous within themselves. The burned gas is taken to be in thermodynamic equilibrium at any instant in time consisting of an evenly distributed mixture of combustion products. Temperature gradients are therefore excluded. The unburned region presents a much simpler case as the reactants are a quiescent mixture of gases whose equilibrium depends only on the fuel-air ratio, independent of pressure. The flame front which divides the burned and unburned control volumes is taken to be infinitesimally thin, and it is assumed that heat transfer occurs only between the burned gas region and the walls of the BDCB contacting that zone.

Knowing the temperature for each zone, and having a pressure common to both, allows one to determine the thermodynamic properties for each using REAC and PER subroutines, developed by the author and by Olikara and Borman (10) respectively. As the thermochemical properties for hydrocarbons in the JANAF data tables were limited to methane when this work was done, the subroutine REAC is

similarly constrained. PER employs a shifting equilibrium for the products consisting of H, O, N, H_2, OH, CO, NO, O_2, H_2O, CO_2, N_2, and Ar. Following these assumptions and having knowledge of the characteristics of the BDCB, a model was derived which is similar to that developed by Foster (19).

The experimental pressure traces used in developing this model were for reactant mixtures of methane and air, taken to behave as perfect gases. As it was already assumed that no heat transfer occurs between the unburned gas and the system boundary, compression is taken to be isentropic. Because the unburned gases are at the same initial temperature as the BDCB and their temperatures remain low, this assumption is justified. Using the experimental pressure curve gives the reactant temperature as

$$T_u = T_o \left(\frac{P}{P_o} \right)^{(k-1)/k} \tag{17}$$

where the subscript u denotes the unburned region. Similarly, the temperature of the adiabatic core T_{ac} of the burned gas can be determined in this manner with its initial temperature being the adiabatic flame temperature, defined as the temperature where the reactants and products have equal enthalpy. The resulting core temperatures provide a means of determining the heat transfer between the burned

gas and the walls of the BDCB.

The heat flux takes place across a thermal boundary layer whose thickness (δ) is time dependent and will reach an estimated maximum of about 2 mm (20). This time dependence varies according to the nature of the flame, be it laminar or turbulent. In the BDCB the mixture is quiescent which gives a burning velocity roughly equal to that of the laminar flame speed and the turbulence intensity approaches zero (21). As a result, the thermal boundary layer will grow as $t^{1/2}$. The laminar flame speed is dependent upon mixture ratios, fuel molecular structure, pressure and temperature of the unburned gas. Following the assumption that R_u is constant and extrapolating data obtained from spherical combustion bomb studies (22), an equation was obtained for the laminar flame speed of methane in cm/s.

$$S_L = [36 - 130\ (\phi - 1)^2] \left(\frac{P T_o}{P_o T_u}\right)^{0.19} \qquad (18)$$

In this case, T_o and P_o refer to the standard temperature and pressure. Knowledge of the flame speed is necessary for determining the wetted area, or the area through which the burned gas transfers its heat to the wall. This represents the only deviation from zero-dimensional analysis used in the model.

The heat flux through the boundary layer is given by

$$\dot{q} = \frac{k_e \ (T_{ac} - T_w)}{\delta} \qquad (19)$$

where k_e is the effective thermal conductivity evaluated at the mean temperature of the adiabatic core and the BDCB wall.

For polyatomic gases, Eucken proposed an empirical correlation for the thermal conductivity based on the assumption that rotational and vibrational energies are less than translational energies.

$$k_e = \frac{\mu \ (9C_p - 5C_v)}{4} \qquad (20)$$

The specific heats are those of the products. The viscosity is obtained using the following equation, taken from Mansouri and Heywood (23), and NASA.

$$\mu = \frac{3.3\times10^{-7} \ T^{0.7}}{1 + 0.27\phi} \qquad (kg/m\ s) \qquad (21)$$

The heat-transfer rate is the product of the heat flux and the wetted area. It is assumed for this analysis that the flame front propagates in a spherical manner, constrained by the cylinder head. Prior to reaching the

cylinder wall, the wetted area is the circular portion of the hemispherical flame defined by the burned gas radius. This radius is geometrically related to the burned gas volume which, in turn can be equated to the wetted area by

$$A_w = \pi^{1/3} \left(\frac{3 V_b}{2} \right)^{2/3} \tag{22}$$

Upon reaching the cylinder wall, the wetted area will be that of the head plus the area encountered by the flame as it proceeds down the wall.

$$A_w = \frac{\pi B^2}{4} + B S_L . t \tag{23}$$

If the reactants are entirely consumed, the wetted area is then the area encompassed by the inside dimensions of the BDCB.

In order for the above equation (22) to be solved, knowledge of the burned volume is necessary. This is obtained by applying the first law of thermodynamics in its time-dependent form to the burned-gas region.

$$\frac{d(mu)_b}{dt} = -P \frac{dV_b}{dt} + \dot{Q}_b + \sum_i \dot{m}_i h_i \tag{24}$$

The use of this equation, as applied to the BDCB, is

illustrated in Figure 11 on the page following. The first term represents the rate at which total internal energy is changed within the burned gas control volume. The sum of the mass flow rate into the region is the conversion rate of reactants into products, or dm_b/dt. The enthalpy is then that of the stagnation absolute enthalpy of the unburned gas h_u. This gives

$$(u_b - h_u)\ \frac{dm_b}{dt} + m_b\ \frac{du_b}{dt} = -P\ \frac{dV_b}{dt} + \dot{Q}_b \qquad (25)$$

Considering the internal energy to be the sum of chemical and sensible energies and constraining the mixture to be in equilibrium means that the internal energy can be expressed as a function of temperature, pressure and fuel/air equivalence ratio. In the case of the BDCB however, no fuel is added once combustion begins, as would be the case for direct fuel injection. The internal energy can then be expressed as the following rate equation.

$$\frac{du_b}{dt} = \frac{\partial u_b}{\partial T_b}\frac{dT_b}{dt} + \frac{\partial u_b}{\partial P}\frac{dP}{dt} \qquad (26)$$

The pressure change rate is determined by applying the Lagrange's five point formula for numerical differentiation (24). The partial derivatives $\partial u/\partial T$ and $\partial u/\partial P$ are readily

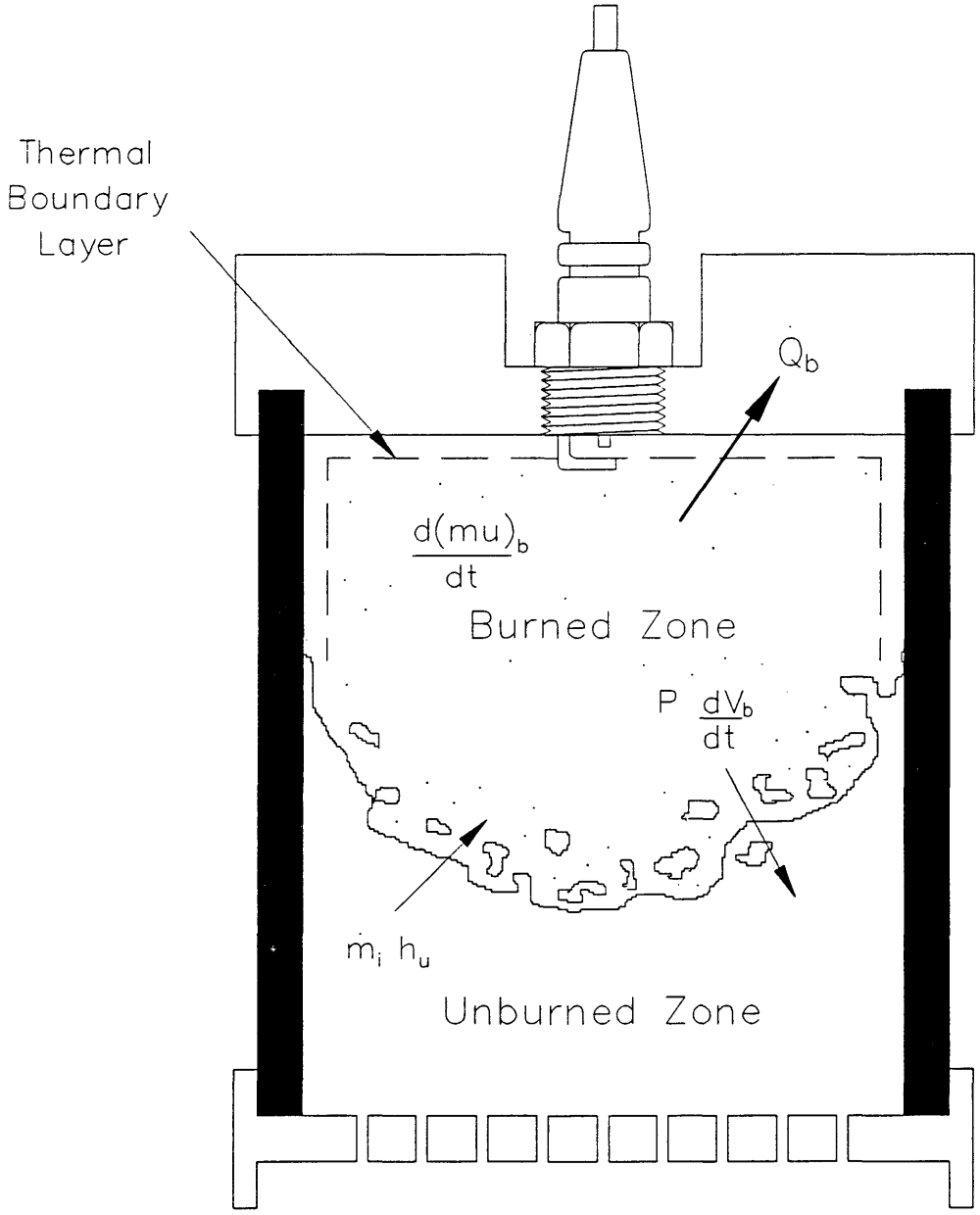

Figure 11 - Illustration of a two-zone thermodynamic model applied to the BDCB.

obtained using the equilibrium subroutine PER. This leaves only the burned-gas temperature change rate as an unknown in the above equation (Eqn. 26). Writing the ideal gas law PV = mRT as a rate equation for the burned-gas control volume

$$\frac{1}{P}\frac{dP}{dt} + \frac{1}{V_b}\frac{dV_b}{dt} = \frac{1}{m_b}\frac{dm_b}{dt} + \frac{1}{R_b}\frac{dR_b}{dt} + \frac{1}{T_b}\frac{dT_b}{dt} \tag{27}$$

allows us to solve for the burned-gas temperature. Just as with the internal energy, the specific gas constant can be expressed as a function of temperature and pressure.

$$\frac{dR_b}{dt} = \frac{\partial R_b}{\partial T_b}\frac{dT_b}{dt} + \frac{\partial R_b}{\partial P}\frac{dP}{dt} \tag{28}$$

Thus, the expression for the burned-gas temperature becomes

$$\frac{dT_b}{dt} = \frac{1}{\alpha}\left(\frac{1}{P}\frac{dP}{dt} + \frac{1}{V_b}\frac{dV_b}{dt} - \frac{1}{m_b}\frac{dm_b}{dt} - \frac{1}{R_b}\frac{\partial R_b}{\partial P}\frac{dP}{dt}\right) \tag{29}$$

$$where\ \alpha = \left(\frac{1}{T_b} + \frac{1}{R_b}\frac{\partial R_b}{\partial T_b}\right)$$

After rearranging terms in the first law analysis (Eqn. 25), we get the following rate equation.

$$\frac{dm_b}{dt}\,(u_b + h_u - \beta) - \dot{Q}_b = - \frac{dP}{dt}\left(\beta\frac{m_b}{P} + m_b\frac{\partial u_b}{\partial P} - \beta\frac{m_b}{R_b}\frac{\partial R_b}{\partial P}\right) - \frac{dV_b}{dt}\left(\beta\frac{m_b}{V_b} + P\right) \tag{30}$$

$$where\ \beta = \frac{1}{\alpha}\frac{\partial u_b}{\partial T_b}$$

Knowing that the total volume is the sum of the unburned and burned volumes and that the total volume is constant, we can relate the two rates by

$$\frac{dV_b}{dt} = -\frac{dV_u}{dt} \tag{31}$$

Employing the ideal gas rate equation to the unburned volume and then making the above substitution provides a means of obtaining the burned-gas volume in terms of the unburned gas variables. The rate of change of the specific gas constant in the unburned region can be excluded as there is no dissociation.

$$\frac{dV_b}{dt} = V_u\left(\frac{1}{P}\frac{dP}{dt} - \frac{1}{T_u}\frac{dT_u}{dt} - \frac{1}{m_u}\frac{dm_u}{dt}\right) \tag{32}$$

Prior to the BDCB exhaust valve opening, a mass balance yields

$$\frac{dm_u}{dt} = -\frac{dm_b}{dt} \tag{33}$$

After the valve opens, the loss of mass in the unburned zone

is due to the conversion of reactants into products as well as that mass which is expelled out of the exhaust valve.

$$\frac{dm_u}{dt} = - \frac{dm_b}{dt} - \dot{m}_o \tag{34}$$

This situation implies that not all of the reactants have been consumed and therefore the mass flow rate out of the blow-down valve is dependent upon the temperature, the specific heats, and specific gas constant of the unburned mixture. These gases will be expelled very rapidly, as the speed of sound for the reactants is much slower than those of the products owing to the their lower temperature. For the condition of choked flow, the mass flow rate is inversely proportional to the speed of sound (see Eqn. 3). Once expelled, all of the remaining mass inside the BDCB is products and their mass rate of change is just that of the new, slower mass flow rate out of the valve.

$$\frac{dm_b}{dt} = - \dot{m}_o \tag{35}$$

If all of the reactants are consumed prior to the valve opening, then the burned mass is fixed until the blow-down phase. Its mass will then be reduced at the rate just cited. In conclusion of this discussion, the mass burning rate can

be expressed as follows.

$$\frac{dm_b}{dt}\left[u_b - u_u + \gamma\left(R_u T_u - R_b T_b\right)\right] =$$

$$\left(m_u R_u \frac{dT_u}{dt} - \dot{m}_o R_u T_u\right)(1 + \gamma) - \dot{Q}_b \qquad (36)$$

$$- \frac{dP}{dt}\left(\gamma V + V_u + m_b \frac{\partial u_b}{\partial P} - \gamma m_b T_b \frac{\partial R_b}{\partial P}\right)$$

$$\text{where } \gamma = \frac{\beta}{R_b T_b}$$

In the above equation (36), the heat transfer rate is taken to be negative as the heat transfer is from the burned-gas control volume to the BDCB wall. Prior to the opening of the blow-down valve, the mass flow rate term is zero and the increase in burned gas mass is by combustion. A complete derivation of this equation (Eqn. 36) is included in Appendix E.

With the equations for the rate of change of mass and volume (Eqns. 36 and 32), as well as their initial values in hand, the Modified Euler method (25) is employed in order that the ideal gas equation may be applied to the burned-gas region. In this manner, an estimate is made such that the thermochemical properties of the following time step are more accurately predicted. Knowing the burned mass m_n and volume V_n at time t_n and employing the previously derived

differential equations, the subroutine PER is called at T_n, P_n, and F.

$$m_{n+1} = m_n + \left(\frac{dm}{dt}\right)_n (t_{n+1} - t_n) \tag{37}$$

$$V_{n+1} = V_n + \left(\frac{dV}{dt}\right)_n (t_{n+1} - t_n) \tag{38}$$

The subroutine is then called at T_n, P_{n+1}, and F with the n+1 derivative values for pressure and temperature being utilized to give the second point estimate for the rate of change in mass and volume.

$$m_{n+1} = m_n + \left[\left(\frac{dm}{dt}\right)_n + \left(\frac{dm}{dt}\right)_{n+1}\right] \frac{t_{n+1} - t_n}{2} \tag{39}$$

$$V_{n+1} = V_n + \left[\left(\frac{dV}{dt}\right)_n + \left(\frac{dV}{dt}\right)_{n+1}\right] \frac{t_{n+1} - t_n}{2} \tag{40}$$

During the blow-down phase after all of the unburned gas has been expelled, the burned volume remains fixed at the BDCB total volume. In addition, mass is no longer convected into the burned-gas control volume and instead is only exhausted. The first law rate equation is then greatly simplified giving

$$m_b \left(\frac{\partial u_b}{\partial T_b} \frac{dT_b}{dt} + \frac{\partial u_b}{\partial P} \frac{dP}{dt}\right) = \dot{Q}_b + \sum_i \dot{m}_i h_i \tag{41}$$

Solving for the burned-gas temperature and using the enthalpy of the products yields

$$\frac{dT_b}{dt} = \left(- \dot{Q}_b - \dot{m}_o h_b - m_b \frac{\partial u_b}{\partial P} \frac{dP}{dt} \right) \left(m_b \frac{\partial u_b}{\partial T_b} \right)^{-1} \qquad (42)$$

Again the heat transfer is taken to be from the burned region to the BDCB. The program which was developed using this model is included in Appendix C. Instructions on usage are included on the comment lines.

The above model deviates from that presented by Foster as the result of the unique design of the BDCB. As has been previously mentioned, the BDCB only emulates the combustion and expansion processes found in real IC engines and does so in a manner quite different from these devices. Instead of being able to use one first law equation for both processes, two are used. The first concerns itself with conditions prior to the blow-down valve opening and a second unique equation is used once this has occurred. Due to the lack of piston motion, no mechanical work is extracted from this device. Instead, flow work is considered as the gases are exhausted out of the combustion chamber. Because values for the specific gas constant are so readily available using PER, no assumptions were made concerning the effects of dissociation and temperature change. Foster assumed these

effects to be negligible and it turns out that this is a valid assumption for most cases.

Having no previously developed model for the BDCB to use as a reference, variable volume models were developed in an attempt to duplicate other results and validate the approach. As an example, a program is included in Appendix C which yields temperature, mass and volume information for both reactants and products in a SI engine. The pressure trace used to drive this model is the one represented by Figure 3. The temperature-time curve resulting from this program is graphically illustrated in Appendix D.

EXPERIMENTAL AND COMPUTATIONAL RESULTS

Initial tests performed on the BDCB were designed to determine the validity of the pressure-decay model. With the pressure transducer, the line power supply, and the digital oscilloscope connected, the BDCB and the blow-down valve were charged with 698 kPa dry air. This was the upper limit of available pressure as this is the maximum setting on the Matheson 3122-590 regulator. The results of a typical test are illustrated on the following page (see Fig. 12). Included on the graph is the curve derived from calculations using Eqn. 4. From this graph it can be seen that the valve delay is 3 to 4 ms, 1 ms greater than theory predicted. Also, the delay associated with the solenoid valves was found to be 10 ms. This is in agreement with the manufacturer of the valves who states the valve delay to be 8-12 ms.

Satisfied with the results of the initial blow-down tests, the next phase of experimentation was to test the BDCB behavior under combustion conditions. With the acquisition of a high-pressure regulator (5200 kPa), the blow-down valve could now be driven at its design pressure (1723 kPa). The apparatus was set up as illustrated in

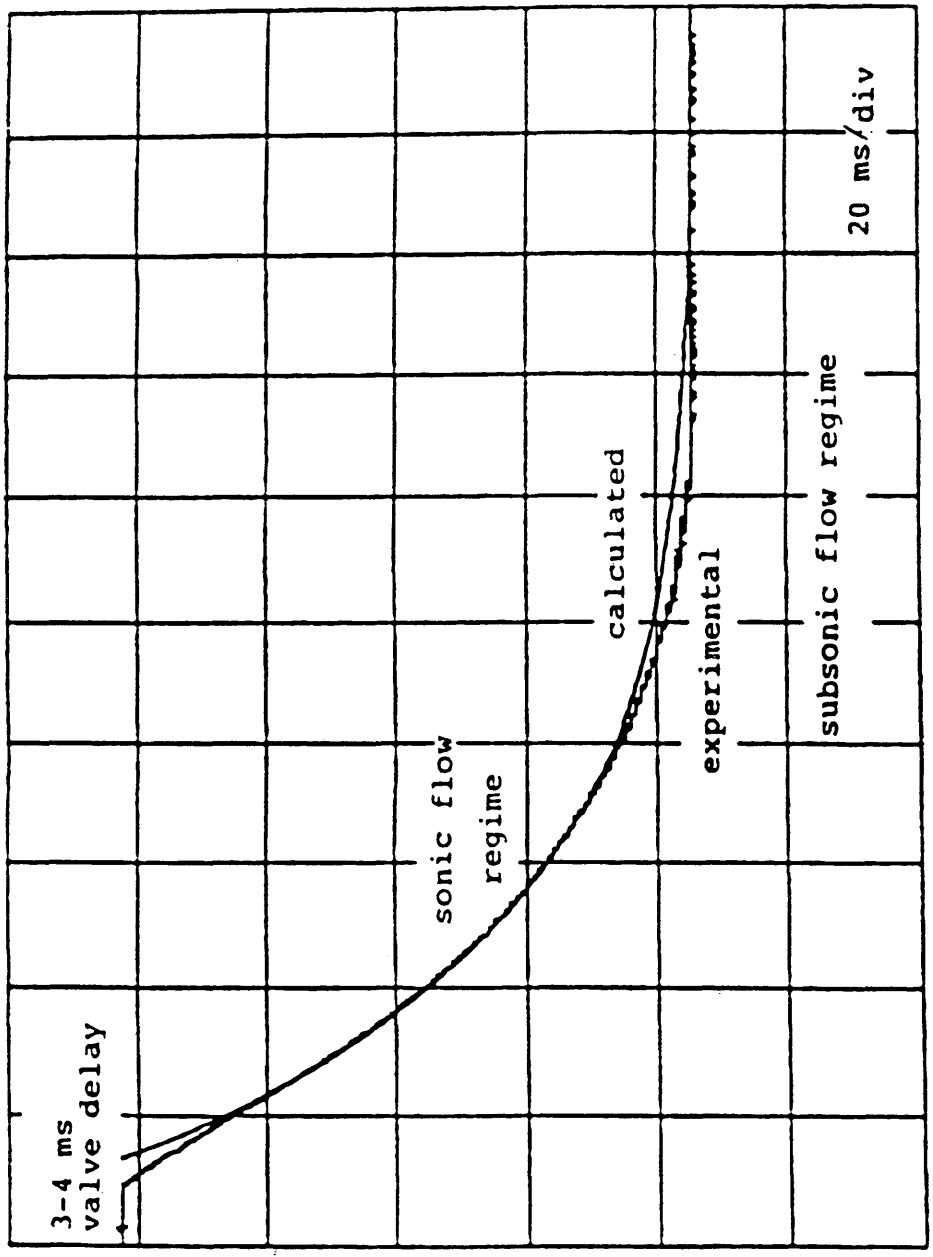

Figure 12 - Theoretical and experimental pressure-time curve for a cold air blow-down test.

Figure 9. The BDCB was first evacuated and then filled with methane to an absolute pressure of 98 kPa. By evacuating the BDCB, peak pressure variations brought about by residual mass fraction interferences were eliminated. 1020 kPa of dry air was then added to give a fuel-air equivalence ratio of 1.0135. This is the ratio where the adiabatic flame temperature is a maximum (see Fig. 13), thereby providing the greatest combustion energy and ensuring the best possible spark initiation. Dry air is preferred as the oxidizing agent, as calculations performed in the subroutine PER are for lower heating values only. Both the fuel and air were introduced into the BDCB at room temperature.

As an example, five consecutive tests were performed in this manner, with the results illustrated in Figure 14. The threshold-pressure control system proved quite effective, limiting the variation of peak pressure to 276 kPa, or 5.3%. This is much less than the cycle-to-cycle variation encountered in IC engines which can exceed values of 19.4% (see Fig. 3). Even research engines which are motored to reduce the residual mass fraction do not improve on the performance of the BDCB, having peak pressure variations of 6.8% (26).

One of the key problems that still remains is the initial burning rate whose variation was previously found to

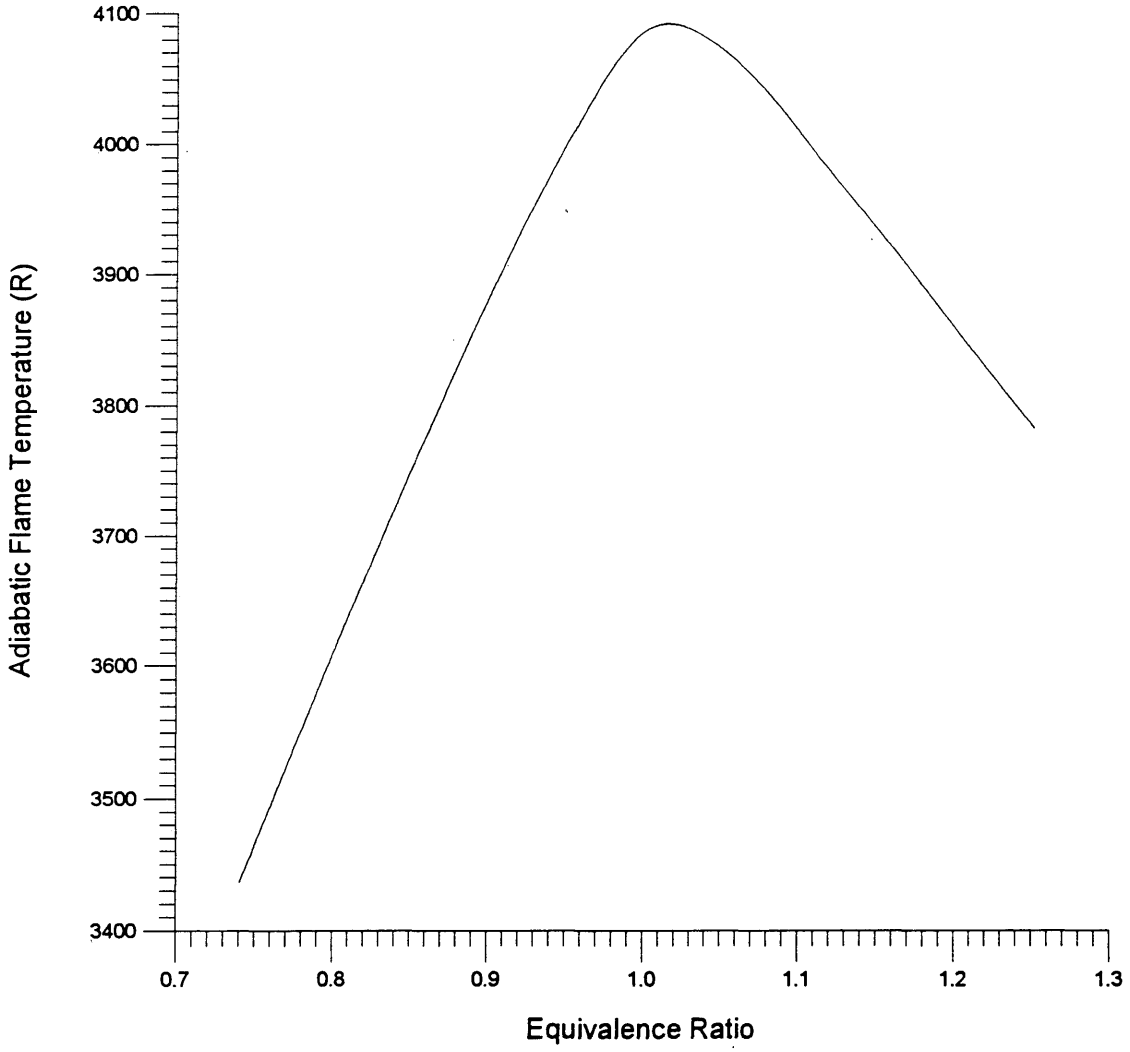

Figure 13 - Adiabatic flame temperature versus equivalence ratio for methane-air combustion.

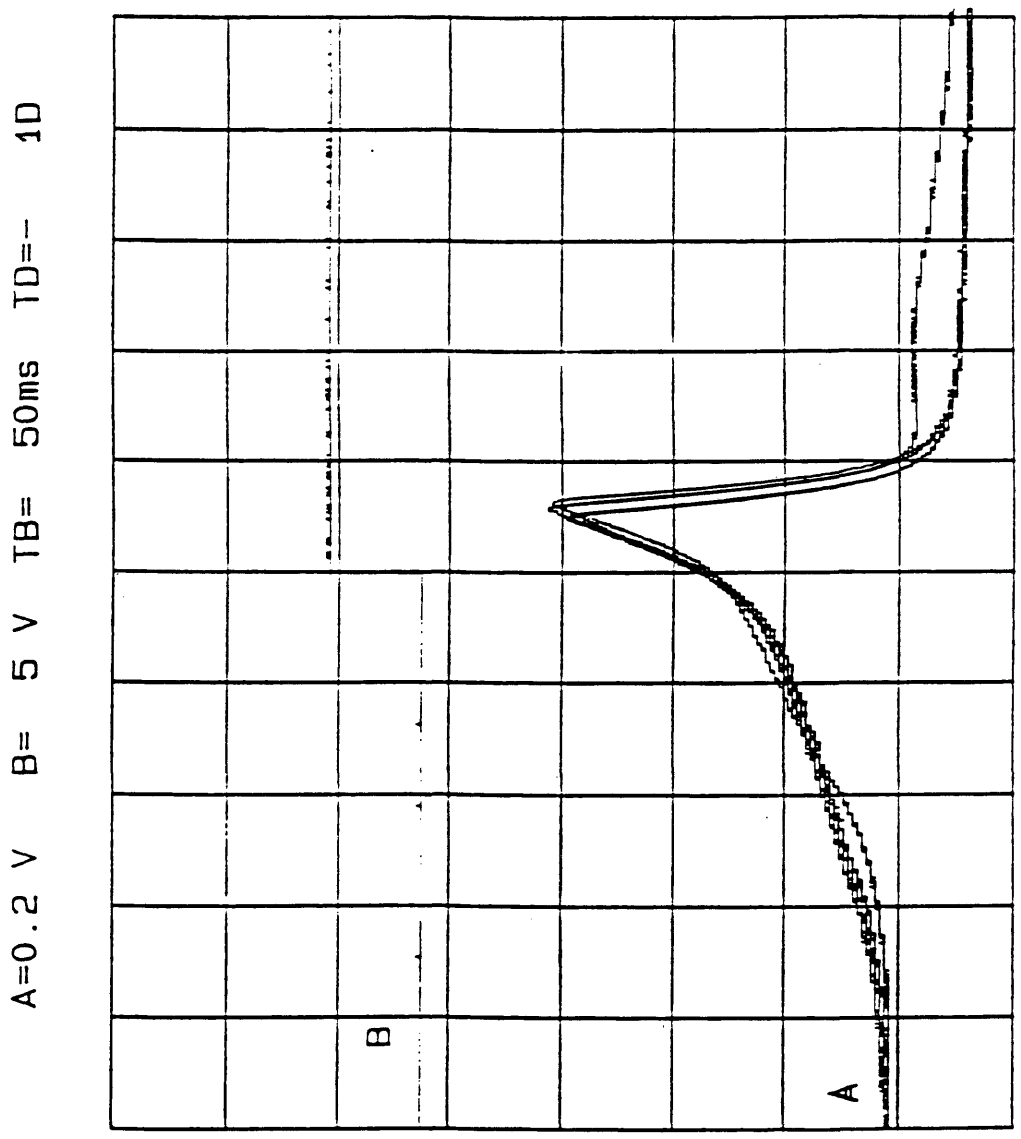

Figure 14 - Five consecutive pressure traces using the BDCB and a methane-air equivalence ratio of 1.035.

be 4.86 MPa/s. This is not an uncommon problem in combustion studies as the development of the ignition kernel can vary substantially. Controlling the development of the spark kernel would further improve the performance of the BDCB. Approaches that can be taken to eliminate this problem will be discussed later.

From Figure 14, the problem associated with using the stainless steel screen as a means of controlling the flow of gases up the fuel-air line can be readily seen. In a random manner, but with increasing frequency as the BDCB became warmer, a pressure rise was observed to occur after the blow-down phase. After exploring other possibilities including oscillatory motion of the valve and wave effects, the cause became apparent. With the cylinder pressure lowered as a result of the blow-down, the fuel-air mixture at 862 kPa began to enter the test section through the stainless steel screen. As the screen had been heated due to the combustion of cylinder gases, it provides the means for ignition of the gases that were now entering the BDCB. Verification of this conclusion came from the output generated by BDCB.FOR using the two-zone model. The secondary pressure rise would result in an increase in the burned gas mass, exceeding the total mass originally contained in the BDCB.

The temperature regime of the BDCB was then determined using the two-zone model previously discussed. The pressure data was converted to tabular form with equal divisions in the time domain after performing a cubic spline to smooth the step-wise pressure increments of the digital plot. This pressure-time data was then used as an input file to the program BDCB.FOR as were the experimental parameters. Several unsuccessful attempts were made to obtain meaningful results until it was determined that a solution would not converge for the orifice-plate flow area used. Losses resulted in a flow coefficient of 0.86, thereby altering the mass flow rate out of the test section. The coefficient for incompressible flow is 0.597, independent of Reynolds number. Using this value and applying the empirical relations put forth by Annand (27), a theoretical compressible flow coefficient of 0.822 was attained which compares favorably to the value determined from numerical calculations. This approach was also used in determining the 17 ms valve delay associated with the newer actuating piston design.

The resulting temperatures for the burned gases, the unburned gases, and the adiabatic core are illustrated in Figure 15. When compared with the temperature regime found in IC engines (see Fig. 4), the BDCB does very well in

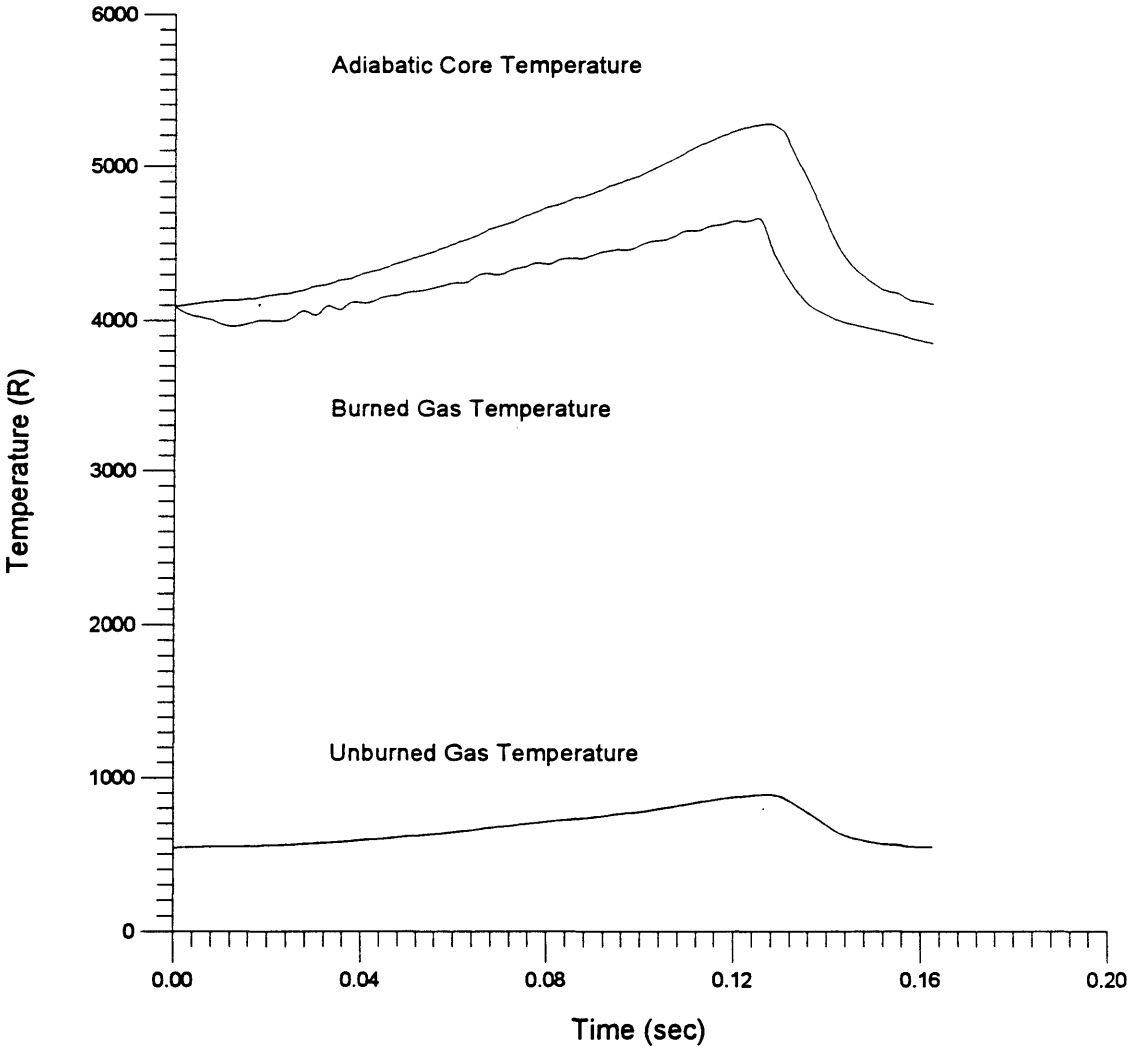

Figure 15 - Unburned, burned, and adiabatic core temperatures as a function of time for the BDCB using a two-zone thermodynamic model.

imitating its IC engine counterpart. The products of combustion in the BDCB therefore experience the same temperatures and pressures as those of real engines.

In addition to determining the temperature of the various constituents, the two-zone model is also used to determine the burned mass and volume as functions of time. These relationships are illustrated on Figure 16 and 17. Included on Figure 17 is a plot of a universal curve for mass-burned fraction versus volume-burned fraction (4). It is termed "universal" as large changes in engine parameters produce little variation in the curve. Its distinctive shape is due to the density change that occurs when reactants are converted to products. The density ratio of unburned to burned gases depends on equivalence ratio, pressure, temperature, and residual gases, but for most SI operating conditions this value is approximately 4. The deviation from the universal curve found with the BDCB is a function of the near stoichiometric mixture of methane and air. By comparison, experimental IC engines normally operate with iso-octane and excess air, resulting in a lower density change than occurred during the experiment using the BDCB.

Additional information gained from the employment of a model using shifting equilibrium is the concentrations of each of the major product species. One such plot is

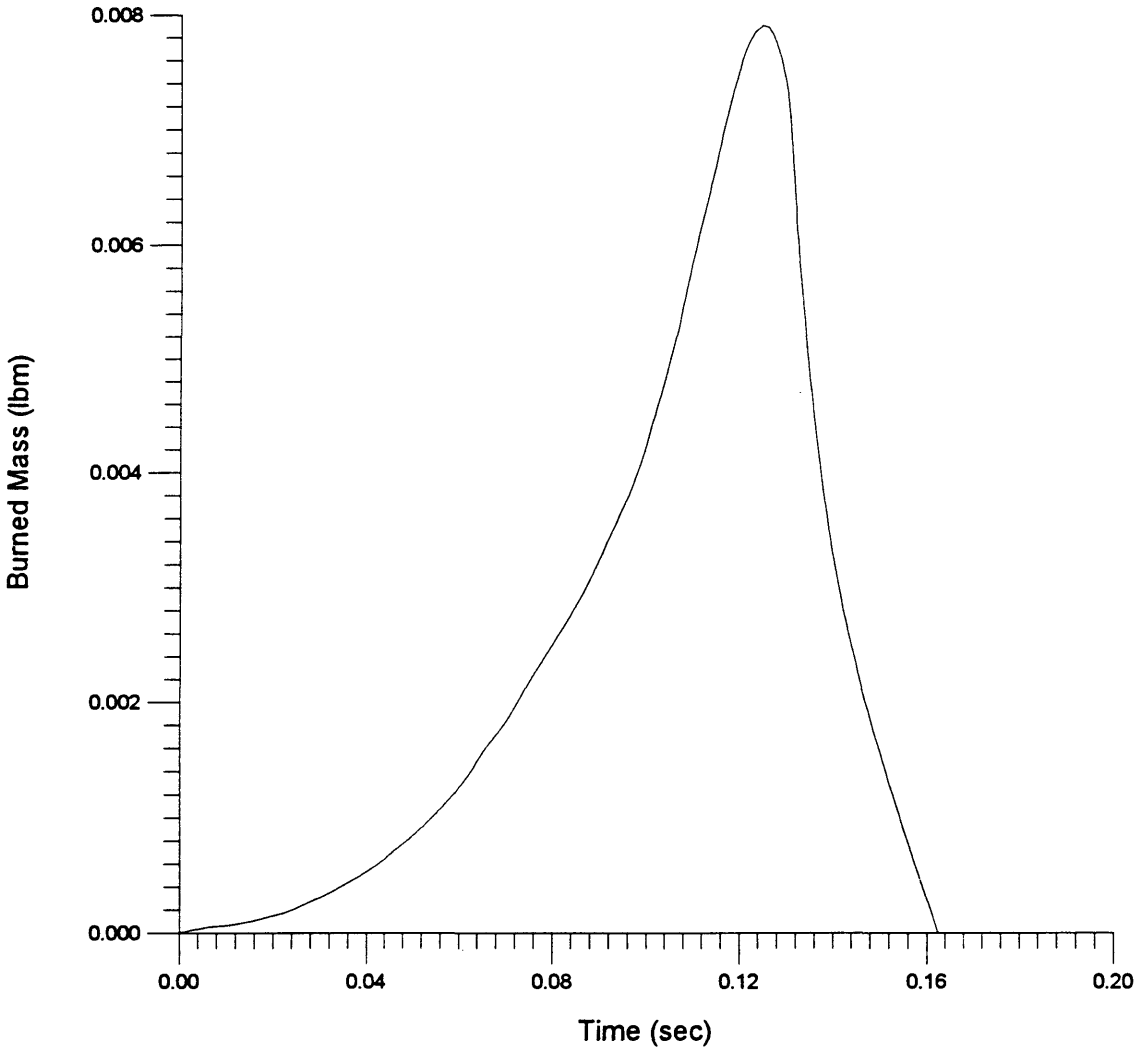

Figure 16 - Burned mass versus time for the BDCB using a two-zone thermodynamic model.

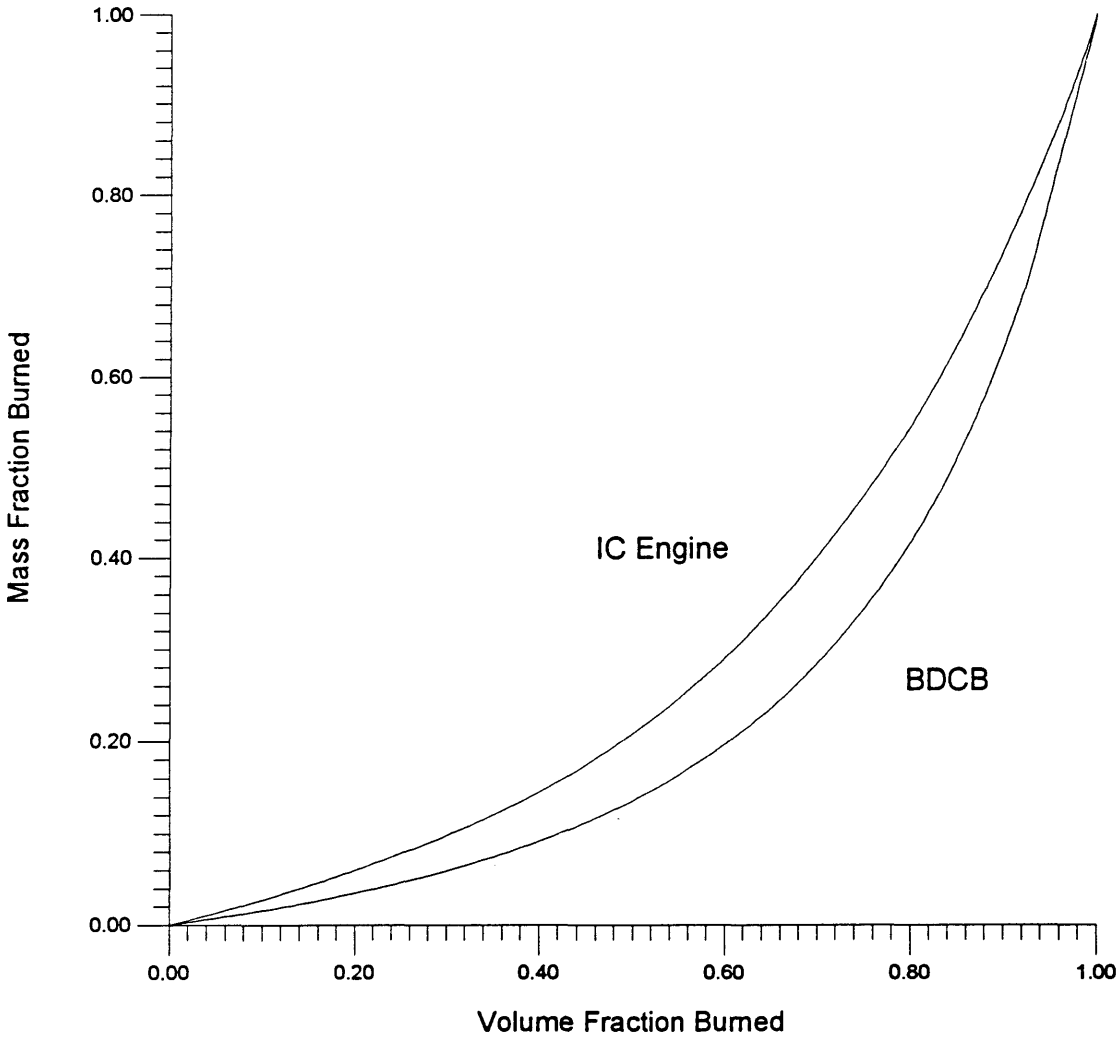

Figure 17 - Burned-mass fraction versus burned-volume fraction for the BDCB and an IC engine.

illustrated in Figure 18 showing the concentration of CO as a function of time. The large oscillations seen in this illustration are the result of instabilities brought about by the large time increment used and the assumption of shifting equilibrium. It would, however, provide an adequate base for confirmation using laser diagnostic techniques. This plot also shows the effect of the rapid evacuation of unburned gases. During the blow down, a large discontinuity in concentration exists brought about by the rapidly changing temperature and pressure which shift the equilibrium composition. After the blow-down phase has been completed, no further reaction takes place and the concentration of the major product species becomes fixed.

Lastly, some of the other parameters calculated using the two-zone model are included in Appendix D, Graphs 1 through 4. Here, the burned-area fraction, flame speed, heat transfer rate, and burned-volume fraction are plotted against experimental time. Of particular interest here is the burned-volume fraction (Graph 4), as this illustrates the rapid expulsion of unburned mass from the test section. At the time of the valve opening, the reactants make up 31.1% of the total mass (see Table III in Appendix A), and yet, are expelled and converted into products in less than one time-step. For the gases being expelled, the flow rate

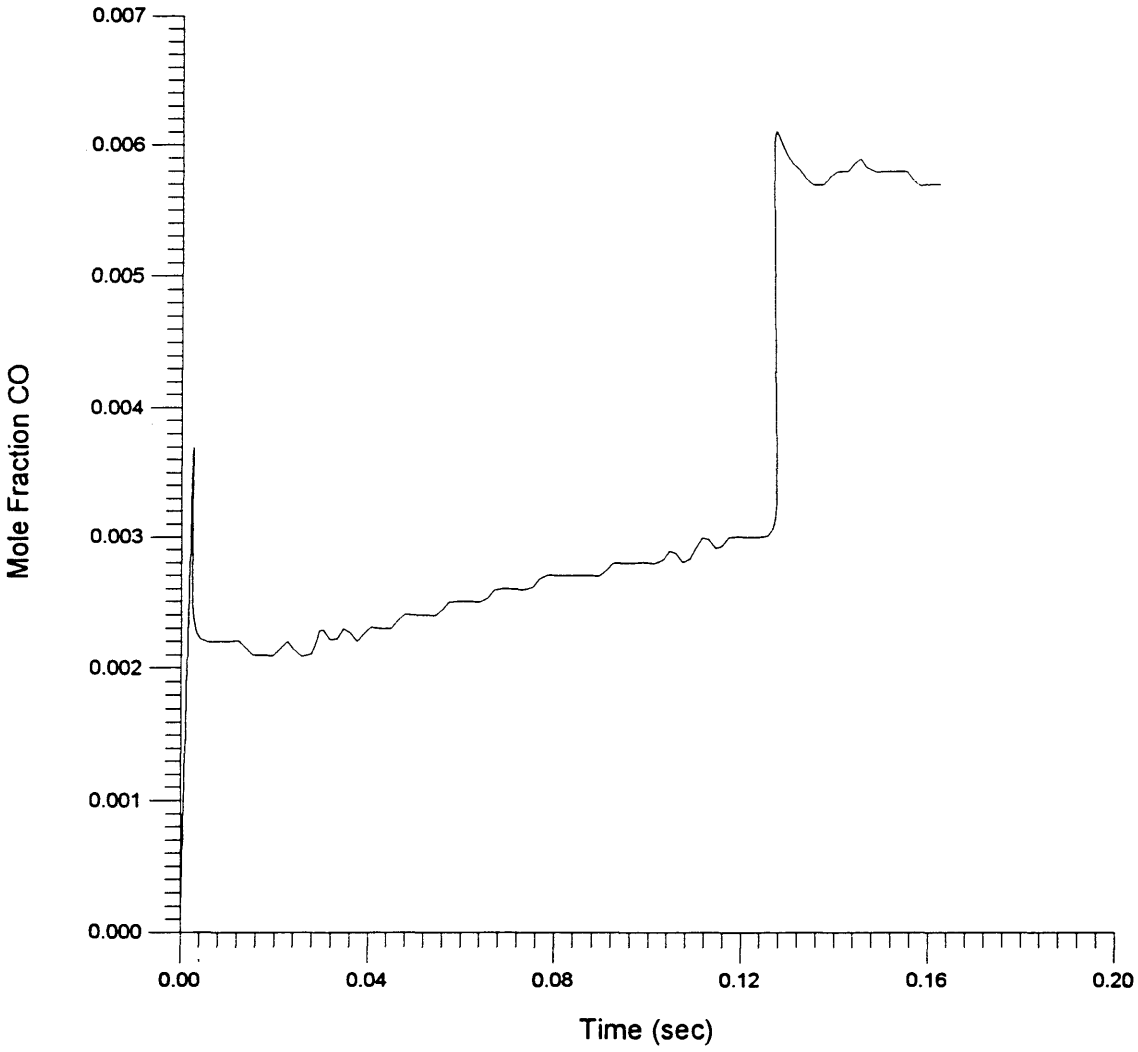

Figure 18 - Mole fraction of CO versus time for the BDCB using a shifting equilibrium.

is controlled by the unburned constituents. As has been previously stated, this is a much higher rate than the burned gases will achieve.

CONCLUSIONS AND RECOMMENDATIONS

From the experiments performed using the BDCB, the usefulness of this new diagnostic tool for combustion studies has been asserted. In addition to emulating the pressure histories found in real IC engines, the combustion products are exposed to similar temperature regimes. In this manner, the BDCB can be used to study chemical kinetics void of turbulent mixing. In reducing this turbulent flow field associated with IC engines, predictable and reproducible results are achieved.

With the elimination of residual gases from the BDCB experiment, pressure traces were observed which were significantly more consistent than the IC engine counterpart. Some improvements to the design could be implemented which would further improve the BDCB performance. To reduce the 5.3% variation in peak pressure, a means of controlling or enhancing the growth of the spark kernel should be pursued. The most obvious approach would be to employ fuels which are much more reactive than methane, as was intended in the original design. Additionally, a cylinder head could be manufactured which houses an array of five spark plugs, one in the center and four around the

perimeter. This would virtually eliminate the 4.87 MPa/s variation in ignition rates common to all spark ignition apparatus. An arrangement of this type would make it possible to apply a two-zone model having a planar flame front which propagates at the flame speed. This is the main reason for not selecting a high-energy arc generator with a large electrode gap. While the increased arc size would enhance ignition, the development of the flame kernel would be difficult to model.

The recommendation just cited for the ignition system would bring about another design variation, as sufficient room would no longer exist in the cylinder head for the pressure transducer and fuel-air inlet port. By fabricating clamps similar to the ones used for the optical windows, but without the interior material removed, a means of facilitating the pressure transducer and inlet port would be achieved. With sufficient room now available, a poppet valve similar to the blow-down valve could be employed. This modification would eliminate the secondary combustion caused by the ignition of gases emerging from the inlet port by the well-heated stainless steel mesh.

Further improvements could be made to the blow-down valve. With the substitution of hydraulic fluid rather than pneumatics, oscillatory motion in the valve would be

eliminated. This would also remedy the increased valve delay brought about by the larger clearance volume when the new actuating piston design was implemented.

While the blow-down valve control system performed admirably, improvements can be made here as well. One of the first things that should be addressed is the manufacturing of a printed circuit board for the control system. Currently, this system resides on a series of bread boards. This substitution would eliminate some of the sporadic behavior exhibited by the system by isolating it from the effects of RF signals. Another area of concern has to do with the transient nature of the piezoelectric pressure transducer, as the fill rate of the fuel-air mixture is sufficiently fast for it to become biased. Therefore, once the fire command is issued by the fuel-air filling program, time must pass before the spark is actually initiated. With a small, but measurable, leak down some of the fuel-air mixture is lost during this time. By implementing a timer to handle the fire sequencing, human error in estimating this duration would be eliminated.

Because the program that was developed using the two-zone thermodynamic model is driven by experimental pressure traces, improvements in acquiring this data should be employed. Instead of transposing the data from a plot, a

digital storage oscilloscope should be used which is capable of storing the information as a data file. This would greatly improve the output from the program BDCB.FOR by reducing the time increment between calculations.

Lastly, an equipment change needs to be made to facilitate capturing the combustion process on high-speed film. Initially, a camera (Nikon N8008) was used which did have the necessary electronic triggering capability and a shutter speed of 1/8000 s. Unfortunately, several hundred milliseconds were required to move the previewing mirror from the film plane. This resulted in the camera-trigger control system initiating the process at the correct time, but the actual exposure occurred after the experiment had been completed. This situation can be corrected by employing a camera with mirror lock-up capabilities. One such camera would be the Nikon F4 which also has a shutter speed of 1/8000 s, equal to the camera previously cited.

With the improvements made to the BDCB that were discussed here, a new diagnostic tool presents itself to the combustion community which is capable of meeting a great many experimental needs. It will allow the researcher to concentrate on chemical kinetics thereby facilitating the development of global conclusions.

REFERENCES

1) Gatowski, J.A., Balles, E.N., Chung, K.M., Nelson, F.E., Ekchian, J.A., Heywood, F.B. 1984. Heat Release Analysis of Engine Pressure Data. SAE 841359 Warrendale, PA: Society of Automotive Engineers.

2) Park, P., Keck, J.C. 1990. Rapid Compression Machine Measurements of Ignition Delays for Primary Reference Fuels. SAE 900027 Warrendale, PA: Society of Automotive Engineers.

3) Belles, E.N., Heywood, J.B. 1988. Fuel-Air Mixing and Diesel Combustion in a Rapid Compression Machine. SAE 880206 Warrendale, PA: Society of Automotive Engineers.

4) Beretta, G.P., Rashidi, M., Keck, J.C. 1983. Turbulent Flame Propagation and Combustion in Spark Ignition Engines. Combust. Flame, vol. 52: 217-245.

5) Kuo, K.K. 1986 Principles of Combustion. New York, NY: John Wiley and Sons.

6) Thomas III, R.W., Callahan, T.J. 1988. Engine and Constant Volume Bomb Studies of Diesel Ignition and Combustion. SAE 881626 Warrendale, PA: Society of Automotive Engineers.

7) Heywood, J.B., Fay, J.A., Linden, L.H. 1971. Jet Aircraft Pollutant production and Dispersion. AIAA J, vol 9: no 5.

8) Newhall, H.K., Shahed, S.M. 1971. Kinetics of Nitric Oxide Formation in High-Pressure Flames. Proceedings of Thirteenth International Symposium on Combustion: The Combustion Institute.

9) Rassweiler, G.M., Withrow, L. 1938. Motion Pictures of Engine Flame Correlated with Pressure Cards. SAE Trans., vol 38.

10) Olikara, C., Borman, G.L. 1975. A Computer program for Calculating Properties of Equilibrium Combustion Products with some Applicatlons to IC Engines. SAE 750468 Warrendale, PA: Society of Automotive Engineers.

11) Taylor, C. 1985. The Internal Combustion Engine in Theory and Practice. Boston, MA: MIT Press.

12) Shapiro, A. 1953. The Dynamics and Thermodynamics of Compressible Fluid Flow. New York, NY: Ronald Press.

13) Lo Russo, J.A., Lavoie, G.A., Kaiser, E.W. 1980. An Electrohydraulic Gas Sampling Valve with Applications to Hydrocarbon Emission Studies. SAE 800045 Warrendale, PA: Society of Automotive Engineers.

14) Guterman, M.M., Nitecki, Z.H. 1984. Differential Equations. New York, NY: CBS College Publishing.

15) Deutschman, A., Michels, W., Wilson, C. 1975. Machine Design Theory and Practice. New York, NY: MacMillan Publishing Co.

16) Boresi, A., Sidebottom, O. 1985. Advanced Mechanics of Materials. New York, NY: John Wiley and Sons.

17) Westergaard, H.M. 1921. Moments and Stresses in Slabs. Proceedings of the American Concrete Institute, vol 17.

18) Lewis, B., von Elba, G. 1961. Combustion Flames and Explosions of Gases. New York, NY: Academic Press.

19) Foster, D.E. 1985. An Overview of Zero-Dimensional Thermodynamic Models for IC Engine Data Analysis. SAE 852070 Warrendale, PA: Society of Automotive Engineers.

20) Heywood, J.B. 1988. Internal Combustion Engine Fundamentals. New York, NY: McGraw-Hill Publishing Co.

21) Keck, J.C. 1982. Turbulent Flame Structure and Speed in Spark-Ignition Engines. Proceedings of the Nineteenth International Symposium on Combustion: The Combustion Institute.

22) Metghalchi, M., Keck, J.C. 1980. Laminar Burning Velocity of Propane-Air Mixtures at High Temperature and Pressure. Combust. Flame, vol 38.

23) Mansouri, S.H., Heywood, J.B. 1980. Correlation for the Viscosity and Prandtl Number of Hydrocarbon-Air Combustion Products. Combust. Sci. Technology, vol 23.

24) Hildebrand, F.B. 1974. Introduction to Numerical Analysis. New York, NY: McGraw-Hill Publishing Co.

25) Burden, R.L., Faires, J.D. 1988. Numerical Analysis. Boston, MA: PWS-Kent Publishing Co.

26) Witze, P.O., Martin, J.K., Borgnakke, C. 1984. Conditionally Sampled Velocity and Turbulence Measurements in a Spark Ignition Engine. Combust. Sci. Technology, vol 36.

27) Annand, W.J.D. 1966. Compressible Flow Through Square-Edged Orifices; an Empirical Approximation for Computer Calculations. J. Mech. Eng. Sci., vol 8: 448.

APPENDIX A

TABLE I - Data For Modeling CFR SI Engine (Pressure Fall)

CRANK ANGLE (deg)	ACTUAL TIME (sec)	EQUATION TIME (sec)	PRESSURE ACTUAL (kPa)	PRESSURE MODEL (kPa)	ERROR (%)
-109	-1.518E-02	0.000E+00	95.5		
-103	-1.429E-02	8.930E-04	111.3		
-96	-1.339E-02	1.786E-03	143.2		
-90	-1.250E-02	2.679E-03	159.2		
-84	-1.161E-02	3.571E-03	182.7		
-77	-1.071E-02	4.464E-03	238.5		
-71	-9.821E-03	5.357E-03	270.2		
-64	-8.929E-03	6.250E-03	326.0		
-58	-8.036E-03	7.143E-03	397.7		
-51	-7.143E-03	8.036E-03	477.0		
-45	-6.250E-03	8.929E-03	572.8		
-39	-5.357E-03	9.821E-03	715.5		
-32	-4.464E-03	1.071E-02	827.1		
-26	-3.571E-03	1.161E-02	954.7		
-19	-2.679E-03	1.250E-02	1113.2		
-13	-1.786E-03	1.339E-02	1312.4		
-6	-8.930E-04	1.429E-02	1630.2		
0	0.000E+00	1.518E-02	2266.4		
6	8.930E-04	1.607E-02	3722.1		
12.86	1.786E-03	0.000E+00	5090.4	5090.4	0.0
19	2.679E-03	8.930E-04	4557.2	4428.8	2.8
26	3.571E-03	1.786E-03	3992.6	3852.6	3.5
32	4.464E-03	2.679E-03	3523.3	3351.6	4.9
39	5.357E-03	3.571E-03	3006.4	2916.2	3.0
45	6.250E-03	4.464E-03	2537.1	2537.0	0.0
51	7.143E-03	5.357E-03	2163.3	2207.1	2.0
58	8.036E-03	6.250E-03	1813.3	1920.1	5.9
64	8.929E-03	7.143E-03	1590.7	1670.4	5.0
71	9.821E-03	8.036E-03	1352.1	1453.2	7.5
77	1.071E-02	8.929E-03	1185.0	1264.2	6.7
84	1.161E-02	9.821E-03	1033.9	1100.0	6.4
90	1.250E-02	1.071E-02	922.6	957.5	3.8
96	1.339E-02	1.161E-02	819.2	832.1	1.6
103	1.429E-02	1.250E-02	723.8	724.2	0.1
109	1.518E-02	1.339E-02	644.2	630.3	2.2
116	1.607E-02	1.429E-02	580.6	547.8	5.7
122	1.696E-02	1.518E-02	540.8	476.8	11.8
129	1.786E-02	1.607E-02	493.1	415.0	15.8
135	1.875E-02	1.696E-02	437.4	361.2	17.4

Model - $P = Po \exp(-156t)$

TABLE II - Unburned, Burned, and Adiabatic Core Temperatures for the BDCB using a Two-Zone Thermodynamic Model.

t (s)	Tu (R)	Tb (R)	Tac (R)
.0000	540.0	4092.0	4092.0
.0025	542.4	4044.4	4102.8
.0050	544.8	4023.7	4113.4
.0075	547.1	4007.3	4123.8
.0100	548.9	3975.0	4131.4
.0125	549.4	3963.7	4133.9
.0150	550.6	3973.2	4139.0
.0175	552.9	3999.1	4149.0
.0200	556.2	3999.1	4163.8
.0225	558.5	3996.6	4173.2
.0250	560.6	4016.9	4182.6
.0275	565.0	4064.7	4201.2
.0300	570.8	4033.6	4225.8
.0325	573.3	4094.9	4235.9
.0350	579.9	4068.0	4263.8
.0375	583.4	4117.5	4276.9
.0400	590.1	4114.4	4304.9
.0425	594.8	4126.3	4322.8
.0450	600.3	4157.9	4344.6
.0475	607.4	4162.5	4372.6
.0500	613.4	4183.8	4395.1
.0525	620.1	4194.2	4420.6
.0550	626.6	4210.3	4444.6
.0575	633.7	4228.7	4470.9
.0600	641.4	4245.6	4498.7
.0625	649.1	4249.2	4526.3
.0650	657.3	4298.4	4555.3
.0675	668.3	4305.1	4594.7
.0700	676.1	4301.4	4619.5
.0725	682.8	4334.0	4641.6
.0750	692.4	4348.0	4675.1
.0775	701.8	4376.2	4705.8
.0800	710.9	4366.2	4735.2
.0825	717.4	4396.5	4754.9
.0850	726.0	4404.9	4783.6
.0875	733.4	4405.6	4806.2
.0900	740.5	4433.6	4829.0
.0925	750.2	4450.6	4860.8
.0950	759.3	4460.7	4888.8
.0975	767.3	4461.0	4913.1
.1000	775.4	4493.8	4938.7
.1025	787.1	4515.9	4976.8

t (s)	Tu (R)	Tb (R)	Tac (R)
.1050	798.9	4521.7	5012.5
.1075	810.1	4552.5	5046.5
.1100	823.8	4583.7	5089.1
.1125	837.3	4584.8	5128.1
.1150	848.1	4613.5	5158.1
.1175	859.9	4622.8	5193.3
.1200	870.1	4644.9	5221.7
.1225	879.4	4640.7	5248.3
.1250	885.2	4663.6	5263.5
.1275	888.3	4508.1	5271.4
.1300	878.7	4350.8	5237.1
.1325	838.0	4222.4	5103.6
.1350	788.4	4130.5	4955.0
.1375	738.3	4067.8	4799.1
.1400	684.2	4026.0	4622.4
.1425	637.6	3996.9	4467.3
.1450	607.1	3974.9	4361.2
.1475	588.1	3957.6	4291.0
.1500	573.3	3939.6	4232.7
.1525	562.8	3921.9	4190.1
.1550	558.4	3903.1	4172.4
.1575	549.4	3884.5	4133.3
.1600	545.9	3865.6	4118.4
.1625	542.4	3846.2	4102.7

TABLE III - Mass Burned, Mass-Burned Fraction, and Volume-Burned Fraction for the BDCB using a Two-Zone Thermodynamic Model.

t (s)	Mb (lbm)	Mb/Mt	Vb/V
.0000	.000000	.00000	.00000
.0025	.000021	.00179	.01308
.0050	.000041	.00355	.02535
.0075	.000055	.00482	.03391
.0100	.000064	.00554	.03854
.0125	.000075	.00651	.04474
.0150	.000096	.00839	.05699
.0175	.000124	.01078	.07213
.0200	.000147	.01278	.08430
.0225	.000171	.01492	.09694
.0250	.000213	.01858	.11810
.0275	.000260	.02268	.14060
.0300	.000304	.02650	.16048
.0325	.000355	.03091	.18227
.0350	.000409	.03563	.20444
.0375	.000469	.04091	.22786
.0400	.000530	.04622	.25005
.0425	.000597	.05199	.27283
.0450	.000676	.05891	.29846
.0475	.000757	.06599	.32294
.0500	.000841	.07330	.34658
.0525	.000931	.08113	.37022
.0550	.001029	.08972	.39445
.0575	.001139	.09923	.41937
.0600	.001254	.10931	.44391
.0625	.001392	.12132	.47090
.0650	.001551	.13522	.49954
.0675	.001692	.14744	.52266
.0700	.001824	.15894	.54281
.0725	.001987	.17321	.56605
.0750	.002172	.18927	.59015
.0775	.002343	.20419	.61080
.0800	.002501	.21793	.62846
.0825	.002669	.23266	.64617
.0850	.002840	.24751	.66289
.0875	.003021	.26326	.67950
.0900	.003240	.28236	.69829
.0925	.003469	.30238	.71656
.0950	.003683	.32097	.73234
.0975	.003922	.34186	.74888
.1000	.004233	.36889	.76865
.1025	.004579	.39910	.78887

t (s)	Mb (lbm)	Mb/Mt	Vb/V
.1050	.004951	.43149	.80863
.1075	.005386	.46939	.82960
.1100	.005840	.50898	.84942
.1125	.006270	.54647	.86654
.1150	.006703	.58417	.88232
.1175	.007130	.62142	.89672
.1200	.007507	.65425	.90855
.1225	.007797	.67951	.91715
.1250	.007905	.68895	.92064
.1275	.007404	.64525	.92064
.1300	.007399	1.00000	1.00000
.1325	.005989	.80950	1.00000
.1350	.004858	.65656	1.00000
.1375	.003968	.53629	1.00000
.1400	.003294	.44520	1.00000
.1425	.002772	.37462	1.00000
.1450	.002334	.31539	1.00000
.1475	.001941	.26239	1.00000
.1500	.001582	.21386	1.00000
.1525	.001245	.16828	1.00000
.1550	.000916	.12379	1.00000
.1575	.000604	.08169	1.00000
.1600	.000299	.04041	1.00000
.1625	.000000	.00000	1.00000

TABLE IV - Area-Burned Fraction, Flame Speed, Heat Transfer Rate, and Mole Fraction of NO for the BDCB using a Two-Zone Thermodynamic Model.

t (s)	Ab/At	Vel (in/s)	Qb (BTU/s)	[CO]
.0000	.00000	21.2727	.0000	.0000
.0025	.01915	21.3189	.3292	.0037
.0050	.02968	21.3646	.4186	.0022
.0075	.03697	21.4096	.4531	.0022
.0100	.03860	21.4431	.4236	.0022
.0125	.04016	21.4541	.4033	.0022
.0150	.04712	21.4762	.4401	.0021
.0175	.05774	21.5198	.5079	.0021
.0200	.06488	21.5842	.5404	.0021
.0225	.06830	21.6266	.5419	.0022
.0250	.07699	21.6684	.5874	.0021
.0275	.09114	21.7505	.6731	.0021
.0300	.09684	21.8603	.6903	.0023
.0325	.10582	21.9093	.7359	.0022
.0350	.11443	22.0331	.7733	.0023
.0375	.12239	22.0982	.8108	.0022
.0400	.13158	22.2247	.8523	.0023
.0425	.13731	22.3126	.8726	.0023
.0450	.15449	22.4151	.9673	.0023
.0475	.17464	22.5475	1.0762	.0024
.0500	.19489	22.6597	1.1849	.0024
.0525	.21525	22.7837	1.2918	.0024
.0550	.23572	22.9038	1.3991	.0024
.0575	.25632	23.0344	1.5070	.0025
.0600	.27705	23.1744	1.6144	.0025
.0625	.29792	23.3161	1.7228	.0025
.0650	.31894	23.4654	1.8394	.0025
.0675	.34010	23.6637	1.9457	.0026
.0700	.36138	23.8067	2.0498	.0026
.0725	.38280	23.9275	2.1639	.0026
.0750	.40437	24.0987	2.2765	.0026
.0775	.42608	24.2684	2.3888	.0027
.0800	.44791	24.4313	2.4921	.0027
.0825	.46986	24.5496	2.6050	.0027
.0850	.49193	24.7014	2.7120	.0027
.0875	.51413	24.8352	2.8198	.0027
.0900	.53648	24.9648	2.9383	.0027
.0925	.55896	25.1366	3.0536	.0028
.0950	.58158	25.3023	3.1654	.0028
.0975	.60435	25.4465	3.2796	.0028
.1000	.62728	25.5932	3.4109	.0028
.1025	.65040	25.7997	3.5413	.0028

t (s)	Ab/At	Vel (in/s)	Qb (BTU/s)	[CO]
.1050	.67371	26.0116	3.6714	.0029
.1075	.69723	26.2141	3.8158	.0028
.1100	.72095	26.4571	3.9577	.0029
.1125	.74486	26.7003	4.0887	.0030
.1150	.76895	26.8983	4.2293	.0029
.1175	.79321	27.1086	4.3613	.0030
.1200	.81761	27.2951	4.4917	.0030
.1225	.84211	27.4644	4.6045	.0030
.1250	.86663	27.5752	4.7050	.0030
.1275	.87888	27.6349	4.7715	.0061
.1300	.89094	27.4822	4.7324	.0059
.1325	.90265	26.7908	4.5251	.0058
.1350	.91395	25.8978	4.2950	.0057
.1375	.92483	24.9794	4.0560	.0057
.1400	.93530	23.9872	3.7880	.0058
.1425	.94545	23.1240	3.5593	.0058
.1450	.95540	22.5499	3.4070	.0059
.1475	.96520	22.1901	3.3093	.0058
.1500	.97489	21.9098	3.2299	.0058
.1525	.98452	21.7100	3.1737	.0058
.1550	.99409	21.6267	3.1533	.0058
.1575	1.00000	21.4542	3.0911	.0057
.1600	1.00000	21.3872	3.0458	.0057
.1625	1.00000	21.3189	3.0003	.0057

APPENDIX B

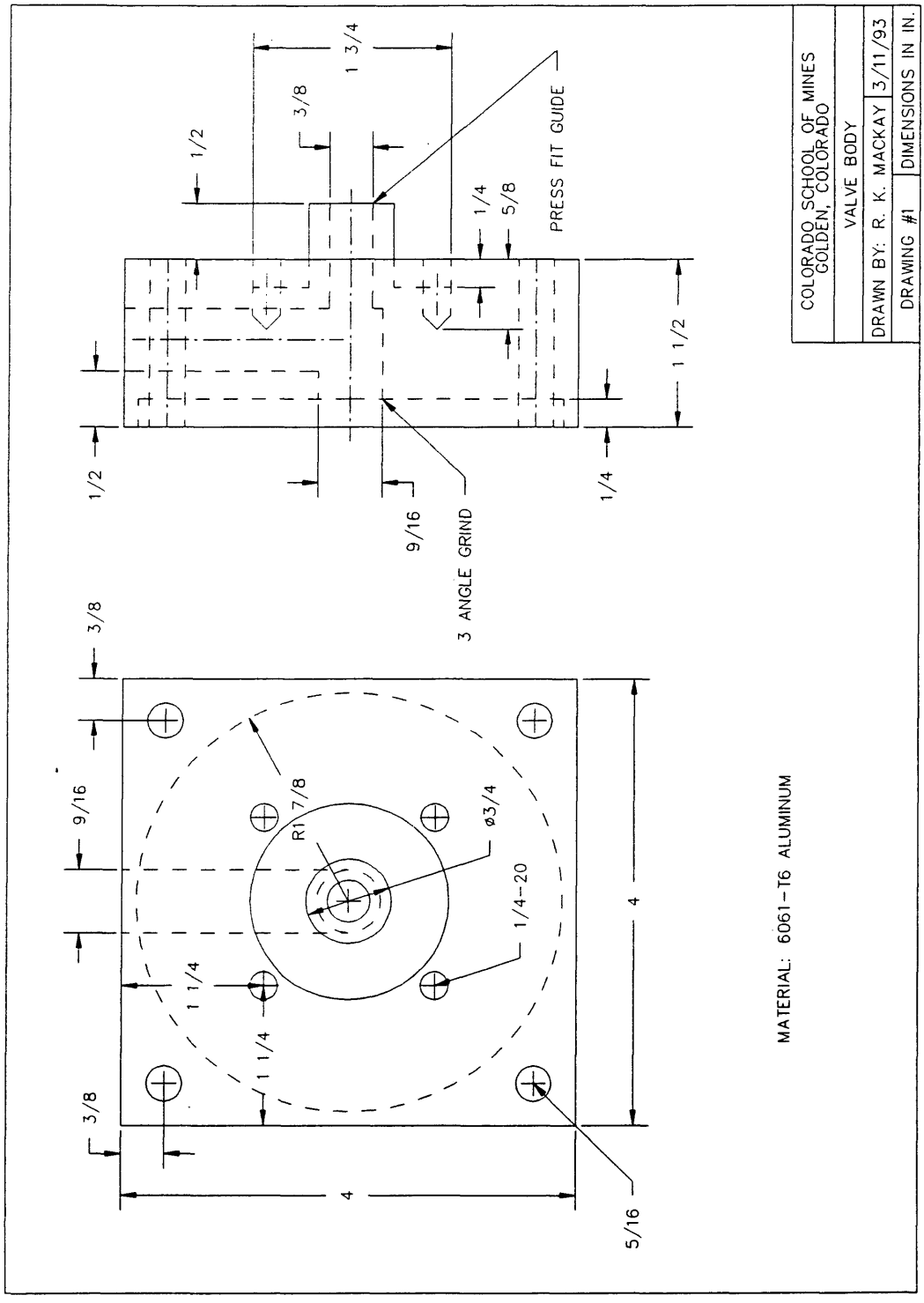
COLORADO SCHOOL OF MINES
GOLDEN, COLORADO
VALVE BODY
DRAWN BY: R. K. MACKAY
3/11/93
DRAWING #1
DIMENSIONS IN IN.
MATERIAL: 6061-T6 ALUMINUM
PRESS FIT GUIDE
3 ANGLE GRIND
1 3/4
3/8
1/2
1/4
5/8
1 1/2
9/16
4
5/16
R1 7/8
ø3/4
1/4-20
1 1/4

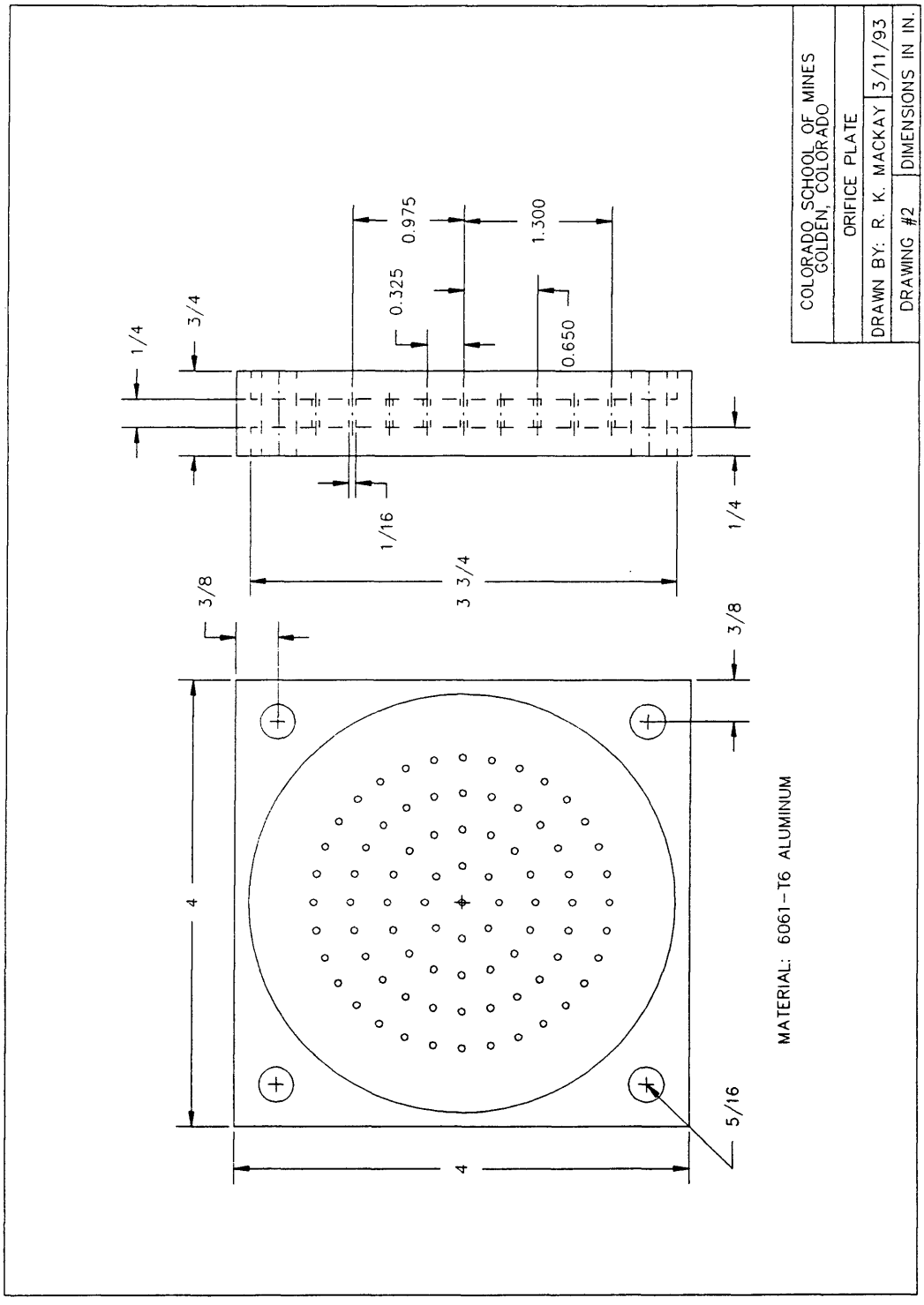
COLORADO SCHOOL OF MINES
GOLDEN, COLORADO
ORIFICE PLATE
DRAWN BY: R. K. MACKAY
3/11/93
DRAWING #2
DIMENSIONS IN IN.
MATERIAL: 6061-T6 ALUMINUM
1/4
3/4
0.325
0.975
1.300
0.650
1/16
3 3/4
1/4
3/8
3/8
4
4
5/16

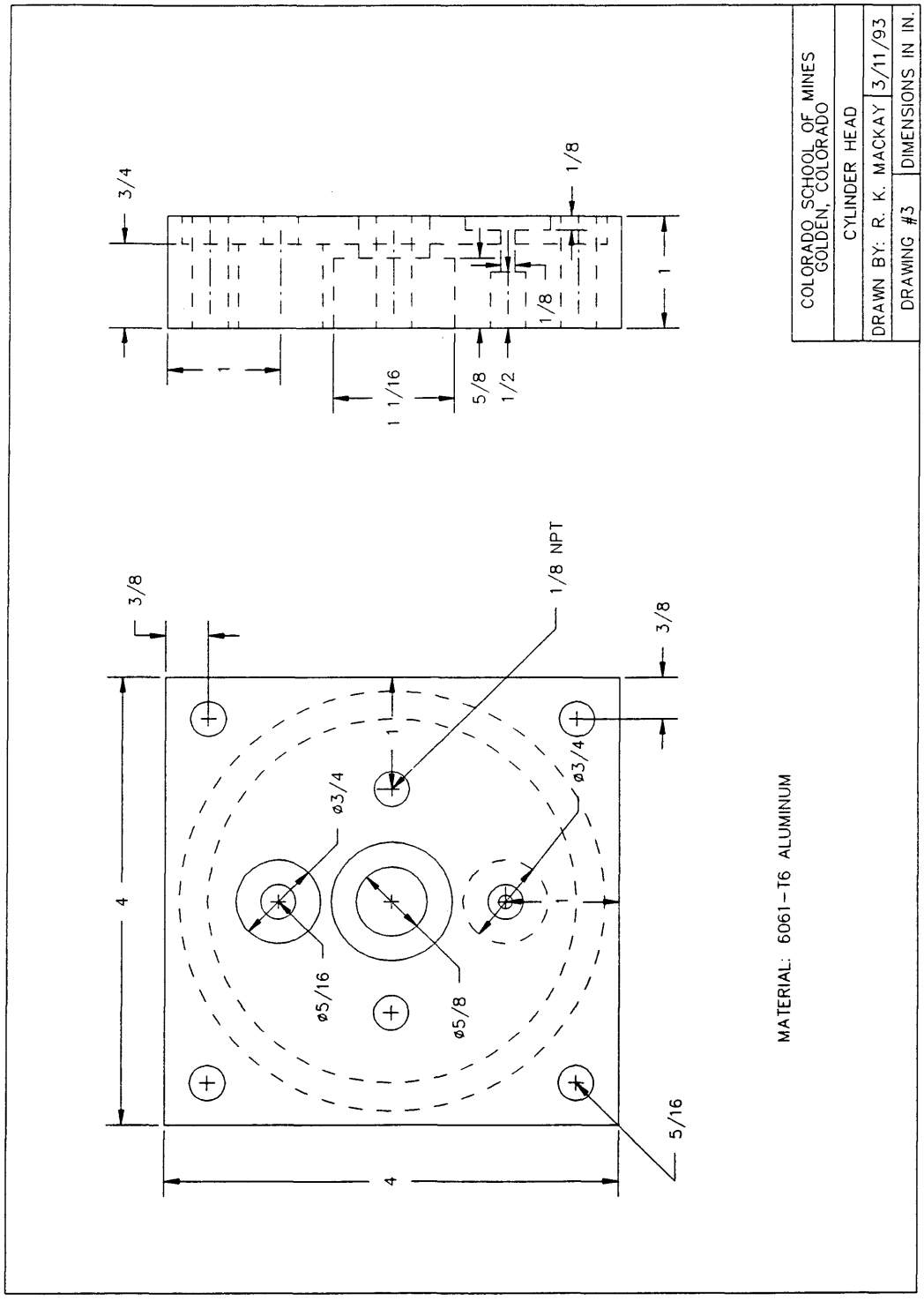
COLORADO SCHOOL OF MINES
GOLDEN, COLORADO
CYLINDER HEAD
DRAWN BY: R. K. MACKAY
3/11/93
DRAWING #3
DIMENSIONS IN IN.
MATERIAL: 6061-T6 ALUMINUM
3/4
1/8
1
1 1/16
5/8
1/2
1/8
3/8
1/8 NPT
3/8
4
ø3/4
ø3/4
ø5/16
ø5/8
1
1
4
5/16

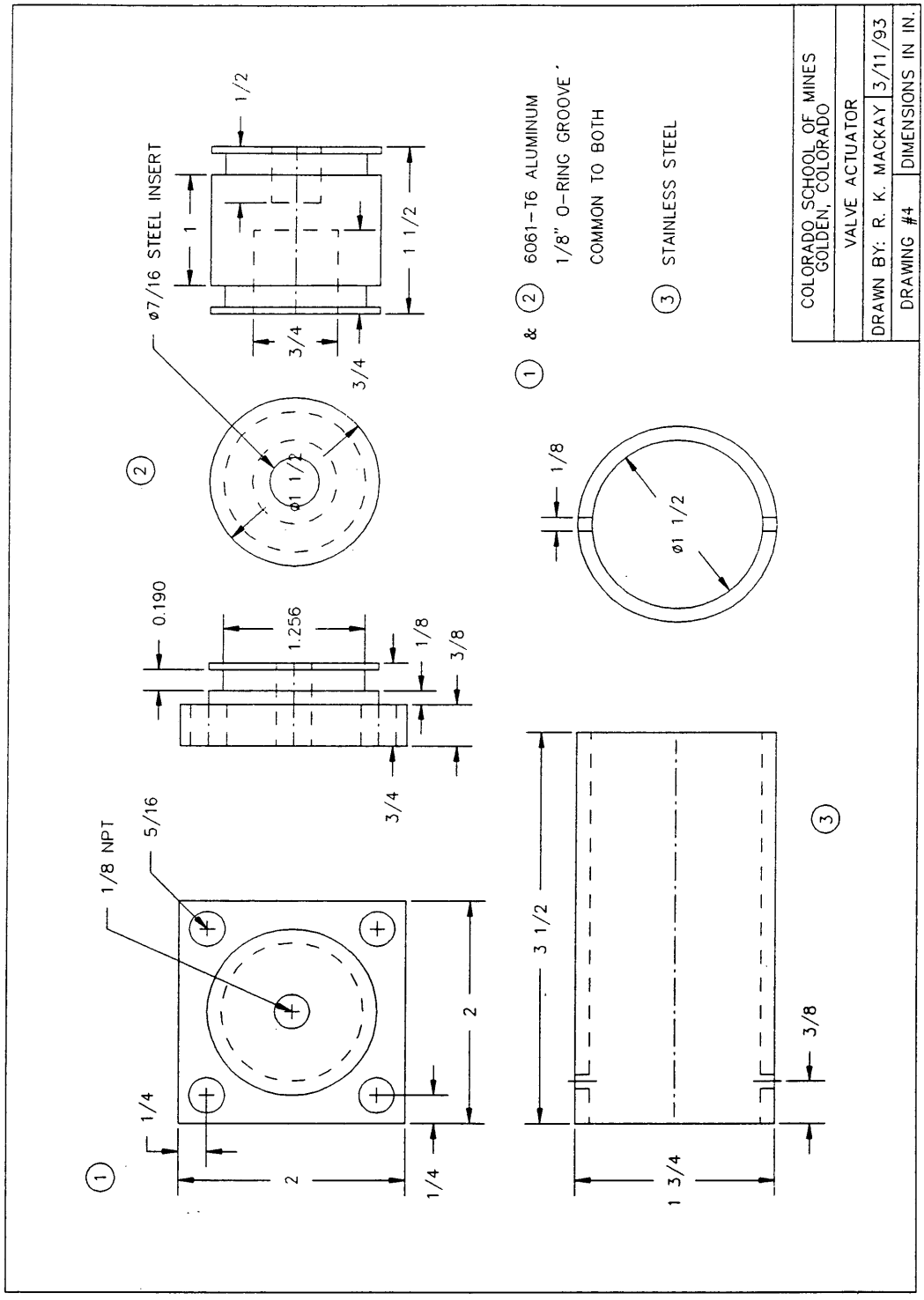
1/8 NPT
5/16
1/4
2
2
1/4
0.190
1.256
1/8
3/8
3/4
ø7/16 STEEL INSERT
1
1/2
1 1/2
3/4
3/4
ø1 1/2
1/8
ø1 1/2
3 1/2
3/8
1 3/4
① & ② 6061-T6 ALUMINUM
1/8" O-RING GROOVE
COMMON TO BOTH
③ STAINLESS STEEL
COLORADO SCHOOL OF MINES
GOLDEN, COLORADO
VALVE ACTUATOR
DRAWN BY: R. K. MACKAY
3/11/93
DRAWING #4
DIMENSIONS IN IN.

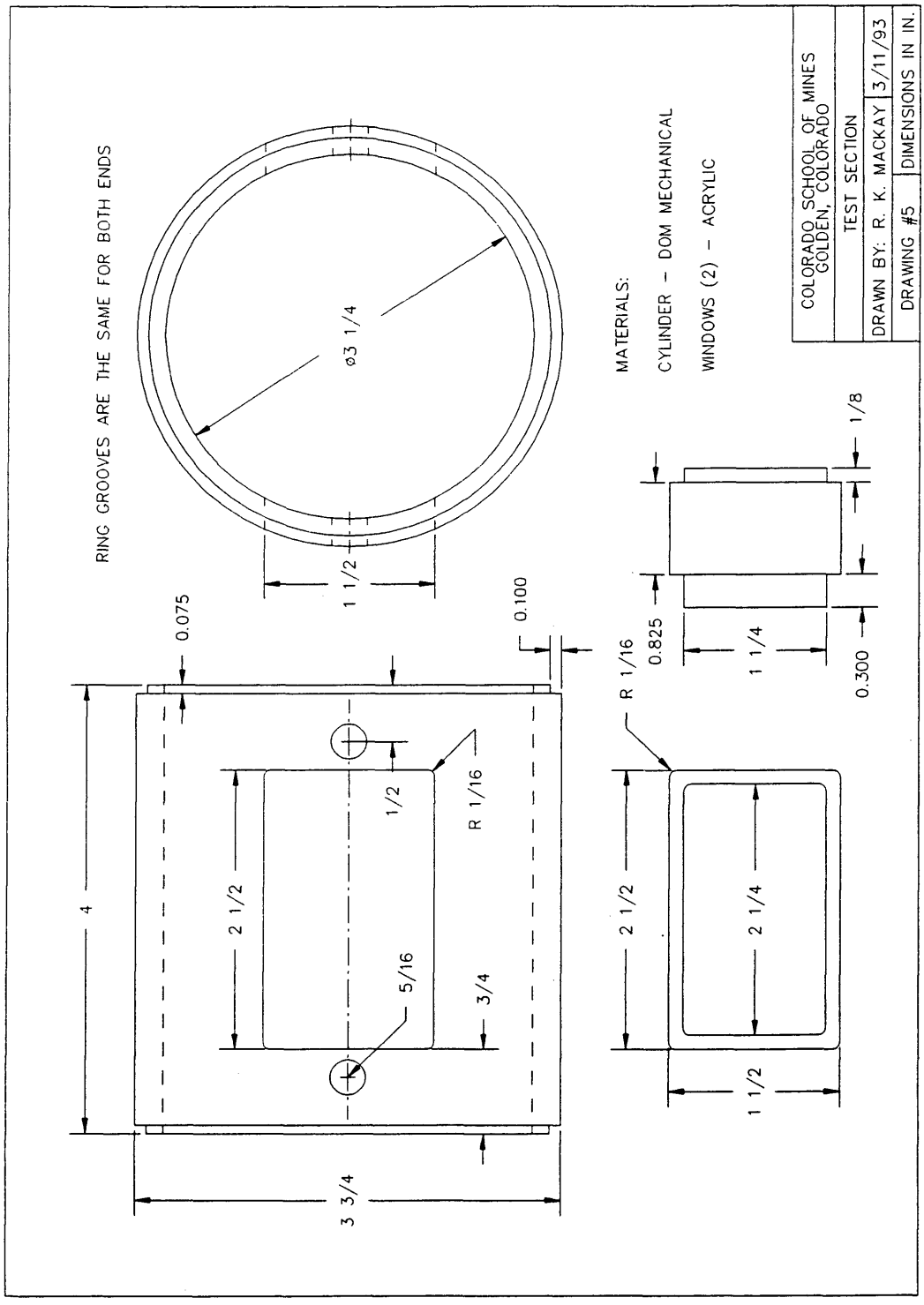
RING GROOVES ARE THE SAME FOR BOTH ENDS
ø3 1/4
1 1/2
0.075
0.100
4
2 1/2
1/2
R 1/16
5/16
3/4
3 3/4
MATERIALS:
CYLINDER - DOM MECHANICAL
WINDOWS (2) - ACRYLIC
R 1/16
0.825
1/8
1 1/4
0.300
2 1/2
2 1/4
1 1/2
COLORADO SCHOOL OF MINES
GOLDEN, COLORADO
TEST SECTION
DRAWN BY: R. K. MACKAY
3/11/93
DRAWING #5
DIMENSIONS IN IN.

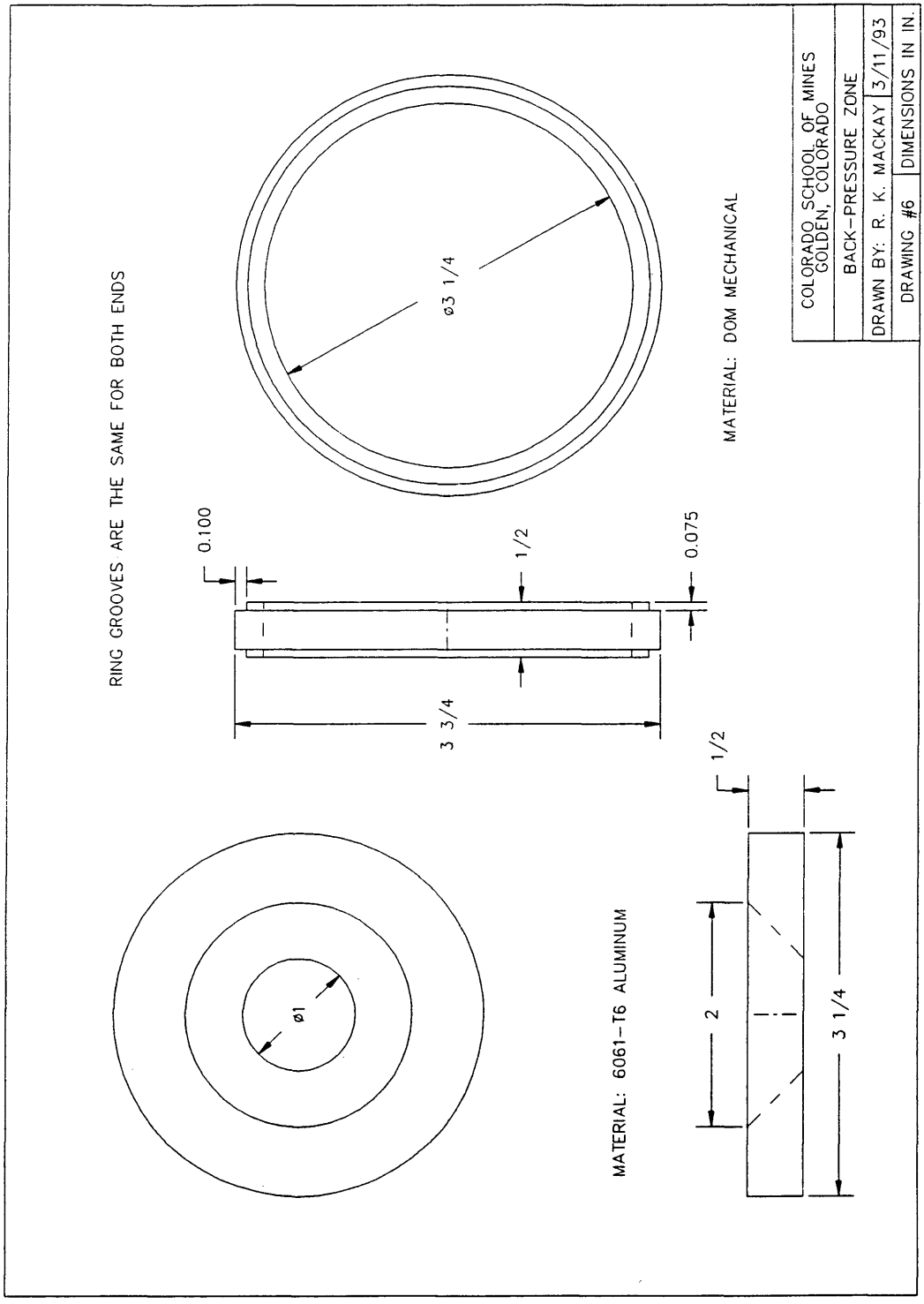
RING GROOVES ARE THE SAME FOR BOTH ENDS
ø3 1/4
0.100
1/2
0.075
3 3/4
MATERIAL: DOM MECHANICAL
ø1
MATERIAL: 6061-T6 ALUMINUM
1/2
2
3 1/4
COLORADO SCHOOL OF MINES
GOLDEN, COLORADO
BACK-PRESSURE ZONE
DRAWN BY: R. K. MACKAY
3/11/93
DRAWING #6
DIMENSIONS IN IN.

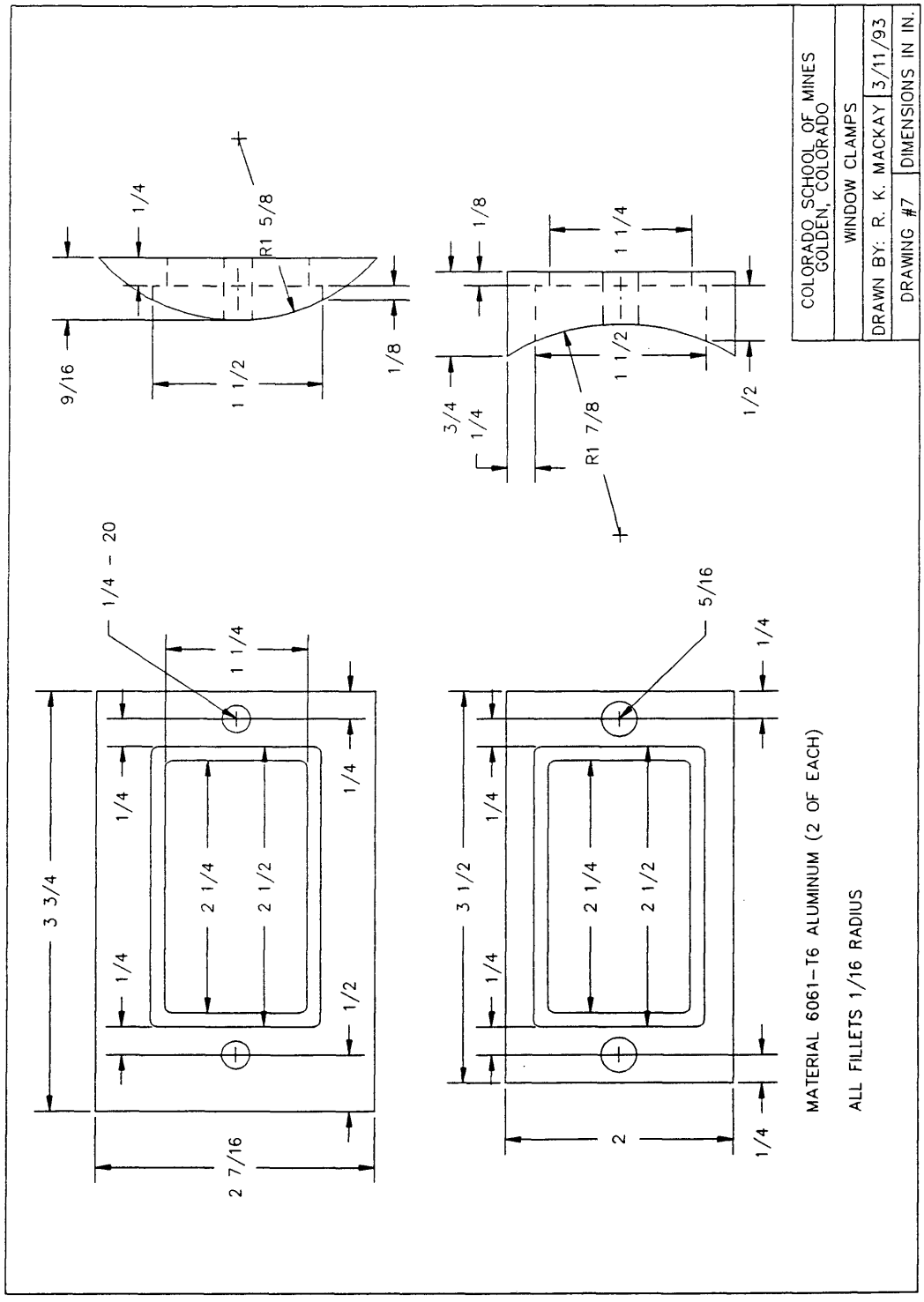
COLORADO SCHOOL OF MINES
GOLDEN, COLORADO
WINDOW CLAMPS
DRAWN BY: R. K. MACKAY
3/11/93
DRAWING #7
DIMENSIONS IN IN.
MATERIAL 6061-T6 ALUMINUM (2 OF EACH)
ALL FILLETS 1/16 RADIUS
1/4 - 20
5/16
R1 5/8
R1 7/8
3 3/4
3 1/2
2 7/16
2
2 1/4
2 1/2
1 1/4
1 1/2
1/4
1/8
1/2
3/4
9/16

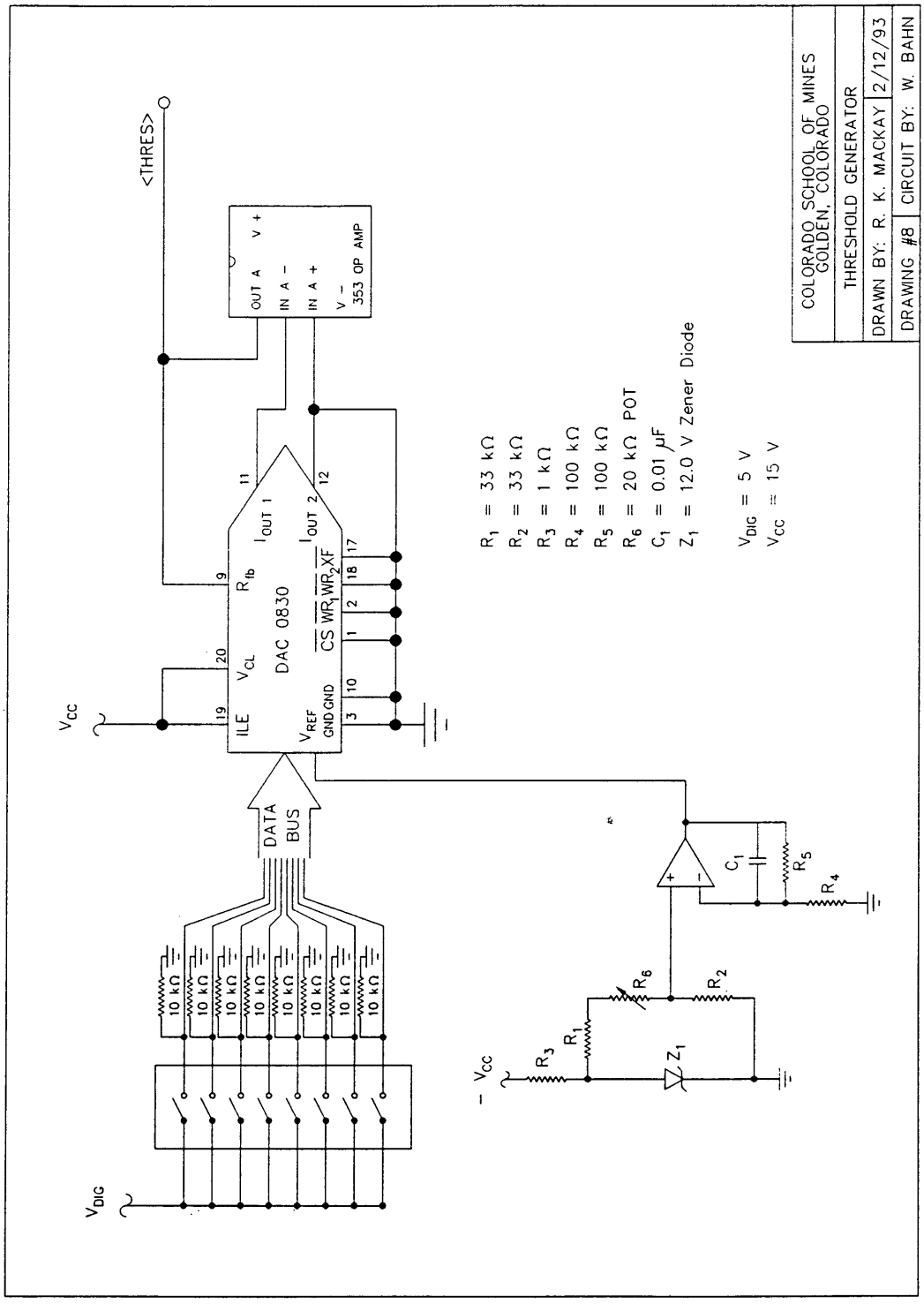
COLORADO SCHOOL OF MINES
GOLDEN, COLORADO
THRESHOLD GENERATOR
DRAWN BY: R. K. MACKAY 2/12/93
DRAWING #8 CIRCUIT BY: W. BAHN
<THRES>
OUT A
V +
IN A −
IN A +
V −
353 OP AMP
DAC 0830
ILE
V_{CL}
R_{fb}
$I_{OUT\ 1}$
$I_{OUT\ 2}$
$\overline{CS}$
$\overline{WR_1}$
$\overline{WR_2}$
XF
V_{REF}
GND
V_{CC}
DATA BUS
V_{DIG}
10 kΩ
R_1 = 33 kΩ
R_2 = 33 kΩ
R_3 = 1 kΩ
R_4 = 100 kΩ
R_5 = 100 kΩ
R_6 = 20 kΩ POT
C_1 = 0.01 μF
Z_1 = 12.0 V Zener Diode
V_{DIG} = 5 V
V_{CC} = 15 V

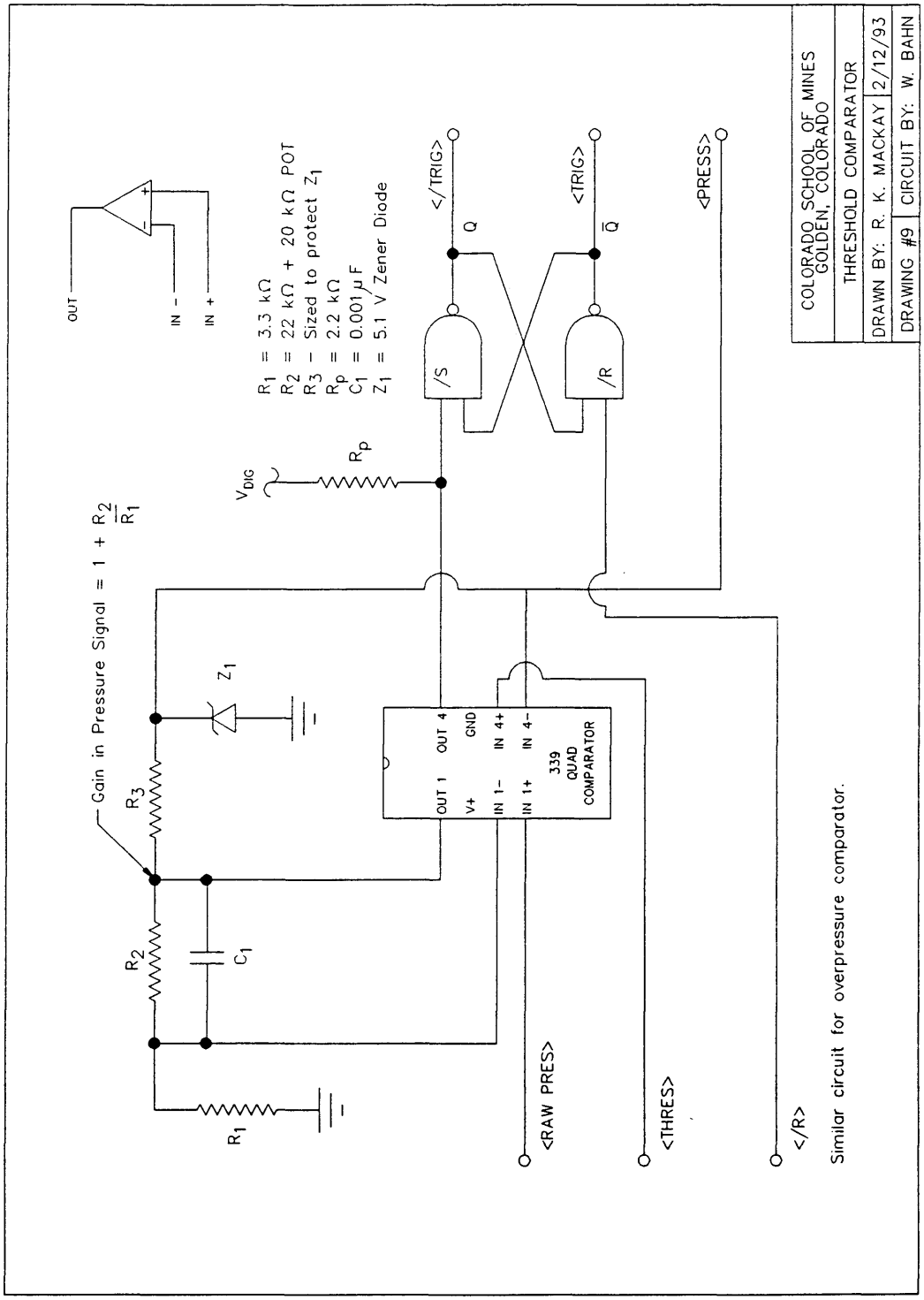
COLORADO SCHOOL OF MINES
GOLDEN, COLORADO
THRESHOLD COMPARATOR
DRAWN BY: R. K. MACKAY 2/12/93
DRAWING #9 CIRCUIT BY: W. BAHN
Gain in Pressure Signal = 1 + R2/R1
R1 = 3.3 kΩ
R2 = 22 kΩ + 20 kΩ POT
R3 - Sized to protect Z1
Rp = 2.2 kΩ
C1 = 0.001 μF
Z1 = 5.1 V Zener Diode
OUT
IN -
IN +
VDIG
Rp
R3
R2
C1
R1
Z1
/S
/R
Q
Q̄
</TRIG>
<TRIG>
<PRESS>
OUT 1
V+
IN 1-
IN 1+
OUT 4
GND
IN 4+
IN 4-
339
QUAD
COMPARATOR
<RAW PRES>
<THRES>
</R>
Similar circuit for overpressure comparator.

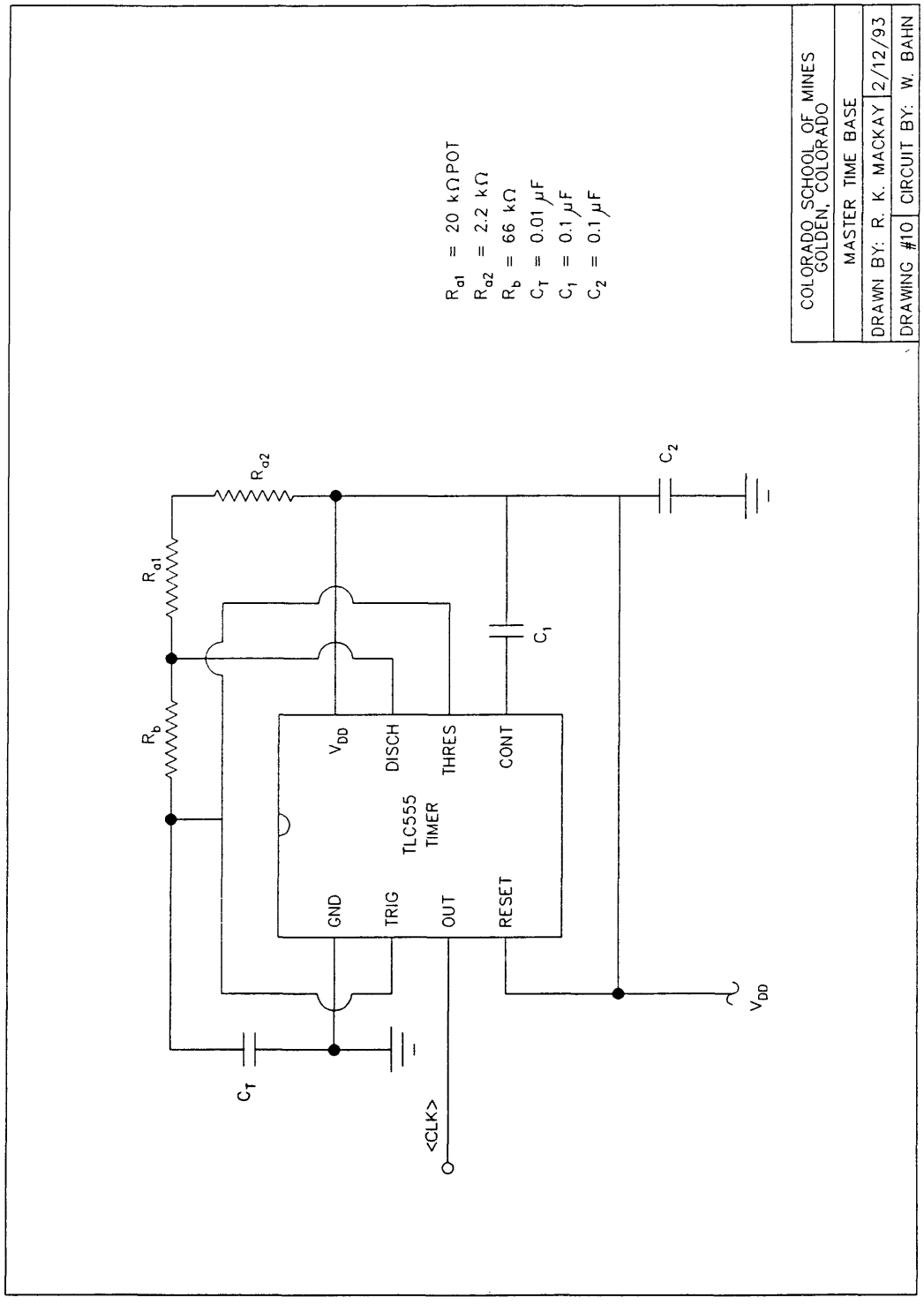
COLORADO SCHOOL OF MINES
GOLDEN, COLORADO
MASTER TIME BASE
DRAWN BY: R. K. MACKAY
2/12/93
DRAWING #10
CIRCUIT BY: W. BAHN
R_{a1} = 20 kΩ POT
R_{a2} = 2.2 kΩ
R_b = 66 kΩ
C_T = 0.01 μF
C_1 = 0.1 μF
C_2 = 0.1 μF
R_{a2}
R_{a1}
R_b
C_2
C_1
C_T
V_{DD}
DISCH
THRES
CONT
TLC555
TIMER
GND
TRIG
OUT
RESET
<CLK>

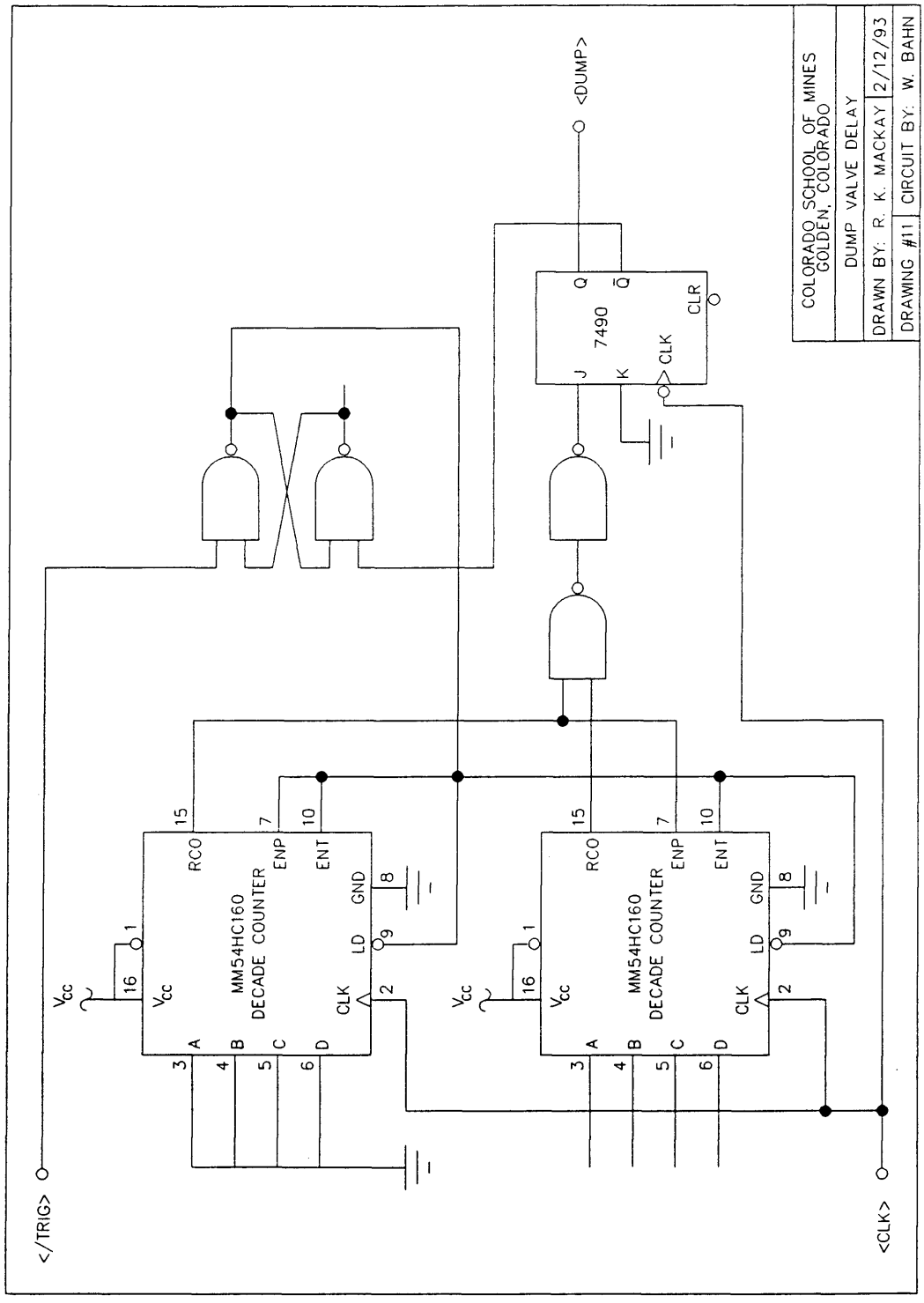
COLORADO SCHOOL OF MINES
GOLDEN, COLORADO
DUMP VALVE DELAY
DRAWN BY: R. K. MACKAY 2/12/93
DRAWING #11 CIRCUIT BY: W. BAHN
<DUMP>
7490
J
K
CLK
Q
Q̄
CLR
MM54HC160
DECADE COUNTER
RCO
ENP
ENT
GND
LD
CLK
A
B
C
D
Vcc
</TRIG>
<CLK>

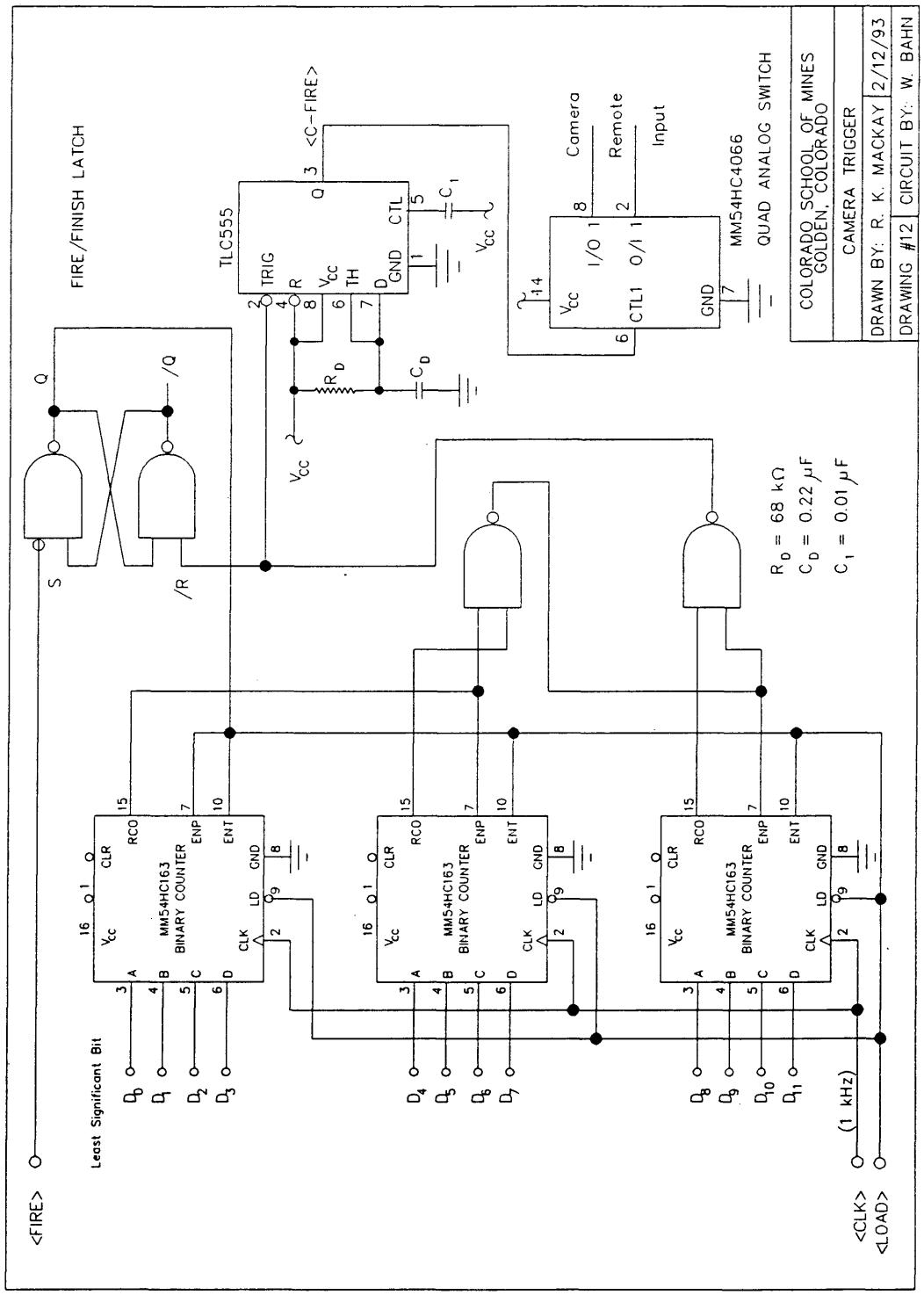
FIRE/FINISH LATCH
TLC555
<C-FIRE>
Camera
Remote
Input
MM54HC4066
QUAD ANALOG SWITCH
COLORADO SCHOOL OF MINES
GOLDEN, COLORADO
CAMERA TRIGGER
DRAWN BY: R. K. MACKAY 2/12/93
DRAWING #12 CIRCUIT BY: W. BAHN
MM54HC163
BINARY COUNTER
Least Significant Bit
(1 kHz)
<FIRE>
<CLK>
<LOAD>
R_D = 68 kΩ
C_D = 0.22 μF
C_1 = 0.01 μF

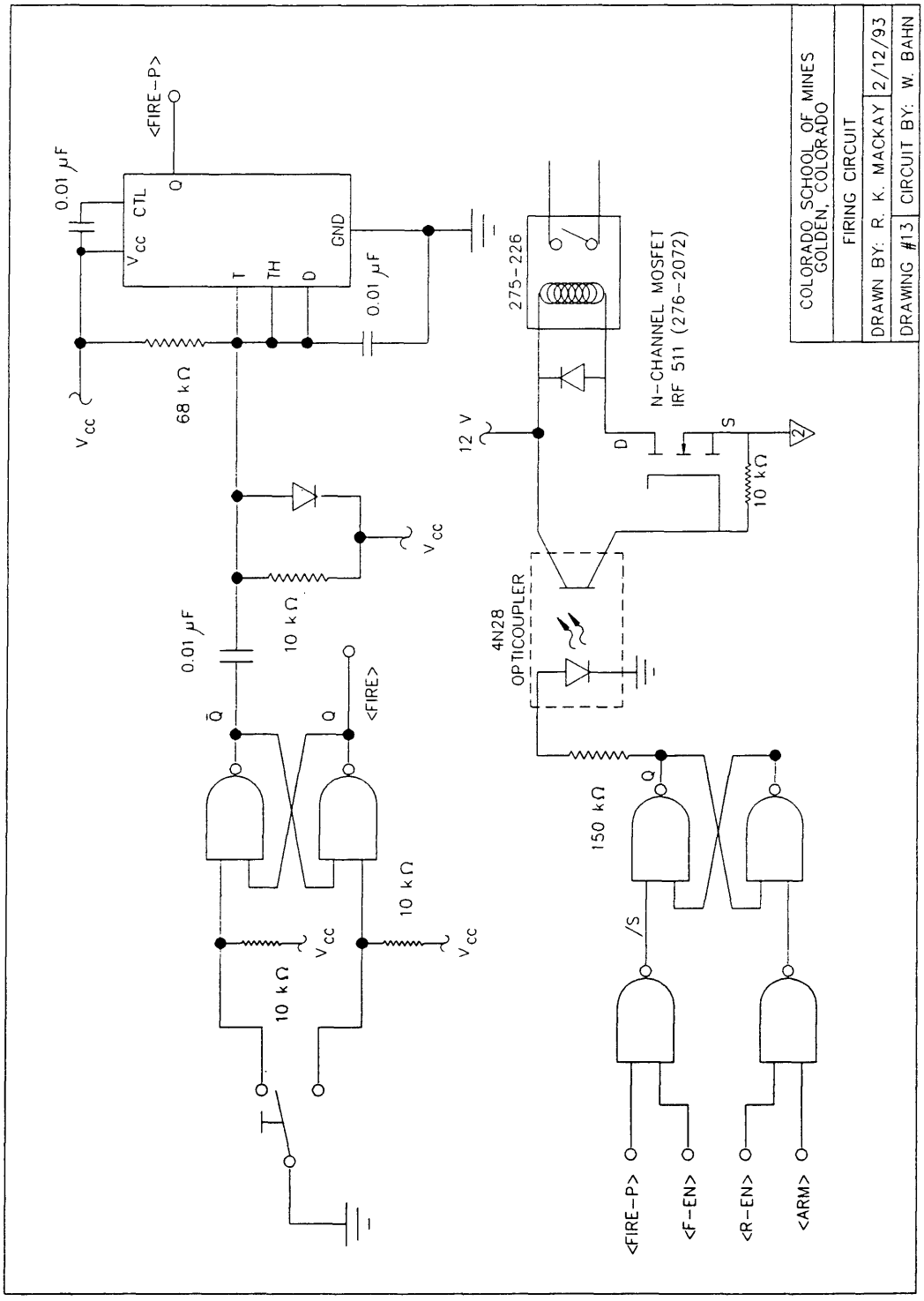
COLORADO SCHOOL OF MINES
GOLDEN, COLORADO
FIRING CIRCUIT
DRAWN BY: R. K. MACKAY 2/12/93
DRAWING #13 CIRCUIT BY: W. BAHN
<FIRE-P>
0.01 μF
CTL
Q
Vcc
GND
T
TH
D
0.01 μF
68 kΩ
Vcc
275-226
N-CHANNEL MOSFET
IRF 511 (276-2072)
12 V
D
S
10 kΩ
4N28
OPTICOUPLER
Vcc
0.01 μF
10 kΩ
Q̄
Q
<FIRE>
150 kΩ
/S
10 kΩ
Vcc
10 kΩ
Vcc
<FIRE-P>
<F-EN>
<R-EN>
<ARM>

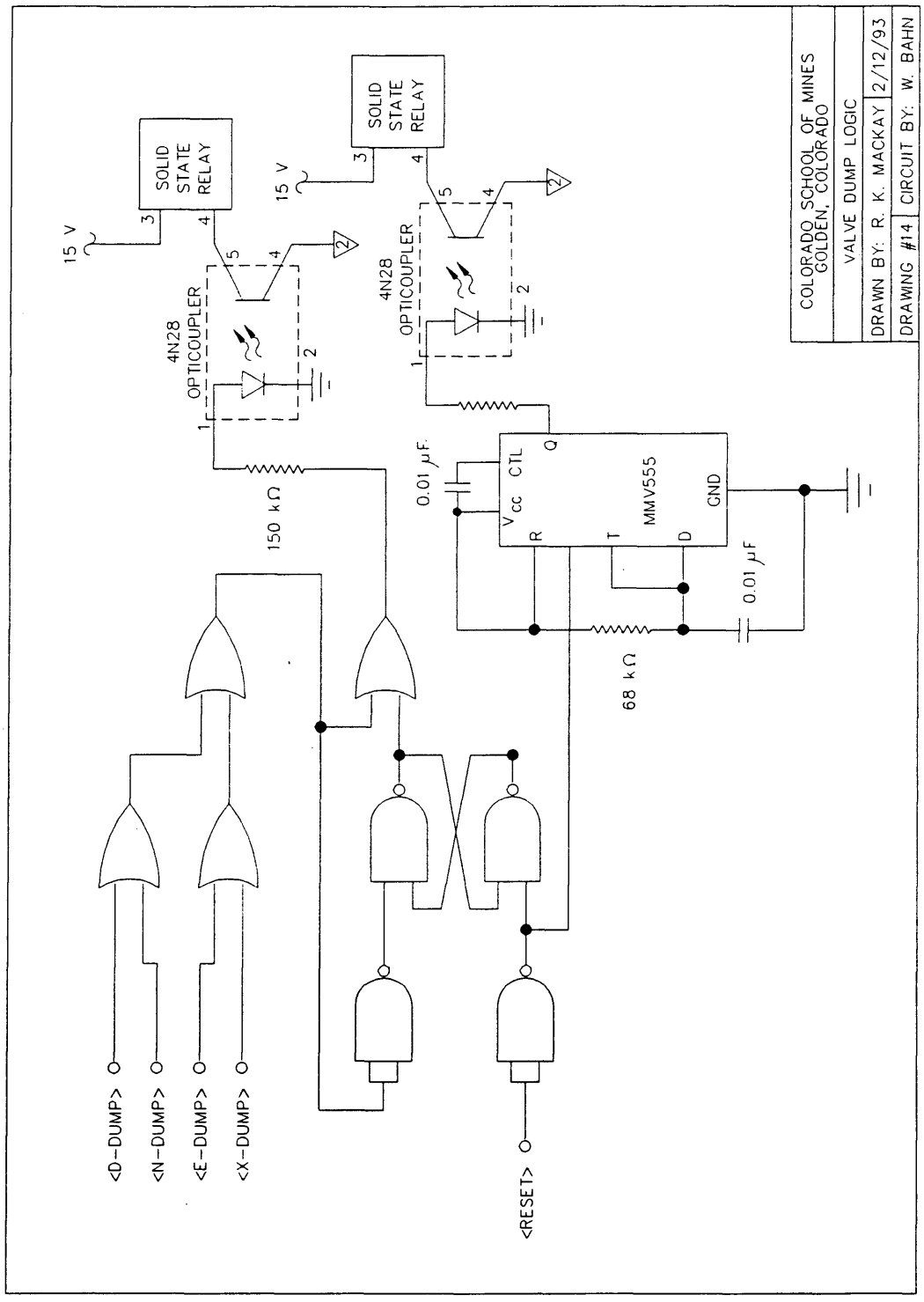
COLORADO SCHOOL OF MINES
GOLDEN, COLORADO
VALVE DUMP LOGIC
DRAWN BY: R. K. MACKAY 2/12/93
DRAWING #14 CIRCUIT BY: W. BAHN
SOLID STATE RELAY
SOLID STATE RELAY
15 V
15 V
4N28 OPTICOUPLER
4N28 OPTICOUPLER
150 kΩ
0.01 μF
MMV555
Vcc CTL Q R T D GND
0.01 μF
68 kΩ
<D-DUMP>
<N-DUMP>
<E-DUMP>
<X-DUMP>
<RESET>

APPENDIX C

```
C    +-----------------------------------------------------+
C    | BDCB.FOR                                            |
C    | Version 1.0                                         |
C    | By R. K. Mackay                                     |
C    | October 1993                                        |
C    |                                                     |
C    | This program will calculate both burned and unburned|
C    | gas temperature, mass fraction, and volume for the  |
C    | combustion of methane in the Blow-Down Combustion   |
C    | Bomb using a two zone thermodynamic model. Additional|
C    | output includes the area burned fraction, flame     |
C    | speed, heat transfer and mole fractions of the      |
C    | product species. The pressure data is entered into  |
C    | the program via an input file labeled INPUT.DAT. The|
C    | time between these data points is entered as an input|
C    | variable whose spacing must be equidistant. Other   |
C    | input variables are vacuum, fuel and air pressures as|
C    | well as reactant temperature and Fast-Acting Dump   |
C    | Valve opening time. The subroutine REAC determines  |
C    | the thermochemical properties of methane and dry air|
C    | for a given temperature while PER determines the same|
C    | for the products given the temperature and pressure.|
C    | A shifting equilibrium is assumed at each time step.|
C    +-----------------------------------------------------+
C
C    +-----------------------------------------------------+
C    | List of Variables                                   |
C    |                                                     |
C    | AN,ANR  Number of C Molecules in Fuel               |
C    | AM,AMR  Number of H Molecules in Fuel               |
C    | AL,ALR  Number of O Molecules in Fuel               |
C    | AK,AKR  Number of N Molecules in Fuel               |
C    | A       Area of Orifice Holes          in^2         |
C    | AW      Wetted Area of Burned Gas      in^2         |
C    | AWMAX   Internal Area of BDCB          in^2         |
C    | ARATIO  Area Fraction Burned                        |
C    | BORE    Internal Diameter of BDCB      in           |
C    | BCON    Boundary Layer Growth Rate     in/sec       |
C    | BRAD    Burned Gas Radius              in           |
C    | CORR    Error in Adiabatic Flame                    |
C    |         Temperature Calculation        R            |
C    | DT      Time Increment                 sec          |
C    | DIST    Flame Travel Distance          in           |
C    | DPDT    Pressure Rate of Change        psia/sec     |
C    | DTUDT   Unburned Gas Temperature                    |
C    |         Rate of Change                 R/sec        |
C    | DTBDT   Burned Gas Temperature Rate                 |
C    |         of Change                      R/sec        |
```

C	DMDT	Burned Mass Rate of Change	lbm/sec
C	DVDT	Volume Burned Rate of Change	in^3/sec
C	DHTR	Constant Pressure Specific Heat for Unburned Gas	BTU/lbm-R
C	DUTR	Constant Volume Specific Heat for Unburned Gas	BTU/lbm-R
C	DHT	Constant Pressure Specific Heat for Burned Gas	BTU/lbm-R
C	DUT	Constant Volume Specific Heat for Burned Gas	BTU/lbm-R
C	DUP	Derivative of Internal Energy wrt Pressure for Burned Gas	BTU/lbm-psia
C	DRT	Derivative of Specific Gas Constant wrt Temperature for Burned Gas	BTU/lbm
C	DRP	Derivative of Specific Gas Constant wrt Pressure for Burned Gas	BTU/lbm-R-psia
C	F,RF	Equivalence Ratio	
C	FRMB	Mass Flow Rate at Burned Gas T, P	lbm/sec
C	FRMU	Mass Flow Rate at Unburned Gas T, P	lbm/sec
C	H	Enthalpy of Burned Gas	BTU/lbm
C	HU	Enthalpy of Unburned Gas	BTU/lbm
C	HEIGHT	Length of Test Section in BDCB	in
C	HEAD	Surface Area of Cylinder Head	in^2
C	INTR	Flag Indicating Maximum Pressure	
C	KOUNT	Total Number of Data Points	
C	MCODE	Flag Indicating No Reactants Left	
C	N	Number of Orifice Holes	
C	PATM	Vacuum Pressure	psia
C	PFUEL	Methane Pressure	psia
C	PAIR	Dry Air Pressure	psia
C	PTOT	Vacuum + Final Gage Pressure	psia
C	PE,P	Data Pressure + PTOT	psia
C	Q	Heat Flux Rate	BTU/in^2-sec
C	QB	Burned Gas Heat Transfer Rate	BTU/sec
C	R	Specific Gas Constant for Products	BTU/lbm-R
C	RU	Specific Gas Constant for Reactants	BTU/lbm-R
C	SFL	Flame Speed at STP	in/sec
C	SFLAME	Flame Speed at Unburned Gas T, P	in/sec

```
C     |  SKB      Ratio of Specific Heats for                          |
C     |           Products                                             |
C     |  SKU      Ratio of Specific Heats for                          |
C     |           Reactants                                            |
C     |  TRG      Valve Opening Time              sec                  |
C     |  TIME     Experimental Time               sec                  |
C     |  TINC     Fraction of Time Between                             |
C     |           Data Points Where Transition                         |
C     |           Occurs                          sec                  |
C     |  TWALL    Wall Temperature of BDCB        R                    |
C     |  TI       Temperature of Reactants                             |
C     |           Before Ignition                 R                    |
C     |  TU       Unburned Gas Temperature        R                    |
C     |  T,TB     Burned Gas Temperature          R                    |
C     |  TAC      Adiabatic Core Temperature      R                    |
C     |  TMEAN    Mean Temperature of Adiabatic                        |
C     |           Core and BDCB Wall              R                    |
C     |  THERM    Thermal Conductivity            BTU/R-in-sec         |
C     |  U        Internal Energy of Products     BTU/lbm              |
C     |  UU       Internal Energy of Reactants    BTU/lbm              |
C     |  V        Total Internal Volume of BDCB   in^3                 |
C     |  VB       Burned Gas Volume               in^3                 |
C     |  VU       Unburned Gas Volume             in^3                 |
C     |  VBF      Volume Burned Fraction                               |
C     |  XCO      Mole Fraction of CO             mole                 |
C     |  ZMB      Burned Mass                     lbm                  |
C     |  ZMU      Unburned Mass                   lbm                  |
C     |  ZMT      Total Mass (Burned +                                 |
C     |           Unburned)                       lbm                  |
C     |  ZMBF     Burned Mass Fraction                                 |
C     |                                                                |
C     |  ** All Other Variables are Used for Intermediate              |
C     |     Calculation **                                             |
C     +----------------------------------------------------------------+
C
      IMPLICIT DOUBLE PRECISION (A-H,O-Z)
      COMMON/BLOC/AN,AM,AL,AK,F,T,P,KLO,IERR,XEQ(12),XPA
      COMMON/TAB/DXT(12),DXP(12),DXF(12)
      COMMON/PROP/AVM,R,H,U,DRT,DHT,DUT,DRP,DHP,DUP,DRF,DHF
     1 ,DUF
      COMMON/RBLOC/ANR,AMR,ALR,AKR,RF,TI,R0R,IERRR
      COMMON/RPROP/AVMR,RU,HU,UU,DHTR,DUTR
C
      PARAMETER(PIE=3.141592654)
      DIMENSION PE(99),DPDT(99),TU(99),DTUDT(99)
      DIMENSION TAC(99),Q(99),SFLAME(99)
      DATA N/75/,A/0.0016/,BORE/3.25/,HEIGHT/4.0/
C
```

```
      OPEN(3,FILE='INPUT.DAT')
      OPEN(5,FILE='TEMP.DAT',STATUS='NEW')
      OPEN(7,FILE='MASS.DAT',STATUS='NEW')
      OPEN(9,FILE='HEAT.DAT',STATUS='NEW')
C
      WRITE(*,*) 'Enter Vacuum Pressure (in. Hg)'
      READ(*,*) PATM
      WRITE(*,*) 'Enter Fuel Pressure (psig)'
      READ(*,*) PFUEL
      WRITE(*,*) 'Enter Fill Pressure (psig)'
      READ(*,*) PTOT
      WRITE(*,*) 'Enter Reactant Temperature (R)'
      READ(*,*) TI
      WRITE(*,*) 'Enter Number of Data Points'
      READ(*,*) KOUNT
      WRITE(*,*) 'Enter the Time Increment (msec)'
      READ(*,*) DT
      WRITE(*,*) 'Enter the Trigger Time (msec)'
      READ(*,*) TRG
      WRITE(*,*) 'Pressure Data is Entered from File'
C
C   +-----------------------------------------------------+
C   | The following section performs initial calculations |
C   | for parameters used later in the program.           |
C   +-----------------------------------------------------+
C
      HEAD=0.25*PIE*(BORE**2)
      V=HEAD*HEIGHT
      AWMAX=2.0*HEAD+PIE*BORE*HEIGHT
      TWALL=TI
      PATM=PATM/29.92127
      PFUEL=PATM+PFUEL/14.696
      PAIR=PTOT/14.696-PFUEL
      PTOT=PATM+PTOT/14.696
      DT=DT/1000.0
      TRG=(TRG+10.0)/1000.0
      BCON=0.07874/SQRT(DT*KOUNT)
C
C   +-----------------------------------------------------+
C   | The following section determines the reactant       |
C   | enthalpy and equivalence ratio for the fuel-air     |
C   | mixture charge in the BDCB.                         |
C   +-----------------------------------------------------+
C
      ANR=1.0
      AMR=4.0
      ALR=0.0
      AKR=0.0
```

```
      COEF=(ANR+0.25*AMR-0.5*ALR)
      RF=PFUEL*4.7718*COEF/PAIR
      ROR=COEF/RF
      CALL REAC(1)
      WRITE(*,5) HU
    5 FORMAT(/' Reactant Enthalpy (BTU/lbm) =',F7.2)
      WRITE(*,10) RF
   10 FORMAT(' Equivalence Ratio =',F7.4)
C
C    +-----------------------------------------------------+
C    | The following section determines the adiabatic flame |
C    | temperature.                                         |
C    +-----------------------------------------------------+
C
      AN=ANR
      AM=AMR
      AL=ALR
      AK=AKR
      F=RF
      KLO=1
      FRATIO=1.0+0.027*F
      SFL=14.173-51.181*(F-1.0)**2
      P=PTOT*14.696
      T=4000.0
   15 CALL PER(1)
      IF(IERR.NE.0) GOTO 85
      CORR=(H-HU)/DHT
      T=T-CORR
      IF(ABS(CORR).LT.1.) THEN
            WRITE(*,20) T
   20       FORMAT(' Flame Temperature (R) =',F8.1,/)
      ELSE
            GOTO 15
      ENDIF
      IF (KOUNT.EQ.1) GOTO 95
C
C    +-----------------------------------------------------+
C    | The following section determines the unburned gas    |
C    | and adiabatic core temperatures for the given        |
C    | fuel-air mixture and pressure trace. The heat flux   |
C    | rate from the adiabatic core to the BDCB is also     |
C    | determined as is the flame speed, which is dependent |
C    | on the temperature of the unburned gases.            |
C    +-----------------------------------------------------+
C
      TIB=T
      TIU=TI
      TIME=0.0
```

```
      DO 25 I = 1,KOUNT
      READ(3,*) PE(I)
      PE(I)=PE(I)/14.696+PTOT
      PE(I)=PE(I)*14.696
      P=PE(I)
      CALL REAC(1)
      CALL PER(1)
      SKU=DHTR/DUTR
      SKB=DHT/DUT
      TU(I)=TIU*(PE(I)/PE(1))**((SKU-1.0)/SKU)
      TAC(I)=TIB*(PE(I)/PE(1))**((SKB-1.0)/SKB)
      TMEAN=(TAC(I)+TWALL)/2
      T=TMEAN
      CALL PER(1)
      THERM=(9.0*DHT-5.0*DUT)*3.0614E-9*(TMEAN**0.7)/FRATIO
      IF(I.NE.1) Q(I)=THERM*(TAC(I)-TWALL)/(BCON*SQRT(TIME))
      SFLAME(I)=SFL*(PE(I)*540.0/(14.696*TU(I)))**0.19
      TI=TU(I)
      T=TAC(I)
      TIME=TIME+DT
   25 CONTINUE
C
C   +-----------------------------------------------------+
C   | The following section calculates the rates of change |
C   | of pressure and unburned gas temperature using       |
C   | Lagrande's five point formula for numerical          |
C   | differentiation. The first and last terms are        |
C   | determined using three point formulas.               |
C   +-----------------------------------------------------+
C
      INTR=0
      DO 30 I=1,KOUNT
      IF (I.LE.2) THEN
            DPDT(I)=(-3.0*PE(I)+4.0*PE(I+1)-PE(I+2))
     1      /(2.0*DT)
            GO TO 30
      ENDIF
      IF (I.GE.(KOUNT-1)) THEN
            DPDT(I)=(PE(I-2)-4.0*PE(I-1)+3.0*PE(I))/(2.0*DT)
            GO TO 30
      ENDIF
      DPDT(I)=(PE(I-2)-8.0*PE(I-1)+8.0*PE(I+1)-PE(I+2))
     1 /(12.0*DT)
      IF(INTR.NE.0) GOTO 30
      IF(DPDT(I).LE.0.0) INTR=I
   30 CONTINUE
C
      DO 35 I=1,KOUNT
```

```
      IF (I.LE.2) THEN
            DTUDT(I)=(-3.0*TU(I)+4.0*TU(I+1)-TU(I+2))
     1      /(2.0*DT)
            GO TO 35
      ENDIF
      IF (I.GE.(KOUNT-1)) THEN
            DTUDT(I)=(TU(I-2)-4.0*TU(I-1)+3.0*TU(I))
     1      /(2.0*DT)
            GO TO 35
      ENDIF
      DTUDT(I)=(TU(I-2)-8.0*TU(I-1)+8.0*TU(I+1)-TU(I+2))
     1 /(12.0*DT)
   35 CONTINUE
C
C   +-----------------------------------------------------+
C   | The following section initialize variables that are |
C   | used to solve the differential equations obtained   |
C   | from the first law of thermodynamics analysis. The  |
C   | output data files TEMP, HEAT, and MASS are also     |
C   | given appropriate headings at this point.           |
C   +-----------------------------------------------------+
C
      TIME=0.0
      DIST=0.0
      MCODE=0
      VB=0.0
      VU=V-VB
      P=PE(1)
      T=TIB
      TB=T
      TI=TIU
      CALL REAC(0)
      CALL PER(0)
      ZMU=P*VU/(RU*TIU*9338.4)
      ZMB=P*VB/(R*TIB*9338.4)
      ZMT=ZMB+ZMU
C
      WRITE(5,40)
   40 FORMAT(6X,'t (s)',6X,'Tu (R)',4X,'Tb (R)',5X,
     1 'Tac (R)',/)
      WRITE(7,45)
   45 FORMAT(8X,'t (s)',6X,'Mb (lbm)',7X,'Mb/Mt',8X,
     1 'Vb/V',/)
      WRITE(9,50)
   50 FORMAT(6X,'t (s)',6X,'Ab/At',3X,'Vel (in/s)',2X,
     1'Qb (BTU/s)',4X,'[CO]',/)
C
C   +-----------------------------------------------------+
```

```
C    ¦ The following section determines the rate of change  ¦
C    ¦ for burned mass, volume and temperature for          ¦
C    ¦ conditions at time t. Calculations are also made as  ¦
C    ¦ to the extent of the reaction with regards to burned ¦
C    ¦ area, mass and volume.                               ¦
C    +------------------------------------------------------+
C
      DO 55 I=1,(KOUNT-1)
      IF(I.EQ.1) GOTO 60
      ZMBH=ZMB
      VBH=VB
      J=I
      P=PE(J)
      TI=TU(J)
      T=TB
      CALL REAC(1)
      CALL PER(1)
      SKU=DHTR/DUTR
      SKB=DHT/DUT
      BRAD=(1.5*VB/PIE)**(1.0/3.0)
      IF(BRAD.LE.(0.5*BORE)) THEN
            AW=PIE*(BRAD**2)
      ELSE
            DIST=DIST+(SFLAME(J+1)+SFLAME(J))*DT/2
            AW=HEAD+PIE*BORE*DIST
      ENDIF
      IF(AW.GE.AWMAX) AW=AWMAX
      QB=AW*Q(J)
C
      SKFB=SQRT(SKB)/((0.5+SKB/2.0)**((SKB+1.0)
     1 /(2.0*SKB-2.0)))
      FRMB=N*A*P*SKFB*0.20333/SQRT(R*T)
      SKFU=SQRT(SKU)/((0.5+SKU/2.0)**((SKU+1.0)
     1 /(2.0*SKU-2.0)))
      FRMU=N*A*P*SKFU*0.20333/SQRT(RU*TI)
      IF(TIME.LT.TRG) FRMU=0.0
      IF(MCODE.EQ.1) THEN
            ZMB=ZMB-FRMB*DT
            GOTO 65
      ENDIF
      IF(((FRMU*DT).GT.ZMU).AND.(MCODE.EQ.0)) THEN
            TINC=ZMU/FRMU
            ZMB=ZMB-FRMB*(DT-TINC)
            ZMT=ZMT-FRMB*(DT-TINC)-FRMU*TINC
            ZMU=0.0
            VB=V
            MCODE=1
            GOTO 65
```

```
      ENDIF
C
      ALFA=DUT/(R+T*DRT)
      BETA=1.0+ALFA
      DMDT1=((ZMU*RU*DTUDT(J)-FRMU*TU(J)*RU)*BETA-QB
     1 -DPDT(J)*(ALFA*V/9338.4+ZMB*DUP+VU/9338.4
     1 -ALFA*ZMB*T*DRP))/(U-UU+ALFA*(RU*TU(J)-R*T))
      DVDT1=VU*(DPDT(J)/P-DTUDT(J)/TU(J))
     1 +9338.4*RU*TU(J)*DMDT1/PE(J)
      IF(DVDT1.LT.0.0) DVDT1=0.0
C
C    +-------------------------------------------------------+
C    | The following section determines the new burned mass  |
C    | and volume using the values of the time derivatives   |
C    | at time t.                                            |
C    +-------------------------------------------------------+
C
      ZMB=ZMB+DMDT1*DT
      IF(ZMB.GE.ZMT) ZMB=ZMT
      VB=VB+DVDT1*DT
      IF(VB.GT.V) VB=V
      ZMU=ZMT-ZMB
      VU=V-VB
      XCO1=XEQ(6)
C
C    +-------------------------------------------------------+
C    | The following section determines the rate of change   |
C    | for burned mass, volume and temperature for           |
C    | conditions at time t+1. Calculations are also made    |
C    | as to the extent of the reaction with regards to      |
C    | burned area, mass and volume.                         |
C    +-------------------------------------------------------+
C
      J=I+1
      P=PE(J)
      TI=TU(J)
      T=TB
      CALL REAC(1)
      CALL PER(1)
      BRAD=(1.5*VB/PIE)**(1.0/3.0)
      IF(BRAD.LE.(0.5*BORE)) THEN
            AW=PIE*BRAD**2
      ELSE
            DIST=DIST+(SFLAME(J+1)+SFLAME(J))*DT/2
            AW=HEAD+PIE*BORE*DIST
      ENDIF
      IF(AW.GE.AWMAX) AW=AWMAX
      QB=AW*Q(J)
```

```
      SKFB=SQRT(SKB)/((0.5+SKB/2.0)**((SKB+1.0)
     1 /(2.0*SKB-2.0)))
      FRMB=N*A*P*SKFB*0.20333/SQRT(R*T)
      SKFU=SQRT(SKU)/((0.5+SKU/2.0)**((SKU+1.0)
     1 /(2.0*SKU-2.0)))
      FRMU=N*A*P*SKFU*0.20333/SQRT(RU*TI)
      IF(TIME.LT.TRG) FRMU=0.0
C
      ALFA=DUT/(R+T*DRT)
      BETA=1.0+ALFA
      DMDT2=((ZMU*RU*DTUDT(J)-FRMU*TU(J)*RU)*BETA-QB
     1 -DPDT(J)*(ALFA*V/9338.4+ZMB*DUP+VU/9338.4
     1 -ALFA*ZMB*T*DRP))/(U-UU+ALFA*(RU*TU(J)-R*T))
      DVDT2=VU*(DPDT(J)/P-DTUDT(J)/TU(J))
     1 +9338.4*RU*TU(J)DMDT2/PE(J)
      IF(DVDT2.LT.0.0) DVDT2=0.0
C
C   +-----------------------------------------------------+
C   | The following section determines the improved values |
C   | for burned mass and volume using the Modified Euler  |
C   | Method. The burned gas temperature is also           |
C   | determined at this time.                             |
C   +-----------------------------------------------------+
C
      ZMB=ZMBH+(DMDT1+DMDT2)*DT/2.0
      IF(ZMB.GE.ZMT) ZMB=ZMT
      VB=VBH+(DVDT1+DVDT2)*DT/2.0
      IF(VB.GT.V) VB=V
      ZMU=ZMT-ZMB
      VU=V-VB
      TB=P*VB/(9338.4*R*ZMB)
      GOTO 60
   65 DTBDT=(-QB-FRMB*H-ZMB*DUP*DPDT(J))/(ZMB*DUT)
      TB=TB+DTBDT*DT
      XCO2=XEQ(6)
C
C   +-----------------------------------------------------+
C   | The following section outputs the calculated values  |
C   | to the DAT files TEMP, MASS and HEAT.                |
C   +-----------------------------------------------------+
C
   60 ZMBF=ZMB/ZMT
      VBF=VB/V
      ARATIO=AW/AWMAX
      XCO=(XCO1+XCO2)/2.0
      WRITE(5,70) TIME,TU(I),TB,TAC(I)
   70 FORMAT(3X,F8.4,3X,F8.1,3X,F8.1,3X,F8.1)
      WRITE(7,75) TIME,ZMB,ZMBF,VBF
```

```
   75 FORMAT(5X,F8.4,5X,F8.6,5X,F8.5,5X,F8.5)
      WRITE(9,80) TIME,ARATIO,SFLAME(I),QB,XCO
   80 FORMAT(3X,F8.4,3X,F8.5,3X,F8.4,3X,F8.4,3X,F8.4)
      TIME=TIME+DT
      IF (IERR.NE.0) GOTO 85
   55 CONTINUE
      IF (IERR.EQ.0) GOTO 95
   85 WRITE(*,90) IERR
   90 FORMAT(/,'Subroutine Error Code No.',I2)
   95 STOP
      END
C
C   +--------------------------------------------------+
C
      SUBROUTINE REAC(JDR)
C
      IMPLICIT DOUBLE PRECISION (A-H,O-Z)
      COMMON/RBLOC/ANR,AMR,ALR,AKR,RF,TI,R0R,IERRR
      COMMON/RPROP/AVMR,RU,HU,UU,DHTR,DUTR
      DIMENSION SHR(4),XR(4),HTF(28),HTO(28),HTN(28)
      DIMENSION CTF(28),CTO(28),CTN(28)
C
       DATA HTF/-13.579,-12.672,-11.635,-10.457, -9.141,
     1          -7.698, -6.137, -4.470, -2.708, -0.863,
     1           1.057,  3.042,  5.084,  7.177,  9.315,
     1          11.491, 13.703, 15.945, 18.214, 20.508,
     1          22.823, 25.158, 27.511, 29.879, 32.262,
     1          34.658, 37.065, 39.484/
       DATA HTO/  2.088,  2.799,  3.530,  4.285,  5.063,
     1           5.861,  6.675,  7.502,  8.341,  9.189,
     1          10.046, 10.910, 11.781, 12.658, 13.540,
     1          14.429, 15.324, 16.224, 17.129, 18.041,
     1          18.957, 19.879, 20.807, 21.739, 22.677,
     1          23.620, 24.568, 25.521/
       DATA HTN/  2.085,  2.782,  3.485,  4.197,  4.925,
     1           5.668,  6.427,  7.201,  7.989,  8.790,
     1           9.601, 10.422, 11.251, 12.087, 12.930,
     1          13.779, 14.632, 15.490, 16.352, 17.221,
     1          18.087, 18.958, 19.833, 20.710, 21.589,
     1          22.470, 23.352, 24.237/
       DATA CTF/  8.535,  9.680, 11.076, 12.483, 13.813,
     1          15.041, 16.157, 17.160, 18.052, 18.842,
     1          19.538, 20.150, 20.688, 21.161, 21.579,
     1          21.947, 22.273, 22.562, 22.820, 23.050,
     1          23.256, 23.441, 23.608, 23.758, 23.894,
     1          24.018, 24.131, 24.233/
       DATA CTO/  7.023,  7.196,  7.431,  7.670,  7.883,
     1           8.063,  8.212,  8.336,  8.439,  8.527,
```

```
     1           8.604,  8.674,  8.738,  8.800,  8.858,
     1           8.916,  8.973,  9.029,  9.084,  9.139,
     1           9.194,  9.248,  9.301,  9.354,  9.405,
     1           9.455,  9.503,  9.551/
      DATA CTN/  6.961,  6.990,  7.069,  7.196,  7.350,
     1           7.512,  7.670,  7.815,  7.945,  8.061,
     1           8.162,  8.252,  8.330,  8.398,  8.458,
     1           8.512,  8.559,  8.601,  8.638,  8.672,
     1           8.703,  8.731,  8.756,  8.779,  8.800,
     1           8.820,  8.838,  8.855/
C
      IF((TI-540.0)*(5400.0-TI)) 100,105,105
  100 IERRR=1
      GO TO 300
  105 TKR=TI/180.0
      ITR=TKR
      FRR=TKR-FLOAT(ITR)
      INR=ITR-2
      SHR(1)=(HTF(INR)+FRR*(HTF(INR+1)-HTF(INR)))*1800.0
      SHR(2)=(HTO(INR)+FRR*(HTO(INR+1)-HTO(INR)))*1800.0
      SHR(3)=(HTN(INR)+FRR*(HTN(INR+1)-HTN(INR)))*1800.0
      SHR(4)=4.968*TI
      XR(1)=1.0/(1.0+4.7718*ROR)
      XR(2)=ROR*XR(1)
      XR(3)=ROR*XR(1)*3.7274
      XR(4)=ROR*XR(1)*0.0444
      AVMR=XR(1)*(ANR*12.011+AMR*1.008+ALR*16.000
     1 +AKR*14.008)+XR(2)*31.999+XR(3)*28.013+XR(4)*39.944
      HU=0.0
      DO 5 I=1,4
      HU=HU+XR(I)*SHR(I)
   5  CONTINUE
      HU=HU/AVMR
      RU=1.987165/AVMR
      UU=HU-RU*TI
      IF (JDR.EQ.0) RETURN
C
      CPF=CTF(INR)+FRR*(CTF(INR+1)-CTF(INR))
      CPO=CTO(INR)+FRR*(CTO(INR+1)-CTO(INR))
      CPN=CTN(INR)+FRR*(CTN(INR+1)-CTN(INR))
      DHTR=XR(1)*CPF+XR(2)*CPO+XR(3)*CPN+XR(4)*4.968
      DHTR=DHTR/AVMR
      DUTR=DHTR-RU
  300 RETURN
      END
C
C   +--------------------------------------------------+
C
```

```
      SUBROUTINE PER(JDR)
C
C     DEVELOPED BY CHERIAN OLIKARA, GARY L. BORMAN
C     UNIVERSITY OF WISCONSIN, MADISON  VERSION  MAY 1974
C     MODIFICATIONS BY R. K. MACKAY
C
      IMPLICIT DOUBLE PRECISION (A-H,O-Z)
      COMMON /BLOC/ AN,AM,AL,AK,PHI,T,P,KLO,IERR,X(13)
      COMMON /TAB/ DXT(12),DXP(12),DXF(12)
      COMMON /PROP/ AVM,R,H,U,DRT,DHT,DUT,DRP,DHP,DUP,DRF
     1 ,DHF,DUF
      DIMENSION SH(12),SM(12),HT(351),CT(351)
      DIMENSION H1(35),H2(35),H3(35),H4(35),H5(35)
      DIMENSION H6(35),H7(35),H8(35),H9(35),H10(36)
      DIMENSION CT1(35),CT2(35),CT3(35),CT4(35),CT5(35)
      DIMENSION CT6(35),CT7(35),CT8(35),CT9(35),CT10(36)
      DATA SM/1.008,16.000,14.008,2.016,17.007,28.001,30.008
     1 ,31.999,18.016,44.010,28.013,39.944/
      DATA H1/ 62.141, 62.645, 63.147, 63.649, 64.149,
     1 64.648, 65.148, 65.646, 66.145, 66.643, 67.141,
     1 67.639, 68.137, 68.635, 69.133, 69.631, 70.129,
     1 70.626, 71.124, 71.623, 72.121, 72.620, 73.119,
     1 73.619, 74.119, 74.620, 75.121, 75.623, 76.126,
     1 76.630, 77.134, 77.640, 78.146, 78.654, 79.162/
      DATA H2/115.501,115.997,116.494,116.991,117.488,
     1117.985,118.482,118.978,119.475,119.972,120.469,
     1120.966,121.462,121.959,122.456,122.953,123.450,
     1123.947,124.455,124.942,125.440,125.939,126.438,
     1126.937,127.438,127.940,128.442,128.947,129.452,
     1129.960,130.470,130.981,131.496,132.013,132.532/
      DATA H3/  4.130,  4.832,  5.538,  6.250,  6.968,
     1  7.694,  8.428,  9.172,  9.926, 10.692, 11.470,
     1 12.257, 13.054, 13.860, 14.675, 15.499, 16.331,
     1 17.170, 18.017, 18.872, 19.732, 20.599, 21.472,
     1 22.350, 23.234, 24.122, 25.016, 25.915, 26.818,
     1 27.727, 28.640, 29.559, 30.481, 31.409, 32.341/
      DATA H4/ 13.618, 14.326, 15.037, 15.756, 16.484,
     1 17.223, 17.972, 18.733, 19.504, 20.286, 21.077,
     1 21.878, 22.688, 23.505, 24.330, 25.162, 26.001,
     1 26.845, 27.695, 28.550, 29.410, 30.275, 31.143,
     1 32.016, 32.892, 33.772, 34.655, 35.541, 36.430,
     1 37.322, 38.216, 39.113, 40.013, 40.915, 41.819/
      DATA H5/-22.991,-22.255,-21.501,-20.731,-19.945,
     1-19.145,-18.334,-17.512,-16.682,-15.843,-14.998,
     1-14.148,-13.292,-12.431,-11.567,-10.698, -9.827,
     1 -8.953, -8.076, -7.197, -6.315, -5.432, -4.546,
     1 -3.659, -2.771, -1.880,  -.989,  -.096,   .799,
     1  1.694,  2.591,  3.489,  4.388,  5.288,  6.188/
```

```
 DATA H6/ 25.839, 26.595, 27.369, 28.160, 28.966,
1 29.784, 30.613, 31.451, 32.297, 33.149, 34.007,
1 34.870, 35.737, 36.608, 37.482, 38.359, 39.240,
1 40.122, 41.007, 41.894, 42.782, 43.673, 44.564,
1 45.458, 46.353, 47.249, 48.146, 49.045, 49.944,
1 50.845, 51.747, 52.650, 53.553, 54.458, 55.363/
 DATA H7/  4.285,  5.063,  5.861,  6.675,  7.502,
1  8.341,  9.189, 10.046, 10.910, 11.781, 12.658,
1 13.540, 14.429, 15.324, 16.224, 17.129, 18.041,
1 18.957, 19.879, 20.807, 21.739, 22.677, 23.620,
1 24.568, 25.521, 26.478, 27.440, 28.406, 29.377,
1 30.351, 31.329, 32.311, 33.296, 34.284, 35.276/
 DATA H8/-52.227,-51.346,-50.436,-49.496,-48.527,
1-47.526,-46.496,-45.438,-44.352,-43.241,-42.106,
1-40.949,-39.772,-38.576,-37.363,-36.134,-34.890,
1-33.633,-32.364,-31.083,-29.791,-28.490,-27.180,
1-25.861,-24.535,-23.201,-21.860,-20.513,-19.159,
1-17.800,-16.436,-15.067,-13.693,-12.314,-10.931/
 DATA H9/-88.640,-87.492,-86.274,-85.025,-83.743,
1-82.431,-81.095,-79.739,-78.365,-76.977,-75.575,
1-74.162,-72.740,-71.309,-69.870,-68.424,-66.972,
1-65.515,-64.053,-62.586,-61.114,-59.639,-58.160,
1-56.678,-55.192,-53.703,-52.212,-50.717,-49.220,
1-47.721,-46.219,-44.715,-43.209,-41.700,-40.189/
 DATA H10/ 4.197,  4.925,  5.668,  6.427,  7.201,
1  7.989,  8.790,  9.601, 10.422, 11.251, 12.087,
1 12.930, 13.779, 14.632, 15.490, 16.352, 17.218,
1 18.087, 18.958, 19.833, 20.710, 21.589, 22.470,
1 23.352, 24.237, 25.123, 26.011, 26.901, 27.791,
1 28.683, 29.577, 30.471, 31.367, 32.263, 33.161,
1 34.060/
 DATA CT1/ 5.049,  5.029,  5.015,  5.006,  4.999,
1  4.994,  4.990,  4.987,  4.984,  4.982,  4.981,
1  4.979,  4.979,  4.978,  4.978,  4.978,  4.979,
1  4.980,  4.981,  4.984,  4.986,  4.990,  4.994,
1  4.999,  5.004,  5.010,  5.017,  5.025,  5.033,
1  5.041,  5.050,  5.060,  5.070,  5.081,  5.091/
 DATA CT2/ 4.968,  4.968,  4.968,  4.968,  4.968,
1  4.968,  4.968,  4.968,  4.968,  4.968,  4.968,
1  4.968,  4.968,  4.969,  4.969,  4.969,  4.971,
1  4.972,  4.975,  4.978,  4.982,  4.987,  4.993,
1  5.001,  5.011,  5.022,  5.035,  5.050,  5.067,
1  5.086,  5.107,  5.130,  5.156,  5.183,  5.213/
 DATA CT3/ 7.009,  7.036,  7.087,  7.148,  7.219,
1  7.300,  7.390,  7.490,  7.600,  7.720,  7.823,
1  7.921,  8.016,  8.108,  8.195,  8.279,  8.358,
1  8.434,  8.506,  8.575,  8.639,  8.700,  8.757,
1  8.810,  8.859,  8.911,  8.962,  9.012,  9.061,
```

```
     1  9.110,  9.158,  9.205,  9.252,  9.297,  9.342/
      DATA CT4/ 7.057,  7.090,  7.150,  7.233,  7.332,
     1  7.439,  7.549,  7.659,  7.766,  7.867,  7.966,
     1  8.053,  8.137,  8.214,  8.286,  8.353,  8.415,
     1  8.472,  8.526,  8.576,  8.622,  8.665,  8.706,
     1  8.744,  8.780,  8.814,  8.846,  8.876,  8.905,
     1  8.933,  8.959,  8.984,  9.008,  9.031,  9.053/
      DATA CT5/ 7.276,  7.450,  7.624,  7.786,  7.931,
     1  8.057,  8.168,  8.263,  8.346,  8.417,  8.480,
     1  8.535,  8.593,  8.626,  8.664,  8.698,  8.728,
     1  8.759,  8.781,  8.804,  8.825,  8.844,  8.863,
     1  8.879,  8.895,  8.910,  8.924,  8.937,  8.949,
     1  8.961,  8.973,  8.984,  8.994,  9.004,  9.014/
      DATA CT6/ 7.466,  7.655,  7.832,  7.988,  8.123,
     1  8.238,  8.336,  8.419,  8.491,  8.552,  8.605,
     1  8.651,  8.692,  8.727,  8.759,  8.788,  8.813,
     1  8.837,  8.858,  8.877,  8.895,  8.912,  8.927,
     1  8.941,  8.955,  8.968,  8.980,  8.991,  9.002,
     1  9.012,  9.022,  9.032,  9.041,  9.050,  9.058/
      DATA CT7/ 7.670,  7.883,  8.063,  8.212,  8.336,
     1  8.439,  8.527,  8.604,  8.674,  8.738,  8.800,
     1  8.858,  8.916,  8.973,  9.029,  9.084,  9.139,
     1  9.194,  9.248,  9.301,  9.354,  9.405,  9.455,
     1  9.503,  9.551,  9.596,  9.640,  9.682,  9.723,
     1  9.762,  9.799,  9.835,  9.869,  9.901,  9.932/
      DATA CT8/ 8.676,  8.954,  9.246,  9.547,  9.851,
     1 10.152, 10.444, 10.723, 10.987, 11.233, 11.462,
     1 11.674, 11.869, 12.048, 12.214, 12.366, 12.505,
     1 12.634, 12.753, 12.863, 12.965, 13.059, 13.146,
     1 13.228, 13.304, 13.374, 13.441, 13.503, 13.562,
     1 13.617, 13.669, 13.718, 13.764, 13.808, 13.850/
      DATA CT9/11.310, 11.846, 12.293, 12.667, 12.980,
     1 13.243, 13.466, 13.656, 13.815, 13.953, 14.074,
     1 14.177, 14.269, 14.352, 14.424, 14.489, 14.547,
     1 14.600, 14.648, 14.692, 14.734, 14.771, 14.307,
     1 14.841, 14.873, 14.902, 14.930, 14.956, 14.982,
     1 15.006, 15.030, 15.053, 15.075, 15.097, 15.119/
      DATA CT10/7.196,  7.350,  7.512,  7.670,  7.815,
     1  7.945,  8.061,  8.162,  8.252,  8.330,  8.398,
     1  8.458,  8.512,  8.559,  8.601,  8.638,  8.672,
     1  8.703,  8.731,  8.756,  8.779,  8.800,  8.820,
     1  8.838,  8.855,  8.871,  8.886,  8.900,  8.914,
     1  8.927,  8.939,  8.950,  8.962,  8.972,  8.983,
     1  8.993/
C
      DO 5 I=1,351
      IF(I.LE.35) THEN
              HT(I)=H1(I)
```

```
              CT(I)=CT1(I)
        ENDIF
        IF((I.GE.36).AND.(I.LE.70)) THEN
              HT(I)=H2(I-35)
              CT(I)=CT2(I-35)
        ENDIF
        IF((I.GE.71).AND.(I.LE.105)) THEN
              HT(I)=H3(I-70)
              CT(I)=CT3(I-70)
        ENDIF
        IF((I.GE.106).AND.(I.LE.140)) THEN
              HT(I)=H4(I-105)
              CT(I)=CT4(I-105)
        ENDIF
        IF((I.GE.141).AND.(I.LE.175)) THEN
              HT(I)=H5(I-140)
              CT(I)=CT5(I-140)
        ENDIF
        IF((I.GE.176).AND.(I.LE.210)) THEN
              HT(I)=H6(I-175)
              CT(I)=CT6(I-175)
        ENDIF
        IF((I.GE.211).AND.(I.LE.245)) THEN
              HT(I)=H7(I-210)
              CT(I)=CT7(I-210)
        ENDIF
        IF((I.GE.246).AND.(I.LE.280)) THEN
              HT(I)=H8(I-245)
              CT(I)=CT8(I-245)
        ENDIF
        IF((I.GE.281).AND.(I.LE.315)) THEN
              HT(I)=H9(I-280)
              CT(I)=CT9(I-280)
        ENDIF
        IF(I.GE.316) THEN
              HT(I)=H10(I-315)
              CT(I)=CT10(I-315)
        ENDIF
    5   CONTINUE
C
C       SUBROUTINE PER CALLS SUBROUTINE EQMD FOR CALCULATION
C       OF MOLE FRACTIONS AND THEIR PARTIAL DERIVATIVES.
C
        CALL EQMD(JDR)
        IF(IERR.NE.0) RETURN
C
C       SECTION 100 CALCULATES AVM, R, H, U.
C
```

```
      TK=T/180.0
      IT=TK
      FR=TK-FLOAT(IT)
      SH(1)=92935.8+4.968*T
      SH(12)=4.968*T
      DO 105 I=2,11
      IN=35*(I-2)+(IT-5)
      SH(I)=(HT(IN)+FR*(HT(IN+1)-HT(IN)))*1800.0
  105 CONTINUE
      AVM=0.0
      H=0.0
      DO 110 I=1,12
      AVM=AVM+X(I)*SM(I)
      H=H+X(I)*SH(I)
  110 CONTINUE
      H=H/AVM
      R=1.987165/AVM
      U=H-R*T
      IF(JDR.EQ.0) RETURN
C
C     SECTION 200 CALCULATES THE PARTIAL DERIVATIVES WITH
C     RESPECT TO T, P, AND PHI.
C
      DMT=DXT(1)*SM(1)+DXT(12)*SM(12)
      DHT=X(1)*4.968+DXT(1)*SH(1)+X(12)*4.968+DXT(12)*SH(12)
      DMP=DXP(1)*SM(1)+DXP(12)*SM(12)
      DHP=DXP(1)*SH(1)+DXP(12)*SH(12)
      DMF=DXF(1)*SM(1)+DXF(12)*SM(12)
      DHF=DXF(1)*SH(1)+DXF(12)*SH(12)
      DO 210 I=2,11
      IN=35*(I-2)+(IT-5)
      CP=CT(IN)+FR*(CT(IN+1)-CT(IN))
      DMT=DMT+DXT(I)*SM(I)
      DHT=DHT+X(I)*CP+DXT(I)*SH(I)
      DMP=DMP+DXP(I)*SM(I)
      DHP=DHP+DXP(I)*SH(I)
      DMF=DMF+DXF(I)*SM(I)
      DHF=DHF+DXF(I)*SH(I)
  210 CONTINUE
      DRT=-R*DMT/AVM
      DHT=(DHT-DMT*H)/AVM
      DUT=DHT-R-DRT*T
      DRP=-R*DMP/AVM
      DHP=(DHP-DMP*H)/AVM
      DUP=DHP-DRP*T
      DRF=-R*DMF/AVM
      DHF=(DHF-DMF*H)/AVM
      DUF=DHF-DRF*T
```

```
      RETURN
      END
C
      SUBROUTINE EQMD(JDR)
C
C     DEVELOPED BY CHERIAN OLIKARA, GARY L. BORMAN
C     UNIVERSITY OF WISCONSIN, MADISON  VERSION  APRIL 1974
C
      IMPLICIT DOUBLE PRECISION (A-H,O-Z)
      COMMON /BLOC/AN, AM, AL, AK, PHI, T, P, KLO, IERR,
     1 X1,X2,X3,X4,X5,X6,X7,X8,X9,X10,X11,X12,X13
      COMMON /TAB/ DX1T, DX2T, DX3T, DX4T, DX5T, DX6T,DX7T,
     1 DX8T, DX9T, DX10T, DX11T, DX12T, DX1P, DX2P, DX3P,
     1 DX4P, DX5P, DX6P, DX7P, DX8P, DX9P, DX10P, DX11P,
     1 DX12P, DX1F, DX2F, DX3F, DX4F, DX5F, DX6F, DX7F,
     1 DX8F, DX9F, DX10F, DX11F, DX12F
      DIMENSION A(4,4),B(4),C(4,3)
      DATA JF,PREC/0,1.0E-3/
      IF((T-1080.0)*(7200.0-T)) 102,105,105
  102 IERR=1
      GO TO 710
C
C     SECTION 100 CALCULATES THE CONSTANTS USED IN THE
C     SUBROUTINE.
C
  105 R0=(AN+0.25*AM-0.5*AL)/PHI
      R=R0+0.5*AL
      R1=R0*3.7274+0.5*AK
      R2=R0*0.0444
      IF(R.GT.0.5*AN) GO TO 110
      IERR=2
      GO TO 710
  110 D1=AM/AN
      D2=2.0*R/AN
      D3=2.0*R1/AN
      D4=R2/AN
C
C     THE EQUILIBRIUM CONSTANTS WERE CURVE FITTED (LEAST
C     SQUARES) IN THE RANGE 600 TO 4000 DEG K (1080 TO 7200
C     R) FROM DATA IN JANAF THERMOCHEMICAL TABLES, SECOND
C     EDITION (1971).
C
  115 SQP=SQRT(P/14.696)
      TA=0.005*T/9.0
      ALTA=DLOG(TA)
      TAIN=1.0/TA
      TASQ=TA*TA
      C1=(10.0**(0.432168*ALTA-11.2464*TAIN+2.67269
```

```
     1 -0.745744E-01*TA+0.242484E-02*TASQ))/SQP
      C2=(10.0**(0.310805*ALTA-12.9540*TAIN+3.21779
     1 -0.738336E-01*TA+0.344645E-02*TASQ))/SQP
      C3=(10.0**(0.389716*ALTA-24.5828*TAIN+3.14505
     1 -0.963730E-01*TA+0.585643E-02*TASQ))/SQP
      C5=10.0**(-0.141784*ALTA-2.13308*TAIN+0.853461
     1 +0.355015E-01*TA-0.310227E-02*TASQ)
      C7=10.0**(0.150879E-01*ALTA-4.70959*TAIN+0.646096
     1 +0.272805E-02*TA-0.154444E-02*TASQ)
      C9=(10.0**(-0.752364*ALTA+12.4210*TAIN-2.60286
     1 +0.259556*TA-0.162687E-01*TASQ))*SQP
      C10=(10.0**(-0.415302E-02*ALTA+14.8627*TAIN-4.75746
     1 +0.124699*TA-0.900227E-02*TASQ))*SQP
C
C     SECTION 200 DECIDES WHETHER OR NOT TO MAKE A NEW
C     ESTIMATE OF X4, X6, X8, X11.
C
      IF(KLO-1) 305,205,410
  205 IF(JF.EQ.0) GO TO 305
      IF(ABS(PHI-PHIPR).GT.1.0E-6) GO TO 305
      IF(ABS(T/TPR-1.0).GT.0.02) GO TO 305
      IF(ABS(P/PPR-1.0).GT.0.05) GO TO 305
      X4=X4PR
      X6=X6PR
      X8=X8PR
      X11=X11PR
      GO TO 410
C
C     SECTION 300 CAN MAKE AN INITIAL ESTIMATE OF X4, X6,
C     X8, AND X11.
C
  305 IF(PHI.GT.1.0) GO TO 310
      PAR=1.0/(R+R1+R2+0.25*AM)
      GO TO 315
  310 PAR=1.0/(R1+R2+AN+0.5*AM)
  315 FUN1=2.0*AN*C10
      FUN2=0.5*AM*C9
      FUN3=2.0/PAR
      FUN4=2.0*R
      OX=1.0
  320 SQOX=SQRT(OX)
      FOX=(FUN1*SQOX+AN)/(1.0+C10*SQOX)+FUN2*SQOX
     1 /(1.0+C9*SQOX)+FUN3*OX-FUN4
      IF(FOX) 325,330,335
  335 OX=0.1*OX
      IF(OX.GE.1.0E-30) GO TO 320
      IERR=3
      GO TO 710
```

```
  325 IND=1
  327 FOX=(FUN1*SQOX+AN)/(1.0+C10*SQOX)+FUN2*SQOX
     1 /(1.0+C9*SQOX)+FUN3*OX-FUN4
      DOX=0.25*FUN1/(SQOX*(1.0+C10*SQOX)**2)+0.5*FUN2
     1 /(SQOX*(1.0+C9*SQOX)**2)+FUN3
      RAT=FOX/DOX
      OX=OX-RAT
      SQOX=SQRT(OX)
      IF(ABS(RAT/OX).LE.1.0E-2) GO TO 330
      IND=IND+1
      IF(IND.LE.20) GO TO 327
  330 X4=0.5*AM*PAR/(1.0+C9*SQOX)
      X6=AN*PAR/(1.0+C10*SQOX)
      X8=OX
      X11=R1*PAR
C
C     SECTION 400 CALCULATES THE ELEMENTS OF THE MATRIX OF
C     LINEARIZED EQUATIONS.
C
  410 IND=1
      NCALL=0
  455 SQX4=SQRT(X4)
      SQX8=SQRT(X8)
      SQX11=SQRT(X11)
      X1=C1*SQX4
      X2=C2*SQX8
      X3=C3*SQX11
      X5=C5*SQX4*SQX8
      X7=C7*SQX11*SQX8
      X9=C9*X4*SQX8
      X10=C10*X6*SQX8
  460 T14=0.5*C1/SQX4
      T28=0.5*C2/SQX8
      T311=0.5*C3/SQX11
      T54=0.5*C5*SQX8/SQX4
      T58=0.5*C5*SQX4/SQX8
      T78=0.5*C7*SQX11/SQX8
      T711=0.5*C7*SQX8/SQX11
      T94=C9*SQX8
      T98=0.5*C9*X4/SQX8
      T106=C10*SQX8
      T108=0.5*C10*X6/SQX8
      A(1,1)=T14+2.0+T54+2.0*T94
      A(1,2)=-D1*(1.0+T106)
      A(1,3)=(T58+2.0*T98)-D1*T108
      A(1,4)=0.0
      A(2,1)=T54+T94
      A(2,2)=(1.0+2.0*T106)-D2*(1.0+T106)
```

```
      A(2,3)=(T28+T58+T78+2.0+T98+2.0*T108)-D2*T108
      A(2,4)=T711
      A(3,1)=0.0
      A(3,2)=-D3*(1.0+T106)
      A(3,3)=T78-D3*T108
      A(3,4)=T311+T711+2.0
      A(4,1)=T14+1.0+T54+T94
      A(4,2)=1.0+T106+D4*(1.0+T106)
      A(4,3)=T28+T58+T78+1.0+T98+T108+D4*T108
      A(4,4)=T311+T711+1.0
      IF(NCALL.EQ.1) GO TO 810
      B(1)=-(X1+2.0*X4+X5+2.0*X9)+D1*(X6+X10)
      B(2)=-(X2+X5+X6+X7+2.0*X8+X9+2.0*X10)+D2*(X6+X10)
      B(3)=-(X3+X7+2.0*X11)+D3*(X6+X10)
      B(4)=-(X1+X2+X3+X4+X5+X6+X7+X8+X9+X10+X11+D4
     1 *(X6+X10))+1.0
C
C     SECTION 500 SOLVES THE MATRIX EQUATION BY GAUSSIAN
C     ELIMINATION ROWS ARE INTERCHANGED ONLY IF THE PIVOT
C     POINT IS SMALLER THAN E-05
C
      DO 505 K=1,3
      KP1=K+1
      BIG=ABS(A(K,K))
      IF(BIG.GE.1.0E-05) GO TO 520
      IBIG=K
      DO 510 I=KP1,4
      IF(ABS(A(I,K)).LE.BIG) GO TO 510
      BIG=ABS(A(I,K))
      IBIG=I
  510 CONTINUE
      IF(BIG.GT.0.) GO TO 512
      IERR=4
      GO TO 710
  512 IF(BIG.EQ.K) GO TO 520
      DO 515 J=K,4
      TERM=A(K,J)
      A(K,J)=A(IBIG,J)
      A(IBIG,J)=TERM
  515 CONTINUE
      TERM=B(K)
      B(K)=B(IBIG)
      B(IBIG)=TERM
  520 DO 525 I=KP1,4
      TERM=A(I,K)/A(K,K)
      DO 530 J=KP1,4
      A(I,J)=A(I,J)-A(K,J)*TERM
  530 CONTINUE
```

```
      B(I)=B(I)-B(K)*TERM
  525 CONTINUE
  505 CONTINUE
      IF(ABS(A(4,4)).GT.0.) GO TO 550
      IERR=4
      GO TO 710
  550 B(4)=B(4)/A(4,4)
      B(3)=(B(3)-A(3,4)*B(4))/A(3,3)
      B(2)=(B(2)-A(2,3)*B(3)-A(2,4)*B(4))/A(2,2)
      B(1)=(B(1)-A(1,2)*B(2)-A(1,3)*B(3)-A(1,4)*B(4))/A(1,1)
C
C     SECTION 600 CORRECTS THE ESTIMATE OF THE VARIABLES AND
C     CHECKS PRECISION.
C
  602 NCK=0
      X4=X4+B(1)
      IF(ABS(B(1)/X4 ).GT.PREC) NCK=1
      X6=X6+B(2)
      IF(ABS(B(2)/X6 ).GT.PREC) NCK=1
      X8=X8+B(3)
      IF(ABS(B(3)/X8 ).GT.PREC) NCK=1
      X11=X11+B(4)
      IF(ABS(B(4)/X11).GT.PREC) NCK=1
      IF((X4.GT.0.0).AND.(X8.GT.0.0).AND.(X11.GT.0.0))
     1 GO TO 620
      IERR=5
      GO TO 710
  620 IF(NCK.EQ.0) GO TO 625
      IF(IND.LT.25) GO TO 622
      IERR=6
      GO TO 710
  622 IND=IND+1
      GO TO 455
  625 IF(X6.GE.0.0) GO TO 702
      IERR=5
      GO TO 710
C
C     SECTION 700 CALCULATES THE REMAINING MOLE FRACTIONS.
C
  702 IERR=0
      JF=1
      PHIPR=PHI
      TPR=T
      PPR=P
      X4PR=X4
      X6PR=X6
      X8PR=X8
      X11PR=X11
```

```
      SQX4=SQRT(X4)
      SQX8=SQRT(X8)
      SQX11=SQRT(X11)
      X1=C1*SQX4
      X2=C2*SQX8
      X3=C3*SQX11
      X5=C5*SQX4*SQX8
      X7=C7*SQX11*SQX8
      X9=C9*X4*SQX8
      X10=C10*X6*SQX8
      X13=(X6+X10)/AN
      X12=R2*X13
      IF(JDR-1) 725,800,800
  725 RETURN
  710 JF=0
      RETURN
C
C     SECTION 800 CALCULATES THE ELEMENTS OF THE MATRIX OF
C     THE PARTIAL DIFFERENTIAL EQUATION.
C
  800 NCALL=1
      GO TO 460
  810 ZZ=ALOG(10.)*0.005/9.
      DC1T=X1*ZZ*(.432168*TAIN+11.2464/TASQ-.745744E-1
     1 +.484968E-2*TA)
      DC2T=X2*ZZ*(.310805*TAIN+12.9540/TASQ-.738336E-1
     1 +.689290E-2*TA)
      DC3T=X3*ZZ*(.389716*TAIN+24.5828/TASQ-.963730E-1
     1 +1.171286E-2*TA)
      DC5T=X5*ZZ*(-.141784*TAIN+2.13308/TASQ+.355015E-1
     1 -.620454E-2*TA)
      DC7T=X7*ZZ*(.150879E-1*TAIN+4.70959/TASQ+.272805E-2
     1 -.308888E-2*TA)
      DC9T=X9*ZZ*(-.752364*TAIN-12.4210/TASQ+.259556
     1 -.325374E-1*TA)
      DC10T=X10*ZZ*(-.415302E-2*TAIN-14.8627/TASQ+.124699
     1 -.01800454*TA)
      PP2=.5/P
      DC1P=-X1*PP2
      DC2P=-X2*PP2
      DC3P=-X3*PP2
      D39P=X9*PP2
      DC10P=X10*PP2
      D5AN=-R0*X13/PHI
      DD4F=0.0444*D5AN
      C(1,1)=-(DC1T+DC5T+2.*DC9T-D1*DC10T)
      C(2,1)=-(DC2T+DC5T+DC7T+DC9T+(2.-D2)*DC10T)
      C(3,1)=-(DC3T+DC7T-D3*DC10T)
```

```
      C(4,1)=-(DC1T+DC2T+DC3T+DC5T+DC7T+DC9T+(1.+D4)*DC10T)
      C(1,2)=-(DC1P+2.*DC9P-D1*DC10P)
      C(2,2)=-(DC2P+DC9P+(2.-D2)*DC10P)
      C(3,2)=-(DC3P-D3*DC10P)
      C(4,2)=-(DC1P+DC2P+DC3P+DC9P+(1.+D4)*DC10P)
      C(1,3)=0.
      C(2,3)=2.*D5AN
      C(3,3)=7.4548*D5AN
      C(4,3)=-DD4F
C
C     SECTION 900 SOLVE THE MATRIX EQUATION BY GUASSIAN
C     ELIMINATION USING MAXIMUM PIVOT STRATEGY.
C
      DO 905 K=1,3
      KP1=K+1
      AMAX=ABS(A(K,K))
      MAX=K
      DO 910 I=KP1,4
      IF(ABS(A(I,K)).LE.AMAX) GO TO 910
      AMAX=ABS(A(I,K))
      MAX=I
  910 CONTINUE
      IF(AMAX.GT.0.0) GO TO 912
      IERR=7
      GO TO 710
  912 IF(MAX.EQ.K) GO TO 950
      DO 915 J=K,4
      TERM=A(K,J)
      A(K,J)=A(MAX,J)
      A(MAX,J)=TERM
  915 CONTINUE
      DO 920 J=1,3
      TERM=C(K,J)
      C(K,J)=C(MAX,J)
      C(MAX,J)=TERM
  920 CONTINUE
  950 DO 925 I=KP1,4
      TERM=A(I,K)/A(K,K)
      DO 930 J=KP1,4
      A(I,J)=A(I,J)-A(K,J)*TERM
  930 CONTINUE
      DO 935 J=1,3
      C(I,J)=C(I,J)-C(K,J)*TERM
  935 CONTINUE
  925 CONTINUE
  905 CONTINUE
      IF(ABS(A(4,4)).GT.0.0) GO TO 938
      IERR=7
```

```
      GO TO 710
  938 DO 940 J=1,3
      C(4,J)=C(4,J)/A(4,4)
      C(3,J)=(C(3,J)-A(3,4)*C(4,J))/A(3,3)
      C(2,J)=(C(2,J)-A(2,3)*C(3,J)-A(2,4)*C(4,J))/A(2,2)
      C(1,J)=(C(1,J)-A(1,2)*C(2,J)-A(1,3)*C(3,J)-A(1,4)
     1 *C(4,J))/A(1,1)
  940 CONTINUE
C
C     SECTION 1000 CALCULATES THE PARTIAL DERIVATIVES WITH
C     RESPECT TO T, P, PHI RESPECTIVELY AND RETURNS TO THE
C     CALLING PROGRAM.
C
      DX4T=C(1,1)
      DX6T=C(2,1)
      DX8T=C(3,1)
      DX11T=C(4,1)
      DX4P=C(1,2)
      DX6P=C(2,2)
      DX8P=C(3,2)
      DX11P=C(4,2)
      DX4F=C(1,3)
      DX6F=C(2,3)
      DX8F=C(3,3)
      DX11F=C(4,3)
      DX1T=T14*DX4T+DC1T
      DX2T=T28*DX8T+DC2T
      DX3T=T311*DX11T+DC3T
      DX5T=T54*DX4T+T58*DX8T+DC5T
      DX7T=T78*DX8T+T711*DX11T+DC7T
      DX9T=T94*DX4T+T98*DX8T+DC9T
      DX10T=T106*DX6T+T108*DX8T+DC10T
      DX12T=D4*(DX6T+DX10T)
      DX1P=T14*DX4P+DC1P
      DX2P=T28*DX8P+DC2P
      DX3P=T311*DX11P+DC3P
      DX5P=T54*DX4P+T58*DX8P
      DX7P=T78*DX8P+T711*DX11P
      DX9P=T94*DX4P+T98*DX8P+DC9P
      DX10P=T106*DX6P+T108*DX8P+DC10P
      DX12P=D4*(DX6P+DX10P)
      DX1F=T14*DX4F
      DX2F=T28*DX8F
      DX3F=T311*DX11F
      DX5F=T54*DX4F+T58*DX8F
      DX7F=T78*DX8F+T711*DX11F
      DX9F=T94*DX4F+T98*DX8F
      DX10F=T106*DX6F+T108*DX8F
```

```
      DX12F=D4*(DX6F+DX10F)+DD4F
      RETURN
      END
```

```
10  REM  +-------------------------------------------------+
20  REM  | BDCB.BAS                                        |
30  REM  | Version 1.0                                     |
40  REM  | By R. K. Mackay                                 |
50  REM  | May 1992                                        |
60  REM  |                                                 |
70  REM  | This program automates the filling proceedure   |
80  REM  | for the BDCB using the Helios digital-to-analog |
90  REM  | converter. Once a channel is activated by the   |
100 REM  | program, the Helios will send a 5.0 volt signal |
110 REM  | which is used to trip a solid state relay. The  |
120 REM  | relays are used to open one of the solenoid     |
130 REM  | valves. The duration of time that the valve is  |
140 REM  | open is input from the keyboard. After that     |
150 REM  | time has elapsed, the valve is closed by        |
160 REM  | returning the channel to 0.0 volts. The         |
170 REM  | channels are arranged as follows.               |
180 REM  | CHANNEL (0) - High pressure safety valve        |
190 REM  | CHANNEL (1) - High pressure vacuum valve        |
200 REM  | CHANNEL (2) - Low pressure fuel valve           |
210 REM  | CHANNEL (3) - Low pressure air valve            |
220 REM  +-------------------------------------------------+
230 CLS
240 CLOSE
250 OPEN "COM1:9600,N,8,1,CS,DS,CD" AS#1
260 PRINT #1, "MODE=COMP"
270 INPUT #1, A$
280 IF A$<>"!" THEN GOTO 50
290 PRINT #1, "SEND VERSION$"
300 INPUT #1, A$
310 PRINT "The firmware is ";A$
320 REM ** Helios Control **
330 PRINT #1, "FORMAT=DECIMAL"
340 PRINT "Enter esc to exit, return to continue"
350 PRINT "Enter time for vacuum (0..10)"
360 INPUT VACUUM
370 PRINT "Enter time for fuel (0..10)"
380 INPUT FUEL
390 PRINT "Enter time for air (0..10)"
400 INPUT AIR
410 R%=0:S%=0:T%=0
420 V%=VACUUM*1000
430 F%=FUEL*1000
440 A%=AIR*1000
450 PRINT #1, "DEF CHAN (0) = UNIPOLV"
460 PRINT #1, "DEF CHAN (1) = UNIPOLV"
470 PRINT #1, "DEF CHAN (2) = UNIPOLV"
480 PRINT #1, "DEF CHAN (3) = UNIPOLV"
```

```
490 PRINT #1, "CHAN (0) = 0.0"
500 PRINT #1, "CHAN (1) = 5.0"
510 PRINT #1, "CHAN (2) = 0.0"
520 PRINT #1, "CHAN (3) = 0.0"
530 FOR L%=0 TO 10 STEP 1
540 FOR M%=0 TO V% STEP 1: NEXT M%
550 NEXT L%
560 PRINT #1, "CHAN (1) = 0.0"
570 PRINT #1, "CHAN (0) = 5.0"
580 PRINT #1, "CHAN (3) = 5.0"
590 FOR N%=0 TO 10 STEP 1
600 FOR O%=0 TO F% STEP 1: NEXT O%
610 NEXT N%
620 PRINT #1, "CHAN (3) = 0.0"
630 PRINT #1, "CHAN (2) = 5.0"
640 FOR P%=0 TO 10 STEP 1
650 FOR Q%=0 TO A% STEP 1: NEXT Q%
660 NEXT P%
670 PRINT #1, "CHAN (2) = 0.0"
680 PRINT #1, "CHAN (0) = 0.0"
690 PRINT "Fire immediately"
700 KBRD$=INKEY$
710 IF KBRD$="" THEN GOTO 680
720 KBR=ASC(KBRD$)
730 IF KBR=27 THEN GOTO 730
740 GOTO 330
750 PRINT #1, "RESET CHAN (0..3)"
760 END
```

```
C   +-------------------------------------------------------+
C   | ENGINE.FOR                                            |
C   | Version 1.0                                           |
C   | By R. K. Mackay                                       |
C   | August 1993                                           |
C   |                                                       |
C   | This program will calculate both burned and unburned  |
C   | gas temperature, mass fraction, and volume for the    |
C   | combustion of iso-octane in an IC engine using a two  |
C   | zone thermodynamic model. Additional output includes  |
C   | the turbulent flame speed, heat transfer and mole     |
C   | fractions of the major product species. The pressure  |
C   | data is entered into the program via an input file    |
C   | labeled PRESS.DAT. The angle between these data       |
C   | points is entered as an input variable whose spacing  |
C   | must be equidistant. Other input variables are        |
C   | engine speed, data starting angle, ignition timing,   |
C   | fuel-air mixture temperature, wall temperature and    |
C   | equivalence ratio. The subroutine PER determines the  |
C   | thermochemical properties for the products given the  |
C   | temperature and pressure. A shifting equilibrium is   |
C   | assumed at each time step.                            |
C   +-------------------------------------------------------+
C
C   +-------------------------------------------------------+
C   | List of Variables                                     |
C   |                                                       |
C   | AN      Number of C Molecules in Fuel                 |
C   | AM      Number of H Molecules in Fuel                 |
C   | AL      Number of O Molecules in Fuel                 |
C   | AK      Number of N Molecules in Fuel                 |
C   | AW      Wetted Area of Burned Gas     in^2            |
C   | ANGLE   Angle Increment Between Data                  |
C   |         Points                        deg             |
C   | BORE    Internal Diameter of Engine   in              |
C   | BCON    Boundary Layer Growth Rate    in/sec          |
C   | CORR    Error in Adiabatic Flame                      |
C   |         Temperature Calculation       R               |
C   | CPU     Constant Pressure Specific                    |
C   |         Heat for Unburned Gas         BTU/lbm-R       |
C   | CVU     Constant Volume Specific                      |
C   |         Heat for Unburned Gas         BTU/lbm-R       |
C   | CRANK   Crankshaft Angle              deg             |
C   | DT      Time Increment                sec             |
C   | DPDT    Pressure Rate of Change       psia/sec        |
C   | DTUDT   Unburned Gas Temperature                      |
C   |         Rate of Change                R/sec           |
C   | DTBDT   Burned Gas Temperature                        |
```

C		Rate of Change	R/sec
C	DTHETA	Engine Speed	rad/sec
C	DMDT	Burned Mass Rate of Change	lbm/sec
C	DVBDT	Volume Burned Rate of Change	in^3/sec
C	DVDT	Cylinder Volume Rate of Change	in^3/sec
C	DHT	Constant Pressure Specific Heat for Burned Gas	BTU/lbm-R
C	DUT	Constant Volume Specific Heat for Burned Gas	BTU/lbm-R
C	DUP	Derivative of Internal Energy wrt Pressure for Burned Gas	BTU/lbm-psia
C	DRT	Derivative of Specific Gas Constant wrt Temperature for Burned Gas	BTU/lbm
C	DRP	Derivative of Specific Gas Constant wrt Pressure for Burned Gas	BTU/lbm-R-psia
C	F	Equivalence Ratio	
C	H	Enthalpy of Burned Gas	BTU/lbm
C	HU	Enthalpy of Unburned Gas	BTU/lbm
C	HEAD	Surface Area of Cylinder Head	in^2
C	INTR	Flag Indicating Maximum Pressure	
C	KOUNT	Total Number of Data Points	
C	LCODE	Flag Indicating Ignition Event	
C	MCODE	Flag Indicating All Mass Burned	
C	NCODE	Flag Indicating All Burned Volume	
C	PE,P	Data Pressure	psia
C	Q	Heat Flux Rate	BTU/in^2-sec
C	QB	Burned Gas Heat Transfer Rate	BTU/sec
C	R	Specific Gas Constant for Products	BTU/lbm-R
C	RU	Specific Gas Constant for Reactants	BTU/lbm-R
C	RC	Compression Ratio	
C	ROD	Crankshaft Radius to Rod Length Ratio	
C	RPM	Engine Speed	rpm
C	SFL	Laminar Flame Speed	in/sec
C	SFLAME	Turbulent Flame Speed	in/sec
C	SKB	Ratio of Specific Heats for Products	
C	SKU	Ratio of Specific Heats for Reactants	
C	SPARK	Ignition Event Angle	deg

```
C    |  START   First Data Point Crank Angle  deg              |
C    |  STROKE  Engine Stroke                 in               |
C    |  TIME    Experimental Time             sec              |
C    |  TWALL   Wall Temperature of BDCB      R                |
C    |  TI      Temperature of Reactants                       |
C    |          Before Ignition               R                |
C    |  TU      Unburned Gas Temperature      R                |
C    |  T,TB    Burned Gas Temperature        R                |
C    |  TAC     Adiabatic Core Temperature    R                |
C    |  TMEAN   Mean Temperature of Adiabatic                  |
C    |          Core and Engine Wall          R                |
C    |  THERM   Thermal Conductivity          BTU/R-in-sec     |
C    |  U       Internal Energy of Products   BTU/lbm          |
C    |  V       Total Internal Volume of                       |
C    |          Engine                        in^3             |
C    |  VC      Clearence Volume              in^3             |
C    |  VD      Displaced Volume              in^3             |
C    |  VB      Burned Gas Volume             in^3             |
C    |  VU      Unburned Gas Volume           in^3             |
C    |  VBF     Volume Burned Fraction                         |
C    |  XCO     Mole Fraction of CO           mole             |
C    |  XNO     Mole Fraction of NO           mole             |
C    |  XAIR    Mass Fraction of Air                           |
C    |  XFUEL   Mass Fraction of Fuel                          |
C    |  ZMB     Burned Mass                   lbm              |
C    |  ZMU     Unburned Mass                 lbm              |
C    |  ZMT     Total Mass (Burned +                           |
C    |          Unburned)                     lbm              |
C    |  ZMBF    Burned Mass Fraction                           |
C    |                                                         |
C    |  ** All Other Variables are Used for Intermediate       |
C    |     Calculation **                                      |
C    +---------------------------------------------------------+
C
      IMPLICIT DOUBLE PRECISION (A-H,O-Z)
      COMMON/BLOC/AN,AM,AL,AK,F,T,P,KLO,IERR,XEQ(12),XPA
      COMMON/TAB/DXT(12),DXP(12),DXF(12)
      COMMON/PROP/AVM,R,H,U,DRT,DHT,DUT,DRP,DHP,DUP,DRF,
     1 DHF,DUF
C
      PARAMETER (PI=3.141592654)
      DIMENSION PE(99),DPDT(99),TU(99),DTUDT(99)
      DIMENSION TAC(99),XR(4),Q(99),SFL(99)
      DATA BORE/3.25/,STROKE/4.5/,RC/8.35/,ROD/4.0/
C
      OPEN(3,FILE='PRESS.DAT')
      OPEN(5,FILE='TEMPOUT.DAT',STATUS='NEW')
      OPEN(7,FILE='MASSOUT.DAT',STATUS='NEW')
```

```
      OPEN(9,FILE='HEATOUT.DAT',STATUS='NEW')
C
      WRITE(*,*) 'Enter Equivalence Ratio'
      READ(*,*) F
      WRITE(*,*) 'Enter Engine Speed (RPM)'
      READ(*,*) RPM
      WRITE(*,*) 'Enter Reactant Temperature (R)'
      READ(*,*) TI
      WRITE(*,*) 'Enter Wall Temperature (R)'
      READ(*,*) TWALL
      WRITE(*,*) 'Enter Number of Data Points'
      READ(*,*) KOUNT
      WRITE(*,*) 'Enter the First Angle (deg)'
      READ(*,*) START
      WRITE(*,*) 'Enter the Angle Increment (deg)'
      READ(*,*) ANGLE
      WRITE(*,*) 'Enter the Ignition Time BTDC (deg)'
      READ(*,*) SPARK
      WRITE(*,*) 'Pressure Data is Entered from File'
C
C   +-----------------------------------------------------+
C   ¦ The following section performs initial calculations ¦
C   ¦ for parameters used later in the program.           ¦
C   +-----------------------------------------------------+
C
      HEAD=0.25*PI*(BORE**2)
      VD=HEAD*STROKE
      VC=VD/(RC-1.0)
      CRANK=START
      TIME=0.0
      DT=ANGLE/(6.0*RPM)
      DTHETA=RPM*PI/30.0
      AN=8.0
      AM=18.0
      AL=0.0
      AK=0.0
      KLO=1
      COEF=(AN+0.25*AM-0.5*AL)
      ROR=COEF/F
      XR(1)=1.0/(1.0+4.7718*ROR)
      XR(2)=ROR*XR(1)
      XR(3)=ROR*XR(1)*3.7274
      XR(4)=ROR*XR(1)*0.0444
      AVMR=XR(1)*(AN*12.011+AM*1.008+AL*16.000+AK*14.008)
     1 +XR(2)*31.999+XR(3)*28.013+XR(4)*39.944
      RU=1.987165/AVMR
      FRATIO=1.0+0.027*F
      XFUEL=114.224/(114.224+12.5*28.97/F)
```

```
      XAIR=(28.97*12.5/F)/(114.224+12.5*28.97/F)
      BCON=0.07874/((DT*KOUNT)**0.8)
C
C   +-----------------------------------------------------+
C   | The following section determines the unburned gas   |
C   | and adiabatic core temperatures for the given       |
C   | fuel-air mixture and pressure trace. The heat flux  |
C   | rate from the adiabatic core to the engine is also  |
C   | determined as is the flame speed, which is dependent|
C   | on the temperature of the unburned gases.           |
C   +-----------------------------------------------------+
C
      TIU=TI
      TU(1)=TIU
      TAC(1)=TIU
      DO 10 I = 1,KOUNT
      READ(3,*) PE(I)
      PE(I)=PE(I)*14.696/101.325
      IF (I.EQ.1) GOTO 20
      P=PE(I)
      CPU=XAIR*(0.220+0.0306*TU(I-1)/1000.0)
     1 +XFUEL*(0.105+0.4860*TU(I-1)/1000.0)
      CVU=CPU-RU
      SKU=CPU/CVU
      TU(I)=TU(1)*(PE(I)/PE(1))**((SKU-1.0)/SKU)
      SFL(I)=7.56*((TU(I)/536.4)**2.36)
     1 *((14.696/PE(I))**0.22)
      IF (ABS(CRANK-SPARK).LT.1.0) THEN
            PBI=PE(I)
            HU=XFUEL*(-89680.0/114.224+201.1+0.000243
     1      *(TU(I)**2)+0.105*TU(I)-201.5712)
     1      +XAIR*(172.39+0.0000153*(TU(I)**2)
     1      +0.220*TU(I)-166.33)
            T=4000.0
   15       CALL PER(1)
            CORR=(H-HU)/DHT
            T=T-CORR
            IF(ABS(CORR).LT.1.0) THEN
                  TIB=T
                  TAC(I)=TIB
                  SKB=DHT/DUT
                  GOTO 20
            ELSE
                  GOTO 15
            ENDIF
      ENDIF
      IF (CRANK.LT.SPARK) THEN
            TAC(I)=TU(I)
```

```
      ELSE
            CALL PER(1)
            SKB=DHT/DUT
            TAC(I)=TIB*(PE(I)/PBI)**((SKB-1.0)/SKB)
            TMEAN=(TAC(I)+TWALL)/2.0
            T=TMEAN
            THERM=(9.0*DHT-5.0*DUT)*3.0614E-9
     1      *(TMEAN**0.7)/FRATIO
            Q(I)=THERM*(TAC(I)-TWALL)/(BCON*(TIME**0.8))
      ENDIF
   20 T=TAC(I)
      CRANK=CRANK+ANGLE
      TIME=TIME+DT
   10 CONTINUE
      CRANK=START
C
C    +-----------------------------------------------------+
C    | The following section calculates the rates of change |
C    | of pressure and unburned gas temperature using       |
C    | Lagrande's five point formula for numerical          |
C    | differentiation. The first and last terms are        |
C    | determined using three point formulas.               |
C    +-----------------------------------------------------+
C
      INTR=0
      DO 30 I=1,KOUNT
      IF (I.LE.2) THEN
            DPDT(I)=(-3.0*PE(I)+4.0*PE(I+1)-PE(I+2))
     1      /(2.0*DT)
            GO TO 30
      ENDIF
      IF (I.GE.(KOUNT-1)) THEN
            DPDT(I)=(PE(I-2)-4.0*PE(I-1)+3.0*PE(I))/(2.0*DT)
            GO TO 30
      ENDIF
      DPDT(I)=(PE(I-2)-8.0*PE(I-1)+8.0*PE(I+1)-PE(I+2))
     1 /(12.0*DT)
      IF(INTR.NE.0) GOTO 30
      IF(DPDT(I).LE.0.0) INTR=I
   30 CONTINUE
C
      DO 35 I=1,KOUNT
      IF (I.LE.2) THEN
            DTUDT(I)=(-3.0*TU(I)+4.0*TU(I+1)-TU(I+2))
     1      /(2.0*DT)
            GO TO 35
      ENDIF
      IF (I.GE.(KOUNT-1)) THEN
```

```
            DTUDT(I)=(TU(I-2)-4.0*TU(I-1)+3.0*TU(I))
     1      /(2.0*DT)
            GO TO 35
       ENDIF
       DTUDT(I)=(TU(I-2)-8.0*TU(I-1)+8.0*TU(I+1)-TU(I+2))
     1 /(12.0*DT)
   35 CONTINUE
C
C   +-----------------------------------------------------+
C   | The following section initializes variables that are |
C   | used to solve the differential equations obtained    |
C   | from the first law of thermodynamics analysis. The   |
C   | output data files TEMPOUT, HEATOUT, and MASSOUT are  |
C   | also given appropriate headings at this point.       |
C   +-----------------------------------------------------+
C
      FRAC=VC*(RC-1.0)/2.0
      BRAC=SQRT(ROD**2-SIN(START)**2)
      V=VC+FRAC*(ROD+1.0-COS(START)-BRAC)
      ZMT=PE(1)*V/(RU*TU(1)*9338.4)
      VU=V
      VB=0.0
      ZMB=0.0
      ZMU=ZMT
      LCODE=0
      MCODE=0
      NCODE=0
      WRITE(5,40)
   40 FORMAT(2X,'Angle (deg)',4X,'Tu (R)',5X,'Tb (R)',
     1 4X,'Tac (R)',/)
      WRITE(7,45)
   45 FORMAT(4X,'Angle (deg)',4X,'Mb (lbm)',7X,'Mb/Mt',
     1 8X,'Vb/V',/)
      WRITE(9,50)
   50 FORMAT(2X,'Angle (deg)',1X,'Vel (in/s)',2X,'Qb
     1 (BTU/s)',3X,'[CO]',/)
C
C   +-----------------------------------------------------+
C   | The following section determines the rate of change |
C   | for burned mass, volume and temperature for          |
C   | conditions at time t.                               |
C   +-----------------------------------------------------+
C
      DO 55 I=1,(KOUNT-1)
      J=I
      THETA=CRANK*PI/180.0
      BRAC=SQRT(ROD**2-SIN(THETA)**2)
      V=VC+FRAC*(ROD+1.0-COS(THETA)-BRAC)
```

```
       DVDT=FRAC*SIN(THETA)*DTHETA
      1 +FRAC*SIN(THETA)*COS(THETA)*DTHETA/BRAC
       RADIUS=0.5*BORE*SQRT(VBF)
       AW=RADIUS**2
       IF (CRANK.LT.SPARK) THEN
             VU=V
             T=TAC(I)
             TB=TAC(I)
             GOTO 65
       ENDIF
       LCODE=LCODE+1
       ZMBH=ZMB
       VBH=VB
       TBH=TB
       P=PE(J)
       T=TB
       QB=AW*Q(I)
       CALL PER(1)
       HU=XFUEL*(-89680.0/114.224+201.1+0.000243*(TU(J)**2)
      1 +0.105*TU(J)-201.5712)+XAIR*(172.39+0.0000153
      1 *(TU(J)**2)+0.220*TU(J)-166.33)
       ALFA=1.0+TB*DRT/R
       BETA=DUT/R
       DMDT1=(-QB+(ZMU*RU*DTUDT(J)-PE(J)*DVDT/9338.4)
      1 *(BETA+1.0)-DPDT(J)*(VU/9338.4+ZMB*DUP+BETA
      1 *(VB/ALFA+VU)/9338.4-ZMB*TB*BETA*DRP/ALFA))
      1 /(U-HU+RU*TU(J)*(1.0+BETA)-TB*DUT/ALFA)
       DVBDT1=DVDT+VU*(DPDT(J)/PE(J)-DTUDT(J)/TU(J))
      1 +9338.4*RU*TU(J)*DMDT1/PE(J)
       IF (VB.EQ.V) DVBDT1=DVDT
       IF (LCODE.GT.1) DTBDT1=TB*(DVBDT1/VB-DMDT1/ZMB+DPDT(J)
      1 *(1.0/PE(J)-DRP/R))/ALFA
C
C    +-----------------------------------------------------+
C    | The following section determines the new burned mass |
C    | and volume using the values of the time derivatives  |
C    | at time t. The burned gas temperature is also        |
C    | determined at this time.                             |
C    +-----------------------------------------------------+
C
       TB=TB+DTBDT1*DT
       ZMB=ZMB+DMDT1*DT
       IF(ZMB.GE.ZMT) ZMB=ZMT
       VB=VB+DVBDT1*DT
       IF(VB.GE.V) VB=V
       ZMU=ZMT-ZMB
       VU=V-VB
       XNO1=XEQ(7)
```

```
      XCO1=XEQ(6)
C
C   +-----------------------------------------------------+
C   | The following section determines the rate of change |
C   | for burned mass, volume and temperature for         |
C   | conditions at time t+1.                             |
C   +-----------------------------------------------------+
C
      J=I+1
      T=TB
      P=PE(J)
      CALL PER(1)
      HU=XFUEL*(-89680.0/114.224+201.1+0.000243*(TU(J)**2)
     1 +0.105*TU(J)-201.5712)+XAIR*(172.39+0.0000153
     1 *(TU(J)**2)+0.220*TU(J)-166.33)
      ALFA=1.0+TB*DRT/R
      BETA=DUT/R
      DMDT2=(-QB+(ZMU*RU*DTUDT(J)-PE(J)*DVDT/9338.4)
     1 *(BETA+1.0)-DPDT(J)*(VU/9338.4+ZMB*DUP+BETA
     1 *(VB/ALFA+VU)/9338.4-ZMB*TB*BETA*DRP/ALFA))
     1 /(U-HU+RU*TU(J)*(1.0+BETA)-TB*DUT/ALFA)
      DVBDT2=DVDT+VU*(DPDT(J)/PE(J)-DTUDT(J)/TU(J))
     1 +9338.4*RU*TU(J)*DMDT2/PE(J)
      IF (VB.EQ.V) DVBDT2=DVDT
      DTBDT2=TB*(DVBDT1/VB-DMDT1/ZMB+DPDT(J)
     1 *(1.0/PE(J)-DRP/R))/ALFA
C
C   +-----------------------------------------------------+
C   | The following section determines the improved values|
C   | for burned mass and volume using the Modified Euler |
C   | Method. The burned gas temperature is also          |
C   | determined at this time.                            |
C   +-----------------------------------------------------+
C
      P=(PE(I)+PE(J))/2.0
      IF (J.LT.INTR) TB=P*VB/(9338.4*R*ZMB)
      ZMB=ZMBH+(DMDT1+DMDT2)*DT/2.0
      IF (ZMB.GE.ZMT) MCODE=1
      IF (MCODE.GT.0) ZMB=ZMT
      VB=VBH+(DVBDT1+DVBDT2)*DT/2.0
      IF (VB.GE.V) NCODE=1
      IF (NCODE.GT.0) VB=V
      ZMU=ZMT-ZMB
      VU=V-VB
      IF (J.GE.INTR) TB=P*VB/(9338.4*R*ZMB)
      XNO2=XEQ(7)
      XCO2=XEQ(6)
C
```

```
C   +-----------------------------------------------------+
C   ¦ The following section outputs the calculated values ¦
C   ¦ to the DAT files TEMPOUT, MASSOUT, and HEATOUT.     ¦
C   +-----------------------------------------------------+
C
   65 ZMBF=ZMB/ZMT
      VBF=VB/V
      XNO=(XNO1+XNO2)/2.0
      XCO=(XCO1+XCO2)/2.0
      SFLAME=157.48+SFL(I)
      WRITE(5,70) CRANK,TU(I),TB,TAC(I)
   70 FORMAT(3X,F8.2,3X,F8.1,3X,F8.1,3X,F8.1)
      WRITE(7,75) CRANK,ZMB,ZMBF,VBF
   75 FORMAT(5X,F8.2,5X,F8.6,5X,F8.5,5X,F8.5)
      WRITE(9,80) CRANK,SFLAME,QB,XCO
   80 FORMAT(3X,F8.2,3X,F8.2,3X,F8.4,3X,F8.5)
      CRANK=CRANK+ANGLE
      IF (IERR.NE.0) GOTO 85
   55 CONTINUE
      IF (IERR.EQ.0) GOTO 95
   85 WRITE(*,90) IERR
   90 FORMAT(/,'Subroutine Error Code No.',I2)
   95 STOP
      END
```

APPENDIX D

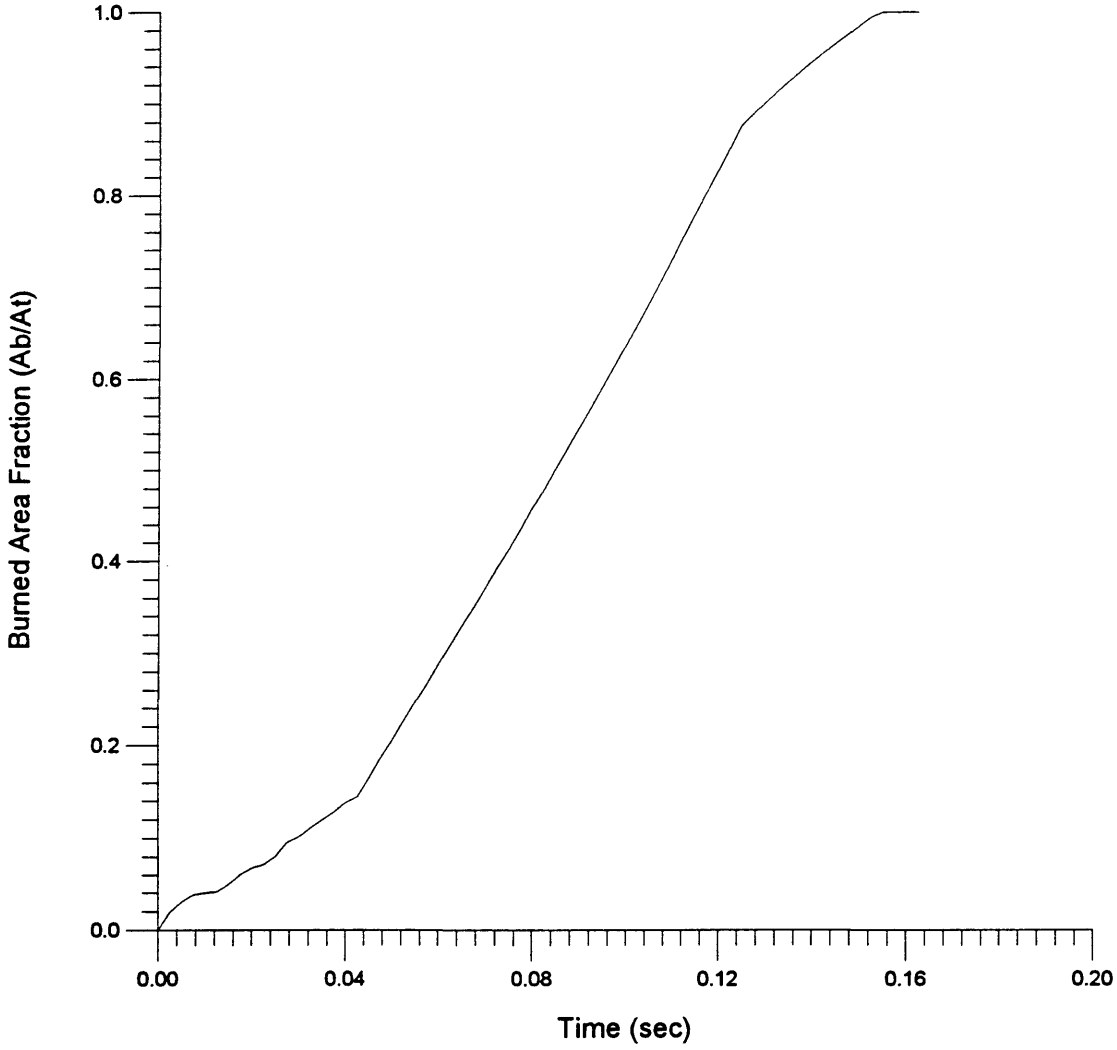

Graph 1 - Burned-Area Fraction versus Time

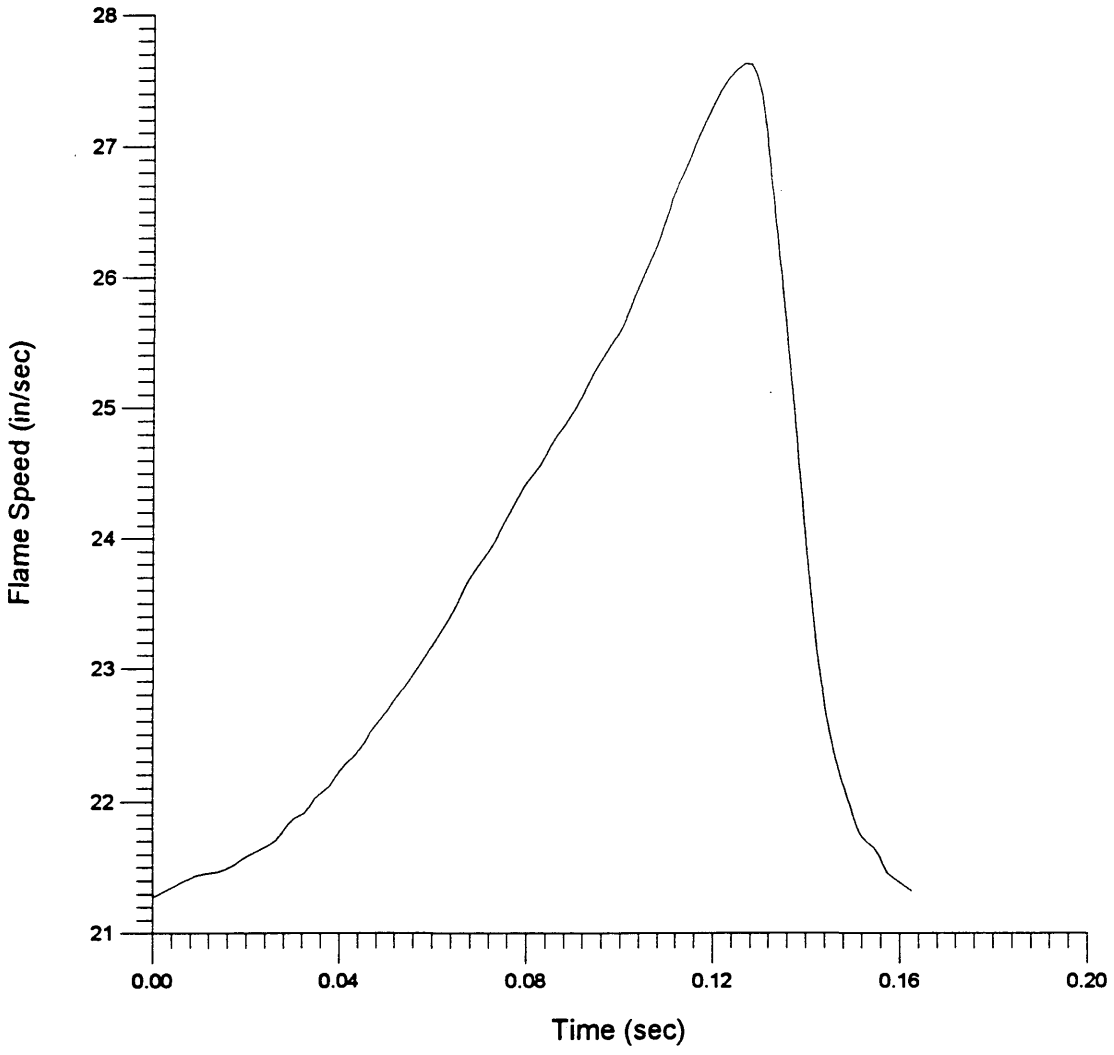

Graph 2 - Flame Speed versus Time

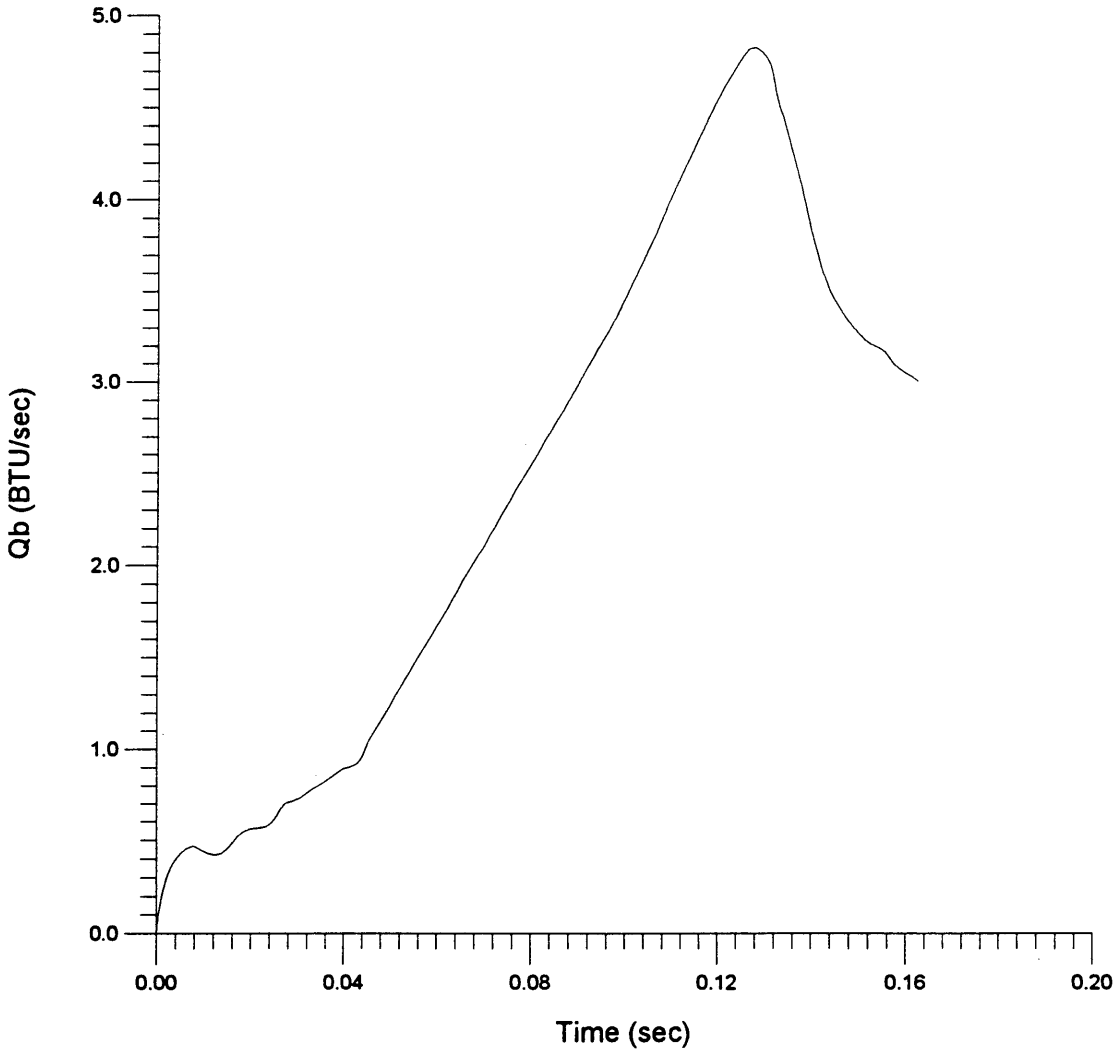

Graph 3 - Heat Transfer Rate versus Time

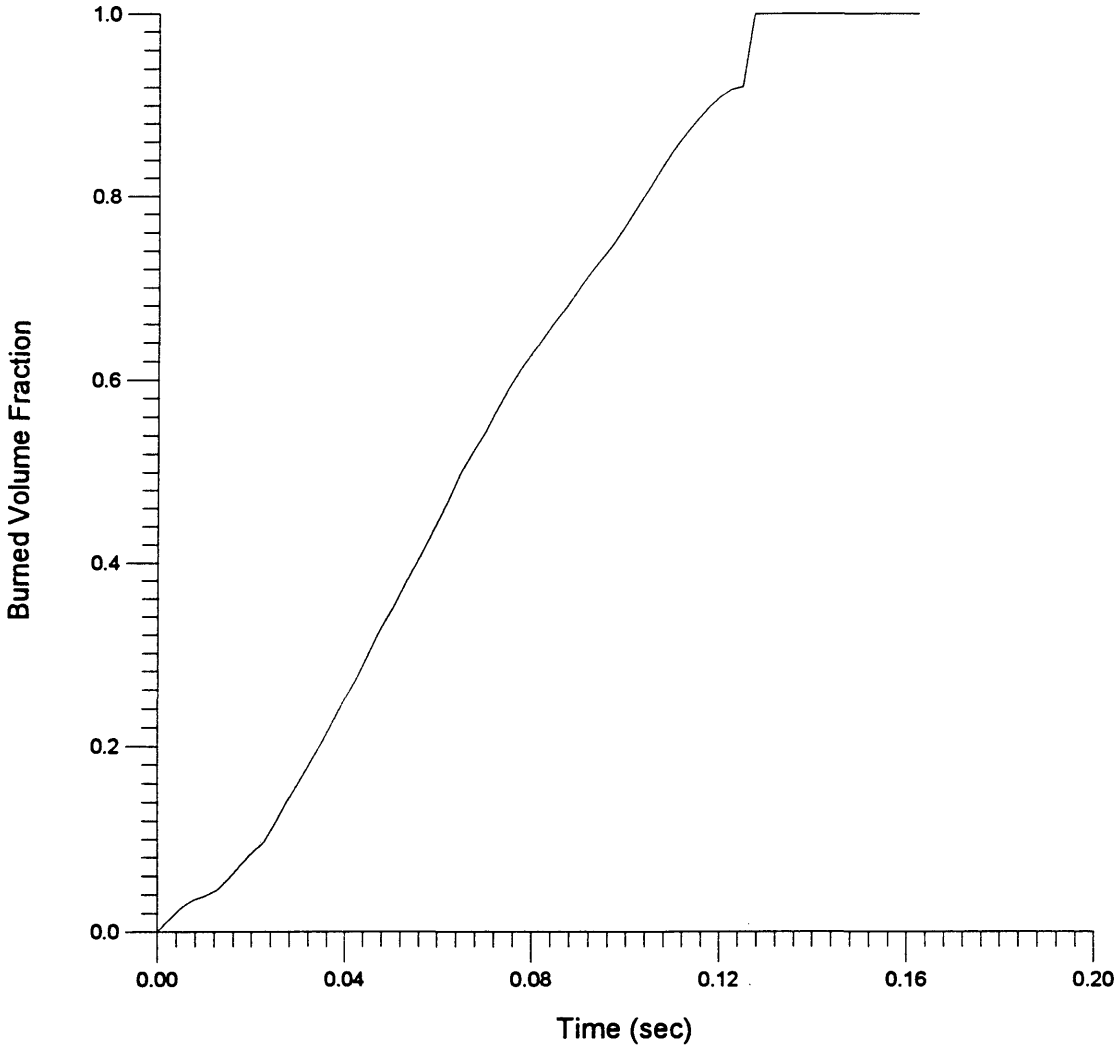

Graph 4 - Burned-Volume Fraction versus Time

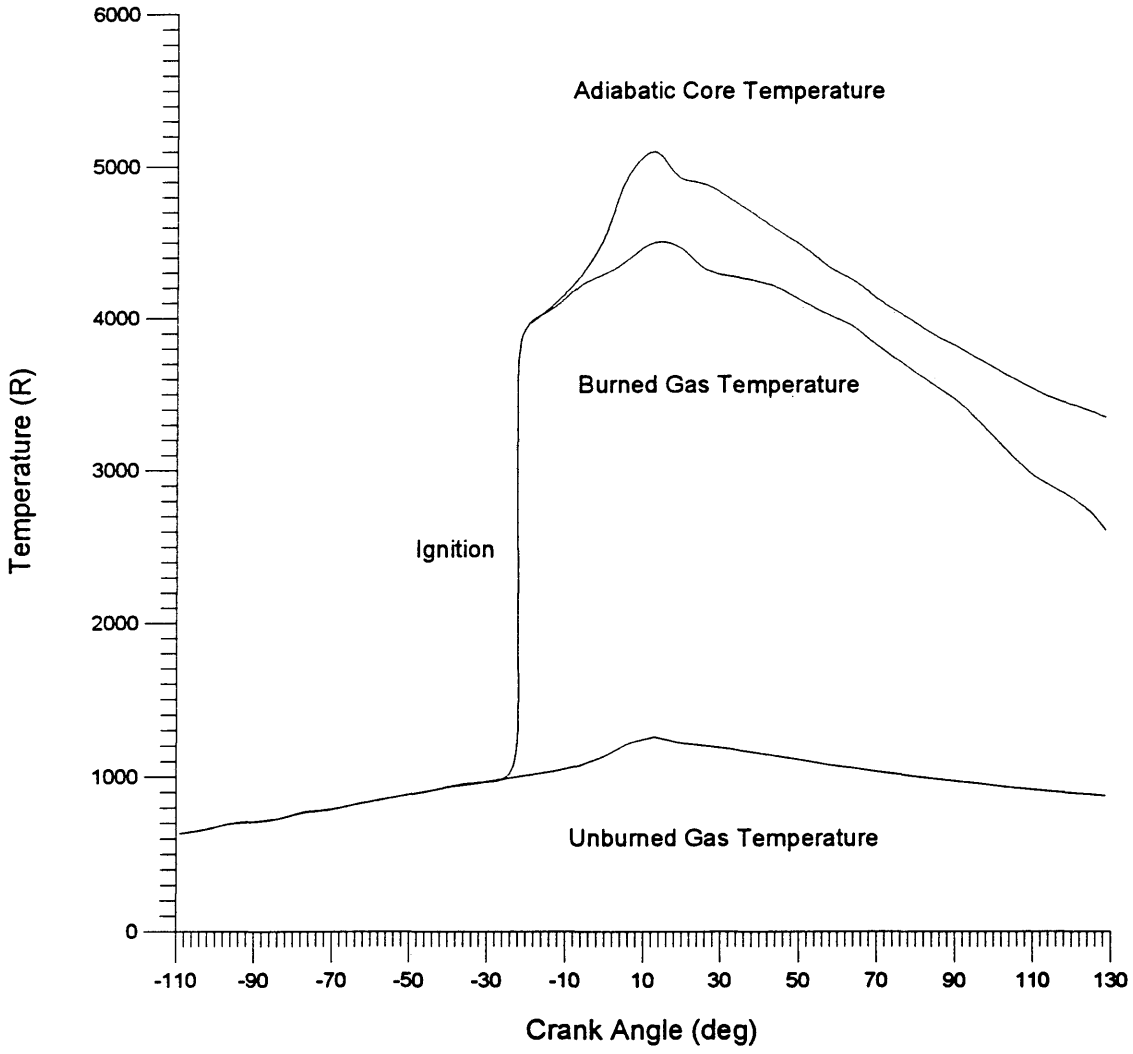

Graph 5 - Temperature versus Time for IC Engine

APPENDIX E

Burned Gas Equation Derivation

The following discussion is intended to further illustrate the development of Equation 36.

Beginning with the First Law of Thermodynamics written as a rate equation and applying this to the burned-gas control volume.

$$\frac{d(mu)_b}{dt} = -P\frac{dV_b}{dt} + \dot{Q}_b + \sum_i \dot{m}_i h_i \qquad (1)$$

At the control volume boundary, reactants are converted into products. This serves to increase the burned mass at the expense of unburned mass. Flow work is also done as this mass crosses the boundary. Lastly, the internal energy of the reactants is added to the burned-gas region as their sensible energy is convected into that zone. The summation in Equation 1 can therefore be written into the First Law as

$$u_b\frac{dm_b}{dt} + m_b\frac{du_b}{dt} = -P\frac{dV_b}{dt} + \dot{Q}_b + \frac{dm_b}{dt}h_u \qquad (2)$$

The internal energy is a function of temperature, pressure, and equivalence ratio. For the BDCB however, no fuel or air is added once the BDCB has been charged. As a result, the equivalence ratio is constant. The internal energy rate of change can now be written as the following

$$\frac{du_b}{dt} = \frac{\partial u_b}{\partial T_b}\frac{dT_b}{dt} + \frac{\partial u_b}{\partial P}\frac{dP}{dt} \qquad (3)$$

Substituting into the First Law rate equation gives

$$\frac{dm_b}{dt}(u_b - h_u) + m_b\left(\frac{\partial u_b}{\partial T_b}\frac{dT_b}{dt} + \frac{\partial u_b}{\partial P}\frac{dP}{dt}\right) = -P\frac{dV_b}{dt} + \dot{Q}_b \qquad (4)$$

dT_b/dt can be solved for by writing the Ideal Gas Law ($PV = mRT$) as a rate equation.

$$V_b\frac{dP}{dt} + P\frac{dV_b}{dt} = m_b R_b\frac{dT_b}{dt} + T_b R_b\frac{dm_b}{dt} + m_b T_b\frac{dR_b}{dt} \qquad (5)$$

As with the internal energy, the specific gas constant is a function of temperature, pressure, and equivalence ratio. With no change in the equivalence ratio occurring, the derivative then becomes

$$\frac{dR_b}{dt} = \frac{\partial R_b}{\partial T_b}\frac{dT_b}{dt} + \frac{\partial R_b}{\partial P}\frac{dP}{dt} \tag{6}$$

Dividing the left-hand side of Equation 5 by PV_b and the right hand side by $m_bR_bT_b$, and substituting Equation 6 for the specific gas constant rate of change yields

$$\frac{1}{T_b}\frac{dT_b}{dt} = \frac{1}{P}\frac{dP}{dt} + \frac{1}{V_b}\frac{dV_b}{dt} - \frac{1}{m_b}\frac{dm_b}{dt} - \frac{1}{R_b}\frac{\partial R_b}{\partial T_b}\frac{dT_b}{dt} - \frac{1}{R_b}\frac{\partial R_b}{\partial P}\frac{dP}{dt} \tag{7}$$

$$\frac{dT_b}{dt}\left(\frac{1}{T_b} + \frac{1}{R_b}\frac{\partial R_b}{\partial T_b}\right) = \frac{1}{P}\frac{dP}{dt} + \frac{1}{V_b}\frac{dV_b}{dt} - \frac{1}{m_b}\frac{dm_b}{dt} - \frac{1}{R_b}\frac{\partial R_b}{\partial P}\frac{dP}{dt} \tag{8}$$

$$setting\ \ \alpha = \left(\frac{1}{T_b} + \frac{1}{R_b}\frac{\partial R_b}{\partial T_b}\right)$$

Substituting back into the First Law rate equation gives

$$\frac{dm_b}{dt}(u_b - h_u) + m_b\left[\frac{\partial u_b}{\partial T_b}\frac{1}{\alpha}\left(\frac{1}{P}\frac{dP}{dt} + \frac{1}{V_b}\frac{dV_b}{dt} - \frac{1}{m_b}\frac{dm_b}{dt} - \frac{1}{R_b}\frac{\partial R_b}{\partial P}\frac{dP}{dt}\right) + \frac{\partial u_b}{\partial P}\frac{dP}{dt}\right]$$

$$= -P\frac{dV_b}{dt} + \dot{Q}_b$$

$$setting\ \ \beta = \frac{1}{\alpha}\frac{\partial u_b}{\partial T_b} \tag{9}$$

$$\frac{dm_b}{dt}(u_b - h_u - \beta) + \frac{dP}{dt}\left(\frac{\beta m_b}{P} - \frac{\beta m_b}{R_b}\frac{\partial R_b}{\partial P} + m_b\frac{\partial u_b}{\partial P}\right) = -\frac{dV_b}{dt}\left(P + \frac{\beta m_b}{V_b}\right) + \dot{Q}_b \tag{10}$$

To solve for the burned-gas volume we consider the total volume to be the sum of the unburned- and the burned-gas volume. Because the BDCB is a constant volume device, the

total volume rate of change is zero. This gives

$$\frac{dV_b}{dt} = -\frac{dV_u}{dt} \tag{11}$$

In this manner, we can relate the burned-gas volume to the physical properties of the unburned-gas region. Applying the Ideal Gas Law rate equation to the unburned-gas control volume gives

$$\frac{1}{V_u}\frac{dV_u}{dt} = \frac{1}{T_u}\frac{dT_u}{dt} + \frac{1}{m_u}\frac{dm_u}{dt} + \frac{1}{R_u}\frac{dR_u}{dt} - \frac{1}{P}\frac{dP}{dt} \tag{12}$$

For the unburned-gas control volume there is no dissociation and the specific gas constant remains fixed, or dR_u/dt is zero. The unburned-mass rate of change is not just the conversion of reactants into products because in the unburned-gas control volume unburned, mass can be expelled out of the blow-down valve.

$$\frac{dm_u}{dt} = -\frac{dm_b}{dt} - \dot{m}_o \tag{13}$$

Prior to the blow-down valve opening, dm_o/dt is zero and the mass exchange is just the conversion of reactants into products. Substituting Equations 12 and 13 into Equation 11 gives an equation for the burned-gas volume.

$$\frac{dV_b}{dt} = V_u\left[\frac{1}{P}\frac{dP}{dt} + \frac{1}{m_u}\left(\frac{dm_b}{dt} + \dot{m}_o\right) - \frac{1}{T_u}\frac{dT_u}{dt}\right] \tag{14}$$

Again, substituting back into the First Law rate equation yields the following.

$$\begin{aligned}\frac{dm_b}{dt}(u_b - h_u - \beta) + \frac{dP}{dt}\left(\frac{\beta m_b}{P} - \frac{\beta m_b}{R_b}\frac{\partial R_b}{\partial P} + m_b\frac{\partial u_b}{\partial P}\right) = \\ -V_u\left[\frac{1}{P}\frac{dP}{dt} + \frac{1}{m_u}\left(\frac{dm_b}{dt} + \dot{m}_o\right) - \frac{1}{T_u}\frac{dT_u}{dt}\right]\left(P + \frac{\beta m_b}{V_b}\right) + \dot{Q}_b\end{aligned} \tag{15}$$

Rearranging and grouping the terms according to the derivative values results in the following.

$$\frac{dm_b}{dt}\left[u_b - h_u - \beta + \frac{V_u}{m_u}\left(P + \frac{\beta m_b}{V_b}\right)\right] =$$

$$-\frac{dP}{dt}\left[\frac{\beta m_b}{P} - \frac{\beta m_b}{R_b}\frac{\partial R_b}{\partial P} + m_b\frac{\partial u_b}{\partial P} + \frac{V_u}{P}\left(P + \frac{\beta m_b}{V_b}\right)\right] \qquad (16)$$
$$+\frac{dT_u}{dt}\frac{V_u}{T_u}\left(P + \frac{\beta m_b}{V_b}\right) - \dot{m}_o\frac{V_u}{m_u}\left(P + \frac{\beta m_b}{V_b}\right) + \dot{Q}_b$$

Substituting $m_b/V_b = P/R_bT_b$ and $V_u/m_u = R_uT_u/P$ we get

$$\frac{dm_b}{dt}\left(u_b - h_u - \beta + R_uT_u + \beta\frac{R_uT_u}{R_bT_b}\right) =$$

$$-\frac{dP}{dt}\left(\frac{\beta m_b}{P} - \frac{\beta m_b}{R_b}\frac{\partial R_b}{\partial P} + m_b\frac{\partial u_b}{\partial P} + V_u + V_u\frac{\beta}{R_bT_b}\right) \qquad (17)$$
$$+\frac{dT_u}{dt}\frac{V_u}{T_u}\left(P + \frac{\beta m_b}{V_b}\right) - \dot{m}_o\frac{V_u}{m_u}\left(P + \frac{\beta m_b}{V_b}\right) + \dot{Q}_b$$

$$\frac{dm_b}{dt}\left[u_b - h_u + R_uT_u + \frac{\beta}{R_bT_b}(R_uT_u - R_bT_b)\right] =$$

$$-\frac{dP}{dt}\left(m_b\frac{\partial u_b}{\partial P} - \frac{\beta m_b}{R_b}\frac{\partial R_b}{\partial P} + V_u + V_b\frac{\beta}{R_bT_b} + V_u\frac{\beta}{R_bT_b}\right) \qquad (18)$$
$$+m_uR_u\frac{dT_u}{dt}\left(1 + \frac{\beta}{R_bT_b}\right) - \dot{m}_oR_uT_u\left(1 + \frac{\beta}{R_bT_b}\right) + \dot{Q}_b$$

$$setting\ \gamma = \frac{\beta}{R_bT_b}$$

and noting that the total volume of the BDCB is the sum of the burned and unburned regions, we greatly simplify the

equation. Also, the unburned internal energy is obtained by subtracting the enthalpy from the flow work, or in this case the product of the unburned-gas temperature and specific gas constant. Making these substitutions gives rise to the following equation which is exactly the same as Equation 36 discussed previously, except that in that case it was assumed that the heat transfer was from the burned-gas region to the surroundings.

$$\frac{dm_b}{dt}\left[u_b - u_u + \gamma\left(R_u T_u - R_b T_b\right)\right] = \left(m_u R_u \frac{dT_u}{dt} - \dot{m}_o R_u T_u\right)(1+\gamma) + \dot{Q}_b - \frac{dP}{dt}\left(\gamma V + V_u + m_b \frac{\partial u_b}{\partial P} - \gamma m_b T_b \frac{\partial R_b}{\partial P}\right) \tag{19}$$